Effect of Arsenic and Phosphate on Microalgae Growth, Nutrient Uptake and the Metabolic Pathways

BY

TANG WENN WENN

BSc Hons

A thesis submitted for the degree of Master at

Monash University in 2023

School of Science

Copyright notice

Abstract

Mining activities release the toxic arsenic into freshwater systems. Microalgae are known photoautotrophic organisms in freshwater systems that uptake and bioremediate arsenic. Recent studies providing a snapshot of the ability of microalgae in arsenic uptake have highlighted the need to identify the effect of various arsenic species and concentrations with an absence or presence of phosphate towards the microalgae growth and efficiency of arsenic uptake. To identify a more suitable microalgae strain as the arsenic bioremediation candidate, we aim to compare the effect of arsenic on the microalgae growth and arsenic uptake capacity in the presence or absence of phosphate. Here we report the comparison between two microalgae strains, *Nostoc* MUM003 (SRR27732368) and *Chlorella* MUM002 (SRR27765439), in terms of the growth and arsenic uptake to determine the most suitable candidate for arsenic bioremediation. Both microalgae strains were treated with 0.01 mg L^{-1}, 0.10 mg L^{-1}, and 1.00 mg L^{-1} As (III) and As (V) under conditions with and without phosphate. The growth of both microalgae strains was measured through the optical density and biomass dry weight method. The arsenic concentrations uptake by the microalgae strains were measured through an ICP-OES instrument. To examine the effect of arsenic on the microalgae's cells, the vegetative cells of the microalgae strain which accumulated the highest arsenic concentration were further observed through SEM-EDX to identify the arsenic concentration adsorb on the cell surface and to identify the consequences of arsenic on the surface morphology. Several arsenic detoxification pathways were also predicted based on the whole genome sequence to understand the pathways that can be found in the microalgae strain. Primer sets were designed based on the predicted pathways and PCR analyses were performed to identify the possible reaction in the microalgae cell. Our results showed that 0.10 mg L^{-1} and 1.00 mg L^{-1} As (III) in the absence of phosphate enhances *Nostoc* growth in comparison to the control treatment in terms of biomass dry weight ($p < 0.05$). Additionally, *Nostoc* strain

demonstrated its ability to uptake a high arsenic concentration percentage ($p < 0.005$) treated with As (III) without phosphate compared to the *Chlorella* strain, particularly when treated with a higher arsenic concentration at 1.00 mg L^{-1}. Whereas, arsenic causes a significant ($p < 0.05$) reduction in *Chlorella* growth and the arsenic uptake reduces throughout the cultivation period. This suggests that *Nostoc* has a comparable advantage in the bioremediation of arsenic compared to the *Chlorella* strain. The structure changes and disruption of *Nostoc* vegetative cells suggest that As (III) adsorbs and damages the vegetative cell surface. The PCR analysis results revealed that the arsenite methyltransferase gene was the only arsenic-related gene expressed. This result indicated that the methylation process of As (III) occurred in the *Nostoc* cell during the 24^{th} day of treatment under 1.00 mg L^{-1} As (III). The intracellular As (III) may not extrude directly from the cell due to the lack of phosphate for ATP formation, whereas the binding of As (III) to glutathione may occur in an earlier stage. Overall, study findings reveal useful insight regarding the suitability of microalgae strains for freshwater arsenic bioremediation.

Declaration

This thesis is an original work of my research and contains no material which has been accepted for the reward of any other degree or diploma at any university or equivalent institution and that, to the best of my knowledge and belief, this thesis contains no material previously published or written by another person, except where due reference is made in the text of the thesis

Signature:

Name: Tang Wenn Wenn

Date: 1st November 2023

Acknowledgement

The successful accomplishment of this project could not have been achieved without the invaluable guidance and assistance from numerous individuals involved directly or indirectly. Taking this opportunity, I would like to extend my heartfelt appreciation for the suggestions, contributions, and support received.

First and foremost, I wish to express my deepest appreciation to my supervisor Dr Foo Su Chern for her unwavering encouragement and supervision throughout this project. Without her guidance, this project could not be performed successfully. Many suggestions and advice were provided throughout the 2 years program to aid me in achieving the goal of this project. I would like to extend my gratitude to Dr Wee Wei Yee for providing invaluable suggestions and guidance that were crucial for the completion of this project. Without his suggestions, the project may not have been completed successfully.

Next, I would like to thank for the encouragement and support from my friends and labmates including Ms Lim Yi An, Ms Zuhaili, and Ms Samantha. Their valuable feedback and suggestions helped overcome challenges faced during the bottleneck period.

In addition, I wish to convey my appreciation to all technical officers from the School of Science and the School of Engineering for their support in terms of lab instruments and facilities. Their assistance ensured the progress of my work to perform smoothly.

On top of that, I wish to extend this appreciation and express my special thanks to all milestone panel examiners including Prof. Adeline, Dr Song and Dr Wan, to the lecturer from the School of Science Dr Patrick Tan, and to all the staff from Monash University Malaysia Genomics Facility for their advice and guidelines for different methodology, troubleshooting problems occurred, and materials that was required for the work completion.

Lastly, I am thankful to both my parents for their financial and emotional support throughout the program. Their encouragement for me to pursue my further studies has brought me to this point of achievement. Without their support and encouragement, this project would not have achieved successful completion. Thank you!

Table of Contents

List of Figures

List of Tables

List of abbreviations and acronyms

%	Percentage
>	More than
µg L^{-1}	Microgram per Litre
µg mg^{-1}	Microgram per Milligram
µm	Micrometre
ANOVA	Analysis of Variance
As (III)	Arsenite
As (V)	Arsenate
BLAST	Basic Local Alignment Search Tool
DMAs (V)	Dimethylarsenic
EDX	Energy Dispersive X-ray
g L^{-1}	Gram per Litre
g L^{-1} d^{-1}	Gram per Litre per day
HCA	Hierarchical Cluster Analysis
i.e.	That is
ICP	Inductively Coupled Plasma
m^{-2} s^{-1}	Meter per Second squared
MA (V)	Methylarsenate
mg kg^{-1}	Milligram per Kilogram

mg L^{-1}	Milligram per Litre
nm	Nanometre
^{o}C	Degree Celsius
OD	Optical density
OES	Optical Emission Spectroscopy
PBS	phosphate-buffered saline
PCA	Principal Component Analysis
PCR	Polymerase Chain Reaction
RNA	Ribonucleic acid
SAM	S-adenosylmethionine
SEM	Scanning Electron Microscope
SGR	Specific growth rate
TBE	Tris-Borate-EDTA
TMA (O)	Trimethylarsine Oxide
UV-vis spectrophotometer	Ultraviolet-visible spectrophotometer
W	Watt
WGS	Whole Genome Sequencing

CHAPTER 1

INTRODUCTION

1.1 Background of Study

The consequences of arsenic exposure via drinking water pose implications for human health. In this chapter, we delve into the factors contributing to arsenic leakage into the water sources, the overview of arsenic implications on human health, and explore the potential of microalgae as an arsenic bioremediation agent.

1.1.1 Freshwater pollution

Freshwater is important for the survival of living organisms on Earth. It is the only water source that can be consumed by humans and animals. Ex-mining lakes are freshwater sources that have potential as alternative raw water sources. One instance, the South Quay Lake in Sunway City is a water reservoir that supplies potable water to many places.

Many of Malaysia's water bodies are ex-mining lakes. According to Samudi Yasir et al. (2008), abandoned mining activities formed the mining lakes in Malaysia. Malaysia was categorized as a prominent tin producers and exporter worldwide and owns multiple tin mining hubs, also represents one of the biggest tin producers and exporters on a global scale (Balamurugan, 1991; Thoburn, 1978). Mining activities involve the iteration of metal ores and water (Grande et al., 2005) and led to the increase of heavy metals concentration in the mining lakes (Samudi Yasir et al., 2008). This translates to the increased arsenic exposure from such water bodies to humans. As arsenic is toxic to both humans and animals, consumption of water sources containing arsenic will lead to health implications. This leads to an alert where the mine water

quality containing arsenic needs to be considered prior to the employment of the mine water as the alternative drinking water source.

1.1.2 Arsenic toxicity

Arsenic is a heavy metal discovered within the earth's crust and widely detected in the environment including the water, air, and land. It is among the most substantial chemical contaminants detected in drinking water worldwide. According to Koki et al. (2018), the era during the increasing global industrialization has led to health consequences, mainly related to exposure to heavy metals in water consumed. The National Research Council (U.S.) (1999) stated that arsenic concentrations are considered low at < 0.29 mg L^{-1}, considered as a medium concentration between the range of 0.3 to 0.59 mg L^{-1}, and considered as a high concentration at > 0.6 mg L^{-1} when exposed to humans. Whereas, the International Agency for Research on Cancer (IARC) graded arsenic as a carcinogen and has affirmed that drinking water contaminated with arsenic will induce cancer in humans.

According to Singh et al. (2011), exposure to arsenic will increase the reactive oxidative species (ROS), DNA damage, and activation of transcription factors in mammalian cells. These changes will lead to several diseases including cancer. Chronic arsenic poisoning mainly is the result of prolonged exposure to drinking water and food contaminated with arsenic. Arsenic (2022) stated that long-term exposure to high arsenic levels can be observed on the skin. The skin changes that can be observed include pigment changes, lesions, and hard patch formation which is also known as hyperkeratosis. These symptoms will appear after approximately 5 years of arsenic exposure and will be the precursor to skin cancer. Arsenic also causes infant mortality during the pregnancy stage and leads to an impact on the child's health. If the utero is exposed to arsenic, the young adult has a high risk of gaining several types of cancers, lung

disease, heart disease, and kidney failure. The cognitive development and intelligence will also be affected by the arsenic exposure (*Arsenic*, 2022).

1.1.3 Microalgae application for arsenic bioremediation

Arsenic can be uptake and metabolized by living aquatic organisms i.e. macrophytes (Singh et al., 2018), bacteria (Takeuchi et al., 2007), and microalgae. Arsenic is metabolized or removed from the environment through accumulation by the microalgae. There were several methods to reduce the arsenic toxicity employed by the microalgae which are metabolization of arsenic and release to the environment, binding to sulfur-containing compounds, or undergoing methylation process to form organic arsenic species with a lower toxicity. *Nostoc* and *Chlorella* are microalgae strains that showed high potential in the accumulation of arsenic. They accumulate 8300 mg kg^{-1} DW (Patel et al., 2021) and 52000 mg kg^{-1} DW (Maeda et al., 1987) of arsenic respectively, multiple times higher compared to aquatic macrophytes and aquatic bacteria.

1.2 Statement of Problem

Natural processes such as the weathering of minerals in hard rocks (Ahmed et al., 2021) and aquifer sediments (Herath et al., 2016) over time release arsenic into water bodies. These processes are exacerbated in mining areas (*Arsenic*, 2022). Arsenic is toxic to humans and animals. To ensure the safety of water for human and animal consumption, arsenic bioremediation to remove its toxicity is significant.

In past studies by Bahar et al., (2013), Karadjova et al. (2008), and Munoz (2014), *Chlorella* sp. was found effective in reducing arsenic toxicity of both the arsenate i.e.: As (V) and arsenite i.e.: As (III). Specifically, *Chlorella* can reduce the toxicity of As (III) through oxidation and form the less toxic As (V). However, different microalgae species contribute to different strategies, efficiencies, and capacities in arsenic bioremediation. At the same time, the growth, adsorption capacity, arsenic speciation, and structural changes will be affected by the arsenic and phosphate concentration exposed to the microalgae. The specific growth rate indicates the adaptation of microalgae to the environment, the adsorption and accumulation of arsenic indicate the bioremediate efficiency of arsenic by the microalgae, while the structural changes indicate the accumulation site of arsenic and other stress occurring on the microalgae. Therefore, this project research question asks, is *Nostoc* strain a more suitable arsenic bioremediation agent compared with the *Chlorella* strain, in terms of the specific growth rate, arsenic adsorption, arsenic accumulation, and arsenic toxicity reduction.

At the same time, studies show that several gene expressions will be regulated when microalgae are exposed to toxic arsenic. A further investigation of the gene expressed in *Nostoc* exposed to arsenic is crucial, as it identifies the pathway corresponding to the accumulation of arsenic by the microalgae. Besides, it was revealed in past studies that the phosphate concentration exposed to the microalgae simultaneously with the arsenic will also affect the uptake mechanism of the arsenic by the microalgae. From here, studies are worthy to not only evaluate

the effectiveness of microalgae in uptake and reducing arsenic toxicity but also to further understand the relationship between genes regulated in the microalgae affected by the arsenic and phosphate concentration. The regulation of genes responsible for the arsenic efflux pump, arsenic redox mechanism, and their relationship with phosphate can be measured to determine the relationship with the arsenic bioremediation processes. For example, upregulation of the genes responsible for As (III) oxidation can be performed under optimal conditions to increase the oxidation rate, thus reducing the arsenic species to As (V) that possess a lesser toxicity to humans and animals.

PCR is an important tool in understanding the expression of targeted genes at the molecular level. The PCR technique can determine the regulation of targeted genes responsible for arsenic bioremediation. Therefore, our second research question asks about the differences in microalgae gene regulation upon long-term arsenic exposure.

In summary, the study's novelty lies in the evaluation of the effectiveness of locally isolated microalgae strains to arsenic bioremediation affected by different phosphate concentrations, and how its genome responds to long-term arsenic and phosphate exposure. Study findings will be useful in the advancing understanding of arsenic bioremediation as well as the proper management and usage of water resources in Malaysia. This is especially important as our current generation is threatened by freshwater insecurity, a cumulative result of water pollution from mining activities in the 1980s, and climate change that increases the frequency of microcystin-releasing microalgae blooms.

Hence, the research question of this project is whether the *Nostoc* MUM003 strain is a more suitable arsenic bioremediation agent compared with the *Chlorella* MUM002 strain, in terms of growth and toxicity?

Therefore, this study was carried out with the following objectives:

a. To investigate the response of selected *Nostoc* strain and *Chlorella* strain under increasing arsenic and phosphate concentration, in terms of microalgae growth, adsorption, accumulation, and excretion of arsenic
b. To identify the expression of targeted arsenic-related gene expression in the *Nostoc* strain that accumulates the highest arsenic concentration

CHAPTER 2

LITERATURE REVIEW

2.1 Freshwater as drinking water

Freshwater is classified as water with less than 0.05% of dissolved salts (*Earth's Fresh Water*, 2023). According to Water Science School (2018), more than 99% of the water on Earth is inoperable by humans and other living organisms. Only 0.3 % of the accessible freshwater is found on the surface of lakes, rivers, and swamps, whereas, more than 68% of the freshwater is found in icecaps and glaciers (Earth's Fresh Water, 2023; Water Science School, 2018). Freshwater ecosystems support the needs of humans and wildlife including approximately 12 % of animals and 40% of fish species (Water Science School, 2018).

Figure 1 shows the distribution of different categories of water on Earth. Ocean stands for the major percentage among the multiple categories of water on Earth, but seawater could not be consumed by humans. Freshwater represents 2.5% of the total water, and only 1.2% of the total freshwater belongs to the surface freshwater which can easily be accessed for daily consumption, in comparison to the groundwater, glaciers and ice caps.

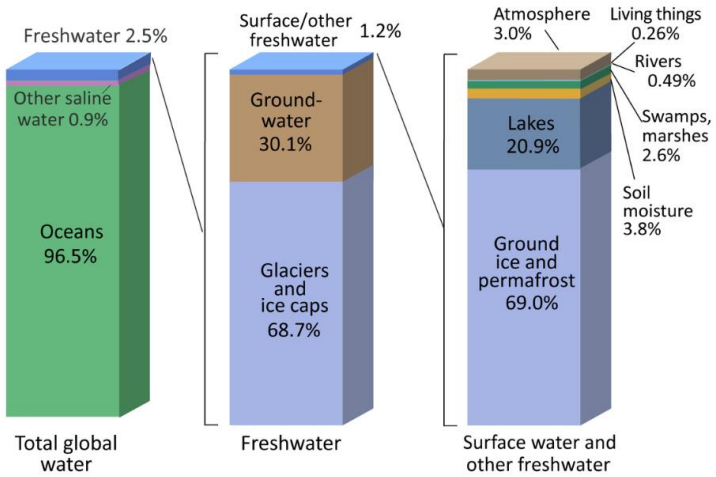

Figure 1. Distributions of different types of water and freshwater. Adapted from USGS Water Science School

2.1.1 Heavy metal arsenic pollution in ex-mining lakes

Arsenic is predominantly detected in the ex-mining waters due to the leakage of impurities from the ores that contain arsenic (Chakraborti et al., 2001; Gemici et al., 2008). As the Mining Acts or environmental protection laws were not fully established before the mining operations, random mining activities led to heavy metal and organic matter contamination in most of the ex-mining ponds (Zuhairi et al., 2009). Due to the heavy pollution with heavy metals, the contaminated ex-mining pools were only used for irrigation or sewage disposals instead of drinking water sources (Orji et al., 2009). Of late, ex-mining lakes in Malaysia are new potential alternative raw water resources (Hani, 2015).

Table 1 shows the arsenic concentration in freshwater lakes reported from past studies. Table 1 shows the arsenic concentration in freshwater lakes reported from past studies. The highest arsenic concentration reported is 66 mg L^{-1} in Bestari Jaya Ex-mining lake. This signifies a concerning situation, given the elevated arsenic concentration could have adverse effects on the health of individuals residing around the lake. Multiple lakes were reported to contain arsenic in Selangor state, followed by the Perak State.

Table 1. List of lakes contaminated with arsenic in Malaysia

Lake	**Arsenic concentration**	**State**	**Reference**
Bau Lake	0.68 mg L^{-1}	Sarawak	Bau Lake Remains Arsenic, n.d.
Jasin Lake	> 0.01 mg L^{-1}	Melaka	Koki et al., 2019
Gunung Lang former mining lake	0.02 mg L^{-1}	Perak	Hashim et al., 2018
Taman Indah former mining lake	0.03 mg L^{-1}		
Kg. Temiang former mining lake	0.03 mg L^{-1}		
Lahat former mining	0.05 mg L^{-1}		
Kg. Engku Hussin former mining lake	0.01 mg L^{-1}		
Bukit Merah Reservoir	12.16 mg kg^{-1}		Abdullah et al., 2020
Sri Serdang Mine Lake	0.0287 to 0.0334 mg L^{-1}	Selangor	Al-Mahdi et al., 2019
Bestari Jaya Ex-mining lake	66 mg L^{-1}		Ashraf et al., 2011
Tasik Kelana Jaya	7.5 ± 0.2 µg L^{-1}		Koki et al., 2019
Tasik Biru	0.53 ± 0.02 µg L^{-1}		
Tasik Saujana Putra	0.67 ± 0.03 µg L^{-1}		

Tasik Putra Perdana	116 ± 2 µg L^{-1}		
Tasik Prima Perdana	42 ± 0.5 µg L^{-1}		
Tasik Titiwangsa	2.13 ± 0.05 µg L^{-1}		
Tasik Taman Jaya	1.13 ± 0.06 µg L^{-1}		
Tasik Perdana	3.8 ± 0.1 µg L^{-1}		
Tasik Shah Alam	3.37 ± 0.2 µg L^{-1}		
Tasik Shah Alam 7	14.4 ± 0.4 µg L^{-1}		
Tasik Putrajaya	7.5 ± 0.3 µg L^{-1}		

2.1.2 Arsenic chemistry and classification

The chemical element of arsenic is represented with the symbol “As” and the atomic number is 33 (Figure 2) in the periodic table. Arsenic is graded as first in the list of poisons by the United States Environmental Protection Agency (EPA). Studies undertaken proved industrial activities including extracting, refining, and burning fossil fuels will leak the arsenic and causes contamination to the soil and water (Wang et al., 2015). Mining is a major source of arsenic leakage to the environment. It releases a considerable amount of arsenic from the arsenopyrite (Gul et al., 2013).

In the natural environment, there are 4 oxidation states of inorganic arsenic. The oxidation states are arsenite (+III), arsenate (+V), arsine (-III), and elemental arsenic (0). These inorganics exist mainly in two oxidative forms i.e. trivalent arsenic, arsenite As (III), and pentavalent arsenic, arsenate As (V) (Yan et al., 2019).

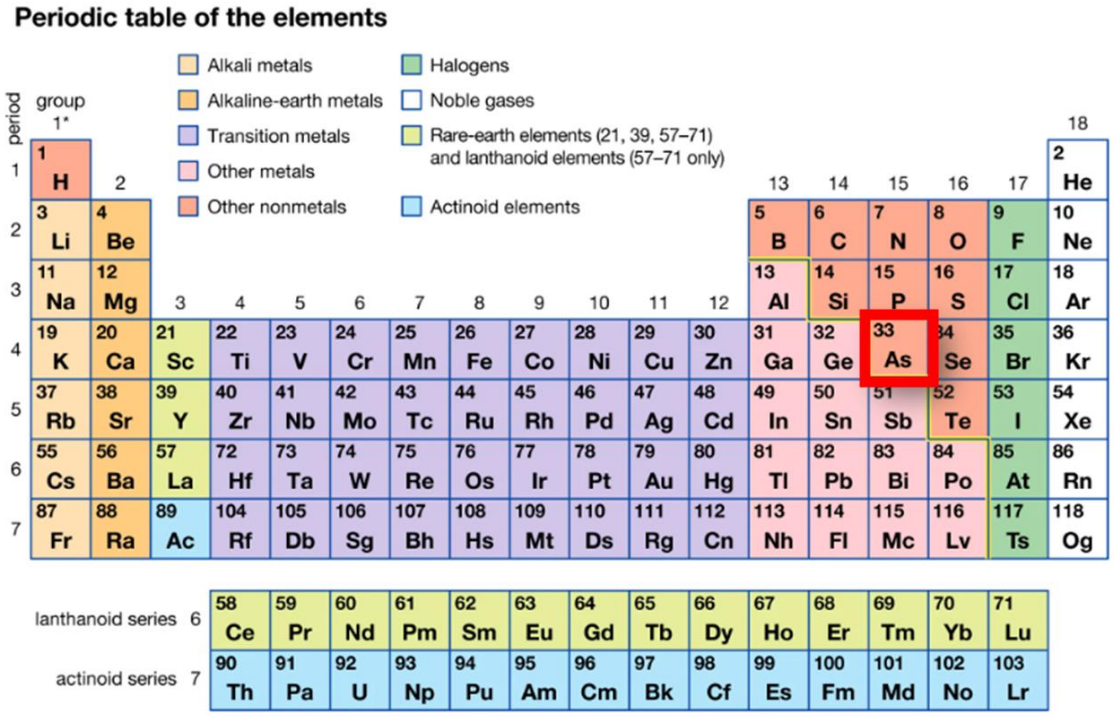

Figure 2. Arsenic is categorized in group 15 and the 4th row of the periodic table

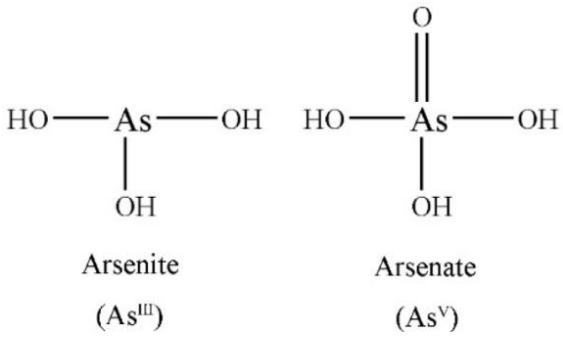

Figure 3. Chemical structure of the As (III) and As (V). Adapted from Shi et al., (2019)

2.1.3 The consequences of arsenic on the humans health

Inorganic arsenic is carcinogen to humans. Humans exposed to high inorganic arsenic concentrations mainly through consuming arsenic-polluted water, utilizing the polluted water to prepare food, watering crops with contaminated water, industrial processes involving arsenic, and consumption of arsenic contaminated food (*Arsenic*, 2022).

Arsenic occurs in either the organic or inorganic form. Inorganic arsenic was mainly found in the water and poses higher toxicity. Whereas, organic arsenic compounds usually in the seafood are less toxic to humans' health (*Arsenic*, 2022). Arsenic poisoning can cause serious health implications in humans, such as kidney, liver, and neurological systems (Table 2). The most characteristic effect of arsenic poisoning is skin lesions and cancer (Arsenic, 2022; Ong et al., 2013; Shanab et al., 2012). Some other symptoms i.e. vomiting, abdominal pain, and diarrhoea were observed as the immediate impact of arsenic poisoning.

The harmful effect of arsenic species on human cells reduces according to the following order i.e. As (III) > As (V) > dimethylarsinic acid DMA (V) > methylarsonic acid MA (V) and trimethylarsine oxide (TMAO) (Miyashita et al., 2015). As (III) binds to the small molecule thiols and the sulfhydryl leads to a higher toxicity compared to As (V). These reactions will inhibit important biochemical processes in organisms (Yan et al., 2019) and reduce the binding to the -SH site of various proteins. As (V) showed a high toxicity due to its function in

substituting phosphate in photophosphorylation and phosphorylation reactions that influence glycolysis and ATP production. However, the products where As (V) substituted phosphate will be unstable compared to the original product and will lead to rapid dissociation. Hence, As (V) exhibited a lower toxicity compared to As (III) (Miyashita et al., 2012).

Table 2. Effects of different arsenic dosages on humans and animals

References	Arsenic species	Arsenic concentration/dosage	Model	Effect
Kapaj et al., 2006	As (III)	0.4 µg L^{-1}	Human	Alter hormone gene transcription
		> 0.5 µg L^{-1}		Bladder cancer
		10 µg L^{-1}		Skin lesions
	Arsenic	50 µg L^{-1}	Child	Effects on memory and intellectual function
National Research Council (U.S.), 1999	Arsenic	200 µg L^{-1}	Human	Bladder cancer
		0.6 mg L^{-1}	Child	Effect on the cardiovascular system
	As (III)	48 mg kg^{-1}	Chicks, golden hamsters, mice	Teratogenic effects
		50 mg L^{-1}	Rabbits and rat	Cardiac output and stroke volume decreased
		160 mg L^{-1}	Rats	Kidney tumour
			Bacteria and mammalian cells	Point mutations, chromosome breakage, chromosomal aberrations, sister chromatid exchange
	Arsenic	Acute intoxication	Human	Abdominal pain, vomit, diarrhoea, muscle pain, flushing of the skin, muscle cramp
		Chronic arsenicism		Dermal lesions, peripheral neuropathy, skin cancer, bladder and lung cancer, peripheral vascular disease, dermal lesions

2.1.4 Aquatic macrophytes and bacteria in arsenic bioremediation

The aquatic macrophytes or plants that accumulate arsenic can be used as biomonitoring and phytoremediator technology to maintain the water quality and prevention in water contamination (Singh et al., 2018). The biomass which is dead macrophytes acts as a simple biosorbent material by absorbing arsenic through the ion exchange mechanism (Miretzky et al., 2006). The concentration of arsenic taken up by the aquatic macrophytes ranged between 1.8 mg As kg^{-1} by *Eichhornia crassipes* (Alvarado et al., 2008) to 1117.65 mg kg^{-1} by *Nakas Marina* (Xing et al., 2013).

Arsenic is harmful to aquatic bacteria. However, several bacteria strains were found to be resistant to the arsenic. This is due to the phosphate-specific transport system found in bacteria does not absorb As (V), or due to the presence of an efflux system in the plasmid. Besides, exposing the bacteria to a higher arsenic concentration can cause the bacteria to acquire arsenic resistance. This is supported by arsenic-resistant bacteria that can be isolated in an arsenic-rich environment. The concentration of arsenic absorbed detected in live cells is lesser than in the heat-killed cells (Takeuchi et al., 2007). Aquatic bacteria can uptake arsenic concentrations ranging from 0.02 µg mg^{-1} by *Tetrahymena thermophilia* (Yin et al., 2011) to 834 mg kg^{-1} by *Marinomonas communis* (Takeuchi et al., 2007).

2.2 Microalgae

Algae are plant-like photosynthetic organisms found in the sea, freshwater, and land. They have chlorophyll and produce their food through photosynthesis. Algae have no true roots, stems, leaves, or vascular tissue (Randrianarison & Ashraf, 2017). Microalgae are diverse groups of microorganisms comprising the eukaryotic photoautotrophic protists and prokaryotic cyanobacteria (Singh & Saxena, 2015). They are mainly found in both seawater and freshwater. There are more than 25,000 species of microalgae determined (Vale et al., 2020), and facilitate half of the photosynthetic activity worldwide.

Microalgae are autotrophic organisms comprising prokaryotic i.e. Cyanophyta or cyanobacteria, or eukaryotic i.e. Chlorophyta such as green microalgae, red microalgae, dinoflagellates, and diatom cells. The diameter of microalgae cells varies from 1 µm to 2 mm (Yaakob et al., 2021). The ideal temperature that supports microalgae growth ranges between 20 ^{o}C to 30 ^{o}C, but reports also mentioned that some strains can grow at temperature conditions beyond the range (Miazek et al., 2015). Microalgae often act as the source of the food chain. They can be cultivated easily in ponds by supplementing carbon dioxide as a carbon source and providing sufficient light energy for their growth (Singh & Saxena, 2015). Most of the microalgae are aerobic photoautotrophs. The basic needs to maintain their growth were water, carbon dioxide, inorganic compounds, and light. Photosynthesis is important for energy metabolism, but some cyanobacteria species can sustain for prolonged periods in total absence of light (Mur et al., 1999). At the lab scale, microalgae can be grown in a medium with adequate nutrients, optimal temperature, and optimal light intensity.

2.2.1 Cyanophyceae, *Nostoc*

Nostoc is the blue-green algae, cyanobacteria, grouped under the Order Nostocales. They are multicellular aerobic photoautotrophs comprising the filamentous organization (Spencer et al., 2011). *Nostoc* exhibits different shapes e.g. gelatinous, amorphous, spherical, filamentous, or forming flat gelatinous colonies, and cells are cylindrical, barrel-shaped up to spherical forms according to their life cycle. The vegetative cells of *Nostoc* are about 4-6 µm long and 4-5 µm wide. *Nostoc* species have an optimal growth rate of 227 µM m^{-2} s^{-1} (Spencer et al., 2011) when grown under 40 µmol photon m^{-2} s^{-1} light intensity (Yu et al., 2009), an optimal temperature of 25 ^{o}C (Møller et al., 2014), and optimal pH at pH 9 (Fernandez Valiente & Leganes, 1990). The cell division of *Nostoc* happens non-uniformly along the filaments, the end of the filament prevails over other parts with faster cell division to provide more space for the inner cells of the trichrome. The sheath of *Nostoc* plays an important role in protecting cells from environmental stresses. To survive under adverse environmental conditions, *Nostocales* can differentiate into resting cells called akinetes during unfavourable conditions. During the development stage, when the sheath is not formed, the cells are susceptible to environmental changes. However, after the sheath was formed, the cells were resistant to severe environmental changes. It seems that the thicker the sheath the higher the survival probability.

Following is the outline of the genus *Nostoc* taxonomy adapted from ITIS - Report: Nostoc Commune, 2023:

Phylum: Cyanobacteria Stanier ex Cavalier-Smith, 2002

Class: Cyanophyceae, Schaffner, 1909

Order: Nostocales Cavalier-Smith, 2002

Family: Nostocaceae Eichler, 1886

Genus: *Nostoc* Vaucher ex Bornet & Flahault, 1886

Past studies have shown that *Nostoc* was able to methylate arsenite As (III) to DMAs (V) and TMA (O), and form arsenosugar phospholipids (Xue et al., 2017). Owing to its size ranging from 10-50 µm, *Nostoc* is one of the few species that has a large size and thus easily harvested using low energy-intensive means i.e. a filtration sieve. This characteristic omits the need for centrifugation which is energy-intensive and therefore advantageously confers an upper hand to environmental applications e.g. bioremediation. However, *Nostoc* is a known producer of cyclic toxins or cyclic heptapeptides called microcystin (Mcy) (Genuário et al., 2010; Gong, Chou, et al., 2009; Ramanan et al., 2000). Microcystin is recognized as one of the most dangerous groups among several cyanotoxin species as they are detrimental to animals' and humans' health (Bártová et al., 2011; Song et al., 1998) at the concentration of 65.4 µg kg^{-1} and 7 mg kg^{-1} (Yoshida et al., 1998). That said, there is a need to evaluate the feasibility of using *Nostoc* species as a bioremediation agent.

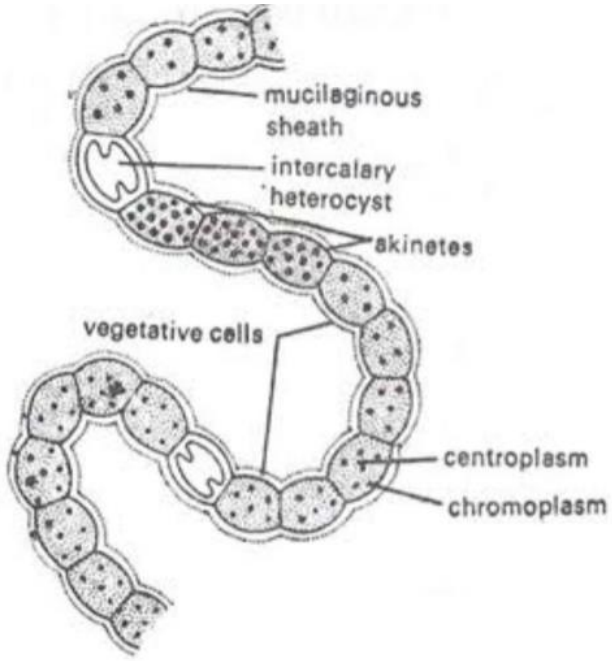

Figure 4. *Nostoc* cell structure. Adapted from: (Alchetron, 2022)

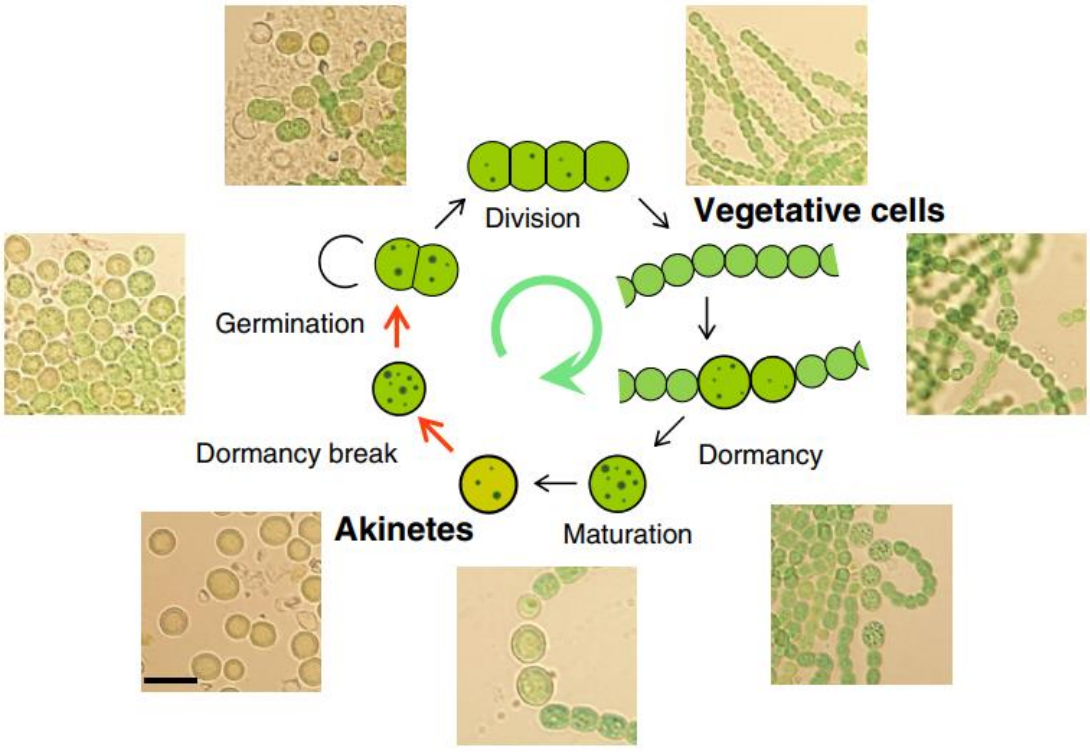

Figure 5. Different growth stages of *Nostoc*. Adapted from Kimura et al., (2020)

2.2.2 Chlorophyceae, *Chlorella*

Chlorella belongs to the green eukaryotic microalgae (Xue et al., 2017), grouped under the Order Chlorellales. It was initially identified in 1890 as the first microalgae consist a well-defined nucleus (Chlorella Vulgaris), n.d.). It illustrated a spherical microscopic cell with a diameter of approximately 2 µm and has various similar structural elements to plants (Safi et al., 2014). It is a microscopic unicellular microalga that can be found in freshwater. *Chlorella* has a biomass growth rate of 2 to 5 g L^{-1} d^{-1} (Safi et al., 2014). The growth conditions that are ideal for *Chlorella* are at the temperature of 25 ^{o}C (Allaguvatova et al., 2019), and light intensity at 110 µM m^{-2} s^{-1} (Khalili et al., 2015).

Following is the outline of the genus *Chlorella* taxonomy adapted from (ITIS - Report, 2023; World Register of Marine Species; LPSN):

Phylum: Chlorophyta, Pascher, 1914

Class: Trebouxiophyceae, Friedl, 1995

Order: Chlorellales Bold & M.J.Wynne, 1978

Family: Chlorellaceae Brunnthaler, 1913

Past studies have shown that *Chlorella* is a known accumulator of approximately 52000 mg kg^{-1} of arsenic (Higashi et al., 1985). Although their small size is not an ideal situation for environmental bioremediation applications, their short growth rate may increase their arsenic uptake efficiency and remediation through an increase in biomass. *Chlorella* was also found effective in reducing the toxic effect for both As (III) and As (V) (Bahar et al., 2013; Karadjova et al., 2008; Munoz, 2014). Specifically, *Chlorella* was found to oxidize As (III) to form As (V), an arsenic species with a lesser toxicity.

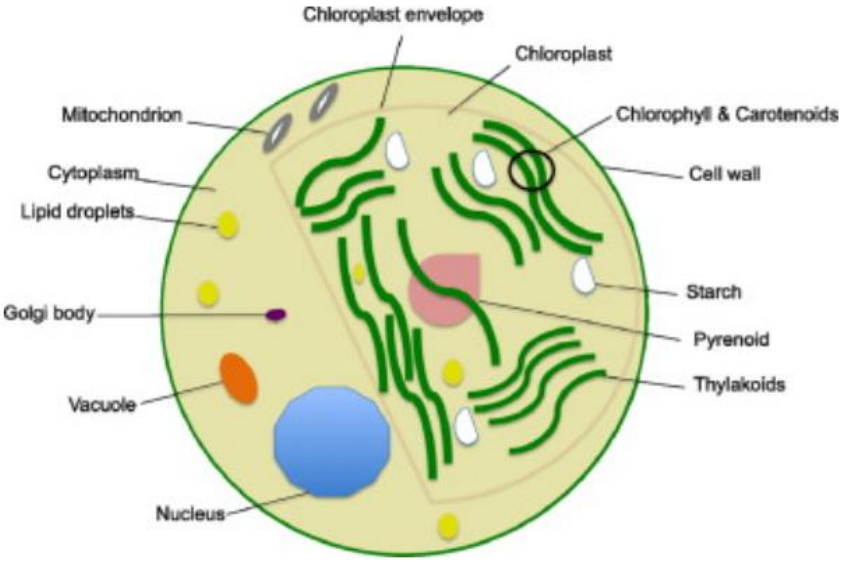

Figure 6. *Chlorella* cell structure. Adopted from Safi et al., (2014)

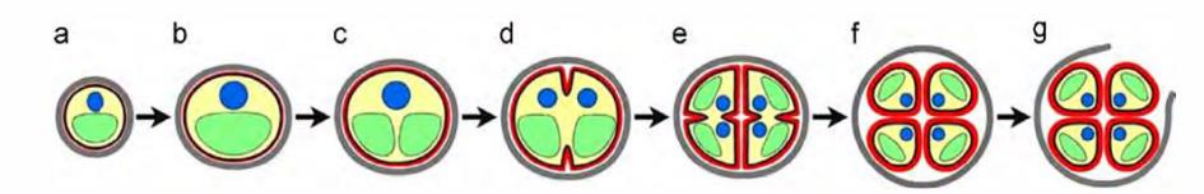

Figure 7. Different growth stages of *Chlorella*. Adopted from Safi et al., (2014)

2.2.3 Microalgae's potential in arsenic bioremediation

Microalgae are important for freshwater aquatic environments. They have a huge potential in the bioremediation of water contaminated with arsenic through absorption or transforming the inorganic arsenic species to lesser toxic species. Arsenic can be absorbed and metabolized by microalgae. Ramanan et al. (2000), stated that As (V) uptake by the cyanobacterial cells through the phosphate transport system, whereas As (III) uptake by the cells through diffusion. As (V) located inside of the cell will be reduced to As (III) and released from the cell. Whereas, As (III) entering the cell will react with cysteine-rich compounds to reduce its toxicity. Besides As (V) and As (III), other inorganic arsenic will be methylated to the methyl group of *S*-adenosylmethionine (SAM) and undergo redox reactions, which form organoarsenicals as the product (Figure 8). The main difference between cyanobacteria with other algae is cyanobacteria lack of organelles such as vacuoles to isolate As (III)-thiol conjugates (Ramanan et al., 2000).

There are several methods utilised for the reduction of arsenic toxicity by microalgae, such as oxidation or reduction, and methylation (Rodriguez et al., 2015; Xiao et al., 2022). Among different methods, the major detoxification process which takes place in the microalgae is the redox reaction between As (III) and As (V), further released from cells (Miyashita et al., 2012). As (III) possesses a higher toxicity compared to As (V) in the human cell. Many As (III) oxidation processes reported were facilitated by As (III) oxidase, which involved the periplasmic protein associated outside of the inner cell membrane. Hence, the oxidation of As (III) to form As (V) is likely the surface oxidation process, which often occurs in the periplasm or outer membrane (Zhang et al., 2014). Whereas, As (V) will be located in the vacuole (Yin et al., 2011). However, studies also show that As (III) will be uptake into cells through the energy-dependent process, mainly via aquaglyceroporins (Zhang et al., 2014), and binds to dithiols which form arsenothiols that alter the protein function and generate oxidative

stress ROS (Sánchez-Riego et al., 2014). The oxidative stress such as superoxide radicals and hydrogen peroxide will damage the membrane lipids and increase lipid peroxidation.

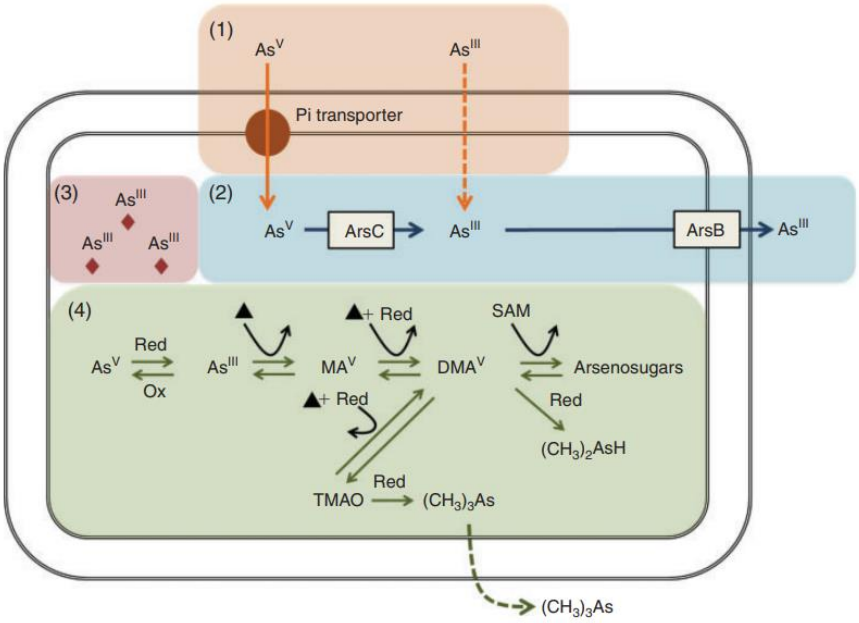

Figure 8. Possible metabolic process of arsenic in cyanobacteria. Adapted from Ramanan et al, (2000)

Microalgae is also a potential arsenic bioremediation agent. It exhibits resilience to arsenic in environmental settings and actively absorbs arsenic to facilitate its removal from the surroundings. Table 3 shows the microalgae species capable of arsenic uptake along with the corresponding uptake concentrations. All microalgae strains can uptake arsenic concentrations higher than detected in the environment as stated in Table 1.

Table 3. Arsenic concentration uptake by microalgae

Reference	**Microalgae species**	**Arsenic concentration uptake**
Ferrari et al., 2013	*Nostoc minutum*	37.4 ± 2.98 mg kg^{-1}
Zhu et al., 2020	*Leptolyngbya boryana*	830 mg kg^{-1}
Maeda et al., 1988	*Chlorella vulgaris*	5200 mg kg^{-1} DW
Sanders and Windom, 1980	*Nostoc* PCC 7120	1523 mg kg^{-1}
Maeda et al., 1987	*Nostoc* sp.	3400 mg kg^{-1}
Leong and Chang, 2020	*Chlorella vulgaris*	3890 mg kg^{-1}
Foster et al., 2008	*Dunaliella teriolecta*	6.1 mg kg^{-1}
	Phaeodactylum tricornutum	1.31 mg kg^{-1}
Suhendrayatna et al., 1997)	*Chlorella vulgaris*	1060 mg kg^{-1} DW
Wang et al., 2013	*Scenedemus obliquus*	2152.2 mg kg^{-1}
Higashi et al., 1985	*Chlorella vulgaris*	52000 mg kg^{-1} DW
Wang et al., 2013	*Microcystis aeruginosa*	260 mg kg^{-1} DW
Maeda et al., 1988	*Phormidium* sp.	2800 mg kg^{-1} DW
Patel et al., 2021	*Nostoc muscorum*	8300 mg As kg^{-1} DW

2.3 Cultivation Parameters of Microalgae

Microalgae requires specific cultivation parameters to sustain its growth. The parameters that are important to maintain the growth include the temperature, light intensity, and nutrients

2.3.1 Temperature Affects the Growth of Microalgae

The ideal temperature required for the growth of microalgae ranges from 15 to 30 ^{o}C (Ahmad et al., 2020). Temperature exceeding this range will lead to cell damage (Ahmad et al., 2020) and affect microalgae growth. Microalgae demonstrated higher biomass productivity and removed higher nutrient content at 25 ^{o}C for *Chlorella*, *Microcystis*, and *Synechocystis* (Gonçalves et al., 2016). The ATCC stated that the optimal growth temperature of *Chlorella* ranged between 20 to 25 ^{o}C, while the optimal growth temperature of *Nostoc* is 26 ^{o}C. Whereas, cyanobacteria can achieve a growth rate of 0.14 doubling per day under 20 ^{o}C, and the maximum growth rate is achieved when the temperatures are above 25 ^{o}C (Mur et al., 1999). Whereas, Li et al. (2014) stated that cells can grow at temperature ranges from 20 ^{o}C to 39 ^{o}C and the most optimal temperature is 32^{o}C.

2.3.2 Light Intensity Affects the Growth of Microalgae

Light is the primary source for the energy production in cyanobacteria (Li et al., 2014). Cyanobacteria consist of chlorophyll *a* pigment to harvest light for the photosynthesis reactions. They do consist of other pigments such as phycobiliproteins that harvest green, yellow, and orange light, falling within the spectrum of 500 to 650 nm. The phycobiliproteins and chlorophyll *a* harvest light efficiently and allow the cyanobacteria to maintain its growth under green light environment (Mur et al., 1999). Cyanobacteria were also responsive to light intensity exposed for prolonged periods. The growth of *Planktothrix agardhii* was inhibited when prolonged exposure to light intensities above 180 µE $m^{-2}s^{-1}$. Exposure to light above 320

μE $m^{-2}s^{-1}$ for a long term is mortal for many cyanobacteria species (Mur et al., 1999). Cyanobacteria can maintain its cell function and structure with low energy consumed. When the light intensity is low, cyanobacteria possess a significantly higher growth rate compared to other phytoplankton organisms which also allows them to compete and grow in deep environments or waters with high turbidity (Mur, Skulberg and Utkilen, 1999)

Chlorella showed an optimal growth rate supplied with light intensity ranging from 500 to 5000 lux (Schor et al., 2020). According to Gonçalves et al. (2016), a higher light intensity will increase the microalgae growth up to a limit. *Chlorella* growth under 7500 lux showed lower growth compared to 5000 lux (Schor et al., 2020) indicating that 7500 lux is too high for *Chlorella* growth. This can be explained when photo-inhibition occurs under increasing light intensity up to a saturation point, whereas, the microalgae growth reduces under lower light intensity (Gonçalves et al., 2016). According to ATCC, *Nostoc* has optimal growth under light intensity ranging from 2000 to 3000 lux.

2.3.3 Phosphate

Microalgae showed sustainable phosphorus storage capacity. They store sufficient phosphorus concentrations to undergo 2 to 4 cycles of cell division, corresponding to approximately 4 to 32-fold biomass increase (Mur et al., 1999). According to Berg and Sutula (2015), cyanobacteria have cellular N:P ratios above 25 which is higher compared with other phytoplankton. As the cyanobacteria have 2 light-harvesting complexes, they require a higher protein association with the light-harvesting pigment compared to the phytoplankton (Mur et al., 1999). This requirement of protein which is peripheral phycobiliproteins increased the N:P ratios of cyanobacteria cells (Mur et al., 1999). Hence, it may be stated that the cyanobacteria uptake nutrients dictated by the macromolecule composition of their tissue, but

does not align with the concentration supplied in water. The N:P ratio can be adjusted within a certain limit to allow the continuous growth of cyanobacteria under changing environments (Mur et al., 1999).

2.3.3.1 Phosphate influences arsenic uptake by microalgae

The arsenic uptake by microalgae, *Synechocystis* is influenced by the phosphate (Zhang et al., 2014). The microalgae uptake As (V) into its cells by two phosphate transporters that are Pst, the protein-specific transporter, and Pit, the protein-inorganic transport system. As the structure of both phosphate and As (V) are similar, high phosphate concentration conditions will lead to competitive binding to the active site of ArsC and the phosphate transport system. This suppresses the As (V) uptake (Zhang et al., 2014) and leads to the failure of As (V) to incorporate into cells (Ferrari et al., 2013). The rate of As (III) oxidizes to As (V) elevated under high phosphate levels (Miyashita et al., 2015), causes the increase of As (V) more rapidly under phosphate-rich conditions over time compared with phosphate-limited conditions (Zhang et al., 2014).

Under low phosphate conditions, microalgae can uptake a higher As (V) concentration compared to phosphate-supplied conditions. In this situation, the extracellular As (III) will oxidize to As (V), then be uptake by microalgae cells to perform arsenic metabolism intracellularly. The total concentration of arsenic will then reduce, where the reduction is 4 times higher compared to phosphate-rich conditions. Hence, total arsenic or As (V) accumulation by cells, arsenic toxicity, and the detoxification system are said to be influenced by the concentration of phosphate (Zhang et al., 2014). There is no clear explanation of the function of phosphate affecting As (III) uptake or metabolism in microalgae.

2.4 DNA and RNA

Nucleic acids, deoxyribonucleic acid (DNA) and ribonucleic acid (RNA) poses the genetic information (Minchin & Lodge, 2019) of an organism which is read in cells to maintain the cellular function.

DNA was discovered in 1860 by a Swiss biochemist, Friedrich Miescher (Minchin & Lodge, 2019). It is a polymer formed of nucleotides. Nucleotides comprise a 5-carbon sugar, deoxyribose, a nitrogenous base, and phosphate groups. The well-known structure of the DNA is in a double helix. The double helix DNA or double-stranded DNA (dsDNA) has two strains bound together by non-covalent bonds (BYJUs, n.d.). It encodes the instruction manual for life and synthesizes nucleotide sequences composed of nucleobase i.e. adenine (A), thymine (T), guanine (G), and cytosine (C). The nucleobase works in pairs where A pairs with T and G pairs with C. The stability of the dsDNA depends on the A-T and G-C ratios. According to (*Genome*, n.d.), the whole set of DNA instructions in the cells are genome. Gene is a specific segment of DNA that regulates the cell function (XX). Besides dsDNA, some viruses have single-stranded DNA (ssDNA). The ssDNA is a single linear strand of nucleic acid sequence (BYJUs, n.d.). As they do not have covalent bonds, they are less stable compared to dsDNA.

RNA is a molecule present in most of the living organisms and viruses (Wang & Farhana, 2023). Similar to DNA, it is formed by nucleotides, which are ribose sugars attached to nitrogenous bases and phosphate groups. RNA contains 4 nucleobases i.e. adenine (A), guanine (G), cytosine (C), and uracil (U). As RNA poses only a single strain, it is more liable compared to DNA (Minchin & Lodge, 2019). The main function of RNA is to synthesise protein. There are 3 main types of RNA involved in protein synthesis i.e. messenger RNA (mRNA), transfer RNA (tRNA), and ribosomal RNA (rRNA). The mRNA contains the genetic blueprint transcribed from the DNA and tRNA translates the mRNA into protein. Whereas, rRNA forms the ribosomes which are essential in protein synthesis (D. Wang & Farhana,

2023). Similar to DNA, RNA poses of double-stranded RNA (dsRNA) presence in the virus or in the host cells during viral replication (Chen & Hur, 2021). It triggers the antiviral and inflammatory immune responses of the host cell. The main difference between dsDNA, ssDNA, dsRNA, and ssRNA is that RNA consists of the uracil (U) base, whereas DNA consists of the thymine (T) base.

2.4.1 Gene expression analysis

Gene expression is dynamic (Scitable, n.d.). It is the phenotypic manifestation of genes by the transcription and translation of genetic information. Gene expression analysis determines the pattern of the gene expressed at the level of genetic transcription under specific circumstances. When genes of an organism are expressed, the sequence on the DNA is transcribed by the mRNA. The mRNA will move to the cytoplasm from the nucleus to synthesize the protein through the translation process (*Gene Expression*, n.d.). The same gene may act differently depending on the conditions (Scitable, n.d.).

The are multiple methods to study the gene expression i.e. Northern blot analysis, Polymerase Chain Reaction (PCR) analysis, real-time PCR (RT-PCR) analysis, microarrays, and RNA sequencing (Scitable, n.d.). PCR is a technique that amplifies a specific or targeted region of the DNA to obtain multiple copies in a few hours, whereas RT-PCR is a similar method that allows the real-time detection of gene expression. To perform the RT-PCR method, a pair of oligonucleotides primers, deoxynucleotide triphosphate (dNTPs), a reaction buffer, a thermostable DNA polymerase, and fluorochrome for fluorescence were added with a specific concentration. The mixture was incubated under the designed temperature for a specific period in a specific instrument with cameras that were able to detect fluorescence. The PCR running condition poses 3 stages, which are denaturation hybridization of primers, and elongation or

polymerization (Segundo-Val & Sanz-Lozano, 2016). Microarray is another technique based on the complementarity between nucleic acid strains that allow the detection of the sequence. There are 2 types of microarrays i.e. expression microarrays, where specific RNA sequences are detected, and genotyping microarrays for detecting specific DNA sequences. The comparison between the results of both methods explained the different transcriptomic responses of the organisms under different conditions (Segundo-Val & Sanz-Lozano, 2016).

CHAPTER 3

GENERAL METHODOLOGY

3.1 Apparatus sterilization technique

All apparatus required for microalgae cultivation i.e. Scott bottles, glass flasks, etc. were soaked in a nitric acid with 10% concentration for 12 hours. After soaking for 12 hours, all apparatus were rinsed with Milli-Q water, dried at 60^{o}C overnight, and sterilized before use. The cultivation medium i.e. BG-11 medium and consumables i.e. micropipette tips required for the cultivation of microalgae were autoclaved for a minimum of 30 minutes at 121^{o}C before the experiment. Analytical grade chemicals and ultrapure Milli-Q water were used for the preparation of stock solutions and mediums (Gong et al., 2011; Gong, Song, et al., 2009).

3.2 Isolation, Purification and Cultivation of *Nostoc* MUM003 and *Chlorella* MUM002 strains

Both the *Nostoc* MUM003 strain and *Chlorella* MUM002 strain were sampled from the freshwater lake in Peninsular Malaysia. The strains were cultivated and maintained in the Microalgae Research Lab, Monash University Malaysia. The microalgae strains collected were pelleted down through centrifugation at 3500 rpm for 5 minutes and the supernatants were discarded. The pellets were platted on a fresh BG-11 agar and incubated at 2500 lux and 25^{o}C until single colonies were clearly observed. The microalgae strains were viewed under a compound microscope and DNA sequencing have been performed to identify the microalgae species. A single colony of the microalgae strains were cultivated in a fresh BG-11 medium and retained as an axenic culture (Minhas et al., 2020).

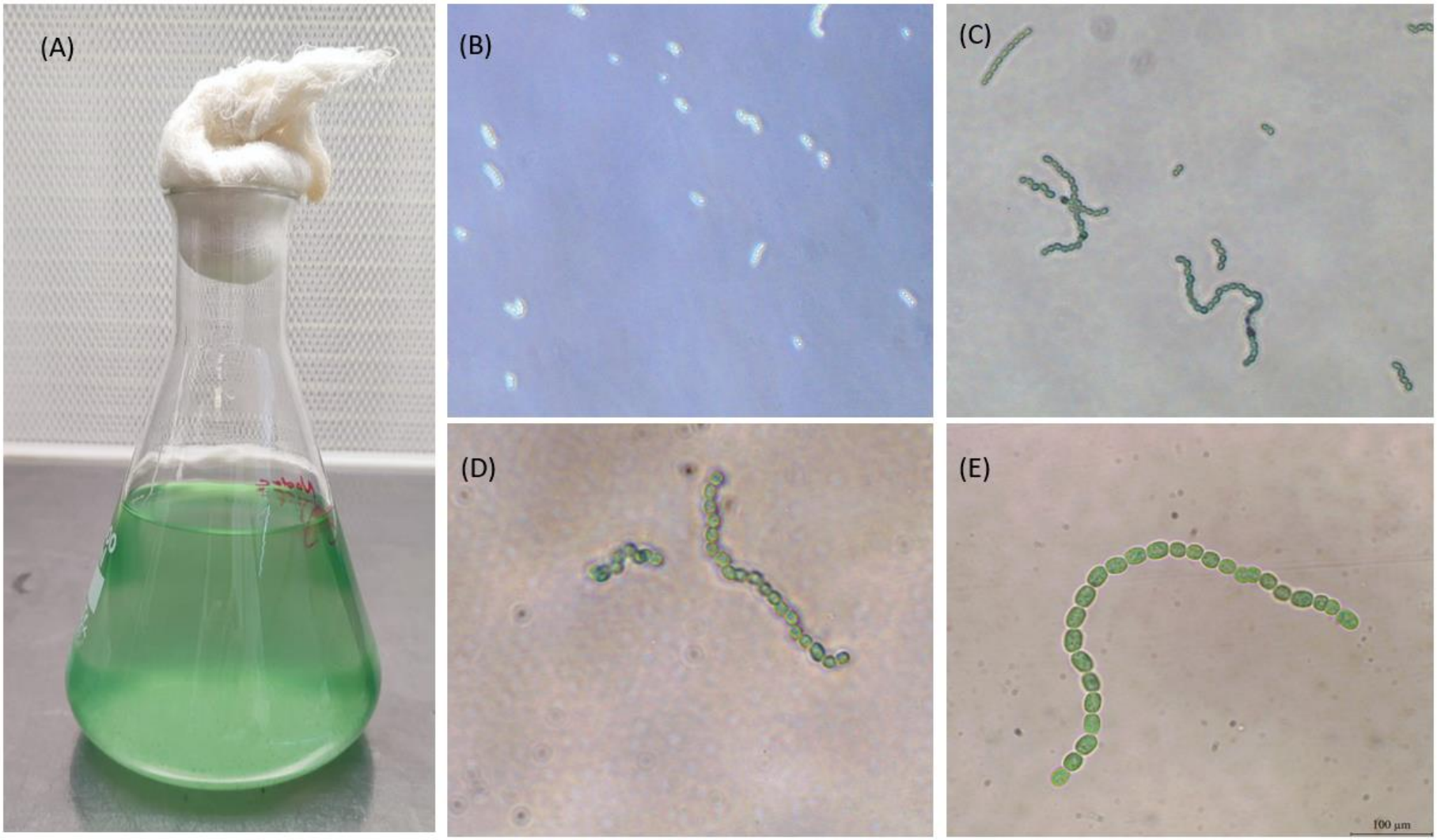

Figure 7. (A) *Nostoc* cells cultivated in BG-11 medium, (B) *Nostoc* cells viewed under 10 X magnification (C) *Nostoc* cells viewed under 20 X (D) *Nostoc* cells viewed under 40 X magnification (E) *Nostoc* cells viewed under 100 X magnification will oil immersion

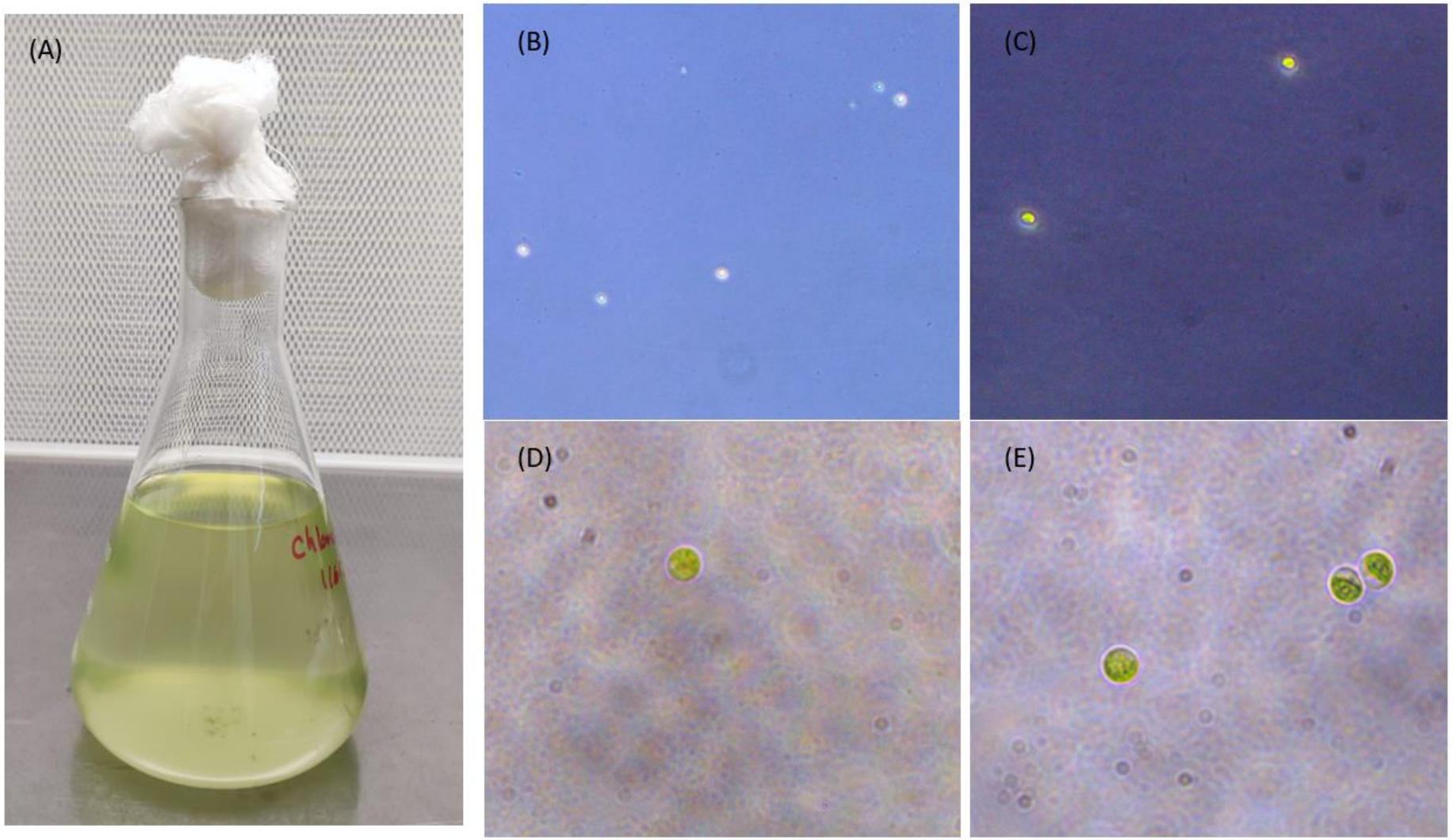

Figure 9. (A) *Chlorella* cells cultivated in BG-11 medium, (B) *Chlorella* cells viewed under 10 X magnification (C) *Chlorella* cells viewed under 20 X (D) *Chlorella* cells viewed under 40 X magnification (E) *Chlorella* cells viewed under 100 X magnification will oil immersion

3.3 Algae Maintenance

Microalgae strains were maintained in BG-11 medium and incubated with 2500 lux for 16 hours at 25 ^{o}C. The purity of microalgae strains was checked periodically under a compound microscope and sub-cultures were platted on BG-11 agar to ensure there was no contamination (Parvin et al., 2007).

3.4 Composition of microalgae cultivation medium (BG-11)

BG-11 medium was selected for the cultivation of both microalgae strains. The composition of the medium was referred to as the Culture Collection of Algae & Protozoa (CCAP, 2019) and the chemicals required for the BG-11 medium preparation were stated in Table 4. To prepare the BG-11 agar plate, 15 g of bacteriological agar was added into 1 L of BG-11 medium. All agars and mediums were prepared freshly, sterilized through autoclave for at least 15 minutes at 121 ^{o}C for 15 minutes at 15 psi and cool down prior to cultivation.

Table 4. Composition of BG-11 medium recommended by CCAP

Chemical	**Amount (mg L^{-1})**
Sodium Nitrate	1500
Dipotassium Hydrogen Phosphate	40
Magnesium Sulphate	75
Calcium Chloride	36
Citric Acid	6
Ammonium Ferric Citrate Green	6
Disodium salt ($EDTANa_2$)	0.1
Sodium Carbonate	20
Boric Acid	2.86
Manganese (II) Chloride	1.81
Zinc Sulphate	0.22
Sodium Molybdate	0.39
Copper Sulphate	0.08
Cobalt (II) nitrate	0.05

CHAPTER 4

EFFECTS OF ARSENIC SPECIES AND CONCENTRATIONS ON THE GROWTH AND PHYSIOLOGICAL RESPONSE OF *Nostoc* NIES 2111 MUM003 AND *Chlorella sorokiniana* MUM002 STRAINS

4.1 Introduction

Arsenic is a toxic heavy metal found in nature. Humans' activities i.e. extracting, melting, and burning of fossil fuels release arsenic into the environment. Microalgae can accumulate arsenic more efficiently compared to other organisms (García-Salgado et al., 2012; Maeda et al., 1987).

Arsenic exists in different forms, known as species. The predominant species of arsenic that exists in water is As (V) as is thermodynamically more stable compared to other arsenic species. As (V) compete with phosphate in enzymatic reactions which will disrupt the phosphorylation and oxidative phosphorylation which interrupts cellular metabolism (Wang et al., 2015). When As (V) enters the cells, it enhances the detoxification mechanism i.e. reduction of As (V), complexation of As (III) to thiol compounds, methylation of arsenic, and excretion out from the cells. The activation of the detoxification mechanism causes increasing stress in the microalgae cells further leading to oxidative stress and inhibiting the division of cells (Levy et al., 2005). Whereas, As (III) entering the cells blocks the sulfhydryl (-SH) groups, causing interruption of cellular proteins i.e. pyruvate dehydrogenase and 2-oxoglutarate dehydrogenase (Lloyd & Oremland, 2006). The interruption produces reactive oxygen species (ROS) which leads to cell membrane degradation and cell death. The detoxification of arsenic in microalgae is performed by adsorbing the arsenic on the cell surface, metabolising the As (III) through the oxidation reaction or reducing As (V) to As (III),

binding the arsenic to the thiol group, and methylate the toxic arsenic species to a lesser toxic species.

Phosphorus is an important element required for growth, lipid synthesis, yield in fatty acid, and metabolic processes i.e. transfer of energy, cellular signalling, and photosynthesis in the microalgae (Huang et al., 2014). It also involves the synthesis of components required by the cells i.e. phospholipids, the construction of membranes, and the storage and replication of genetic information including nucleic acid and ATP. It constitutes below 1 % of the total algal biomass and only 0.03-0.06% of phosphorus is required in the medium to maintain the growth of algae (Huang et al., 2014; Liu et al., 2021; Yaakob et al., 2021). The ideal phosphate concentration required for microalgae is ranged within 0.001g L^{-1} to 0.179 g L^{-1} (Yaakob et al., 2021). Phosphate concentration affects the uptake of arsenic by the microalgae especially when there is a low nutrient condition (Xue et al., 2017). More arsenic will be uptake into the cells under a low nutrient condition compared to a high nutrient condition (Schmidt et al., 2016). Under the phosphate-rich condition, microalgae will uptake lower As (V), which further reduces the As (V) toxicity over a prolonged period. The As (V) competes with the phosphate for uptake by the algae cells (Sanders, 1979). This is due to both the phosphate and As (V) shares the similar chemical structure. The similarity in structure suggests that both elements will show a competitive behaviour for the phosphate uptake system (Ferrari et al., 2013) to enter the cells. As per our current knowledge, there is no report on phosphate affecting the uptake or metabolism of As (III) in microalgae cells.

The removal of arsenic from the freshwater system is crucial, emphasizing the significance of employing microalgae as an arsenic bioremediation agent. This chapter aims to determine the effect of arsenic and phosphate on microalgae growth, to analyse the arsenic uptake in microalgae, and to characterize the ultrastructural surface of microalgae exposed to arsenic.

4.2 Methodology

The working strains for both *Nostoc* and *Chlorella* were collected from the stock culture and cultivated for 14 days to reach the exponential phase. Both strains at the exponential phase were collected and pre-cultivation was performed in BG-11 medium without phosphate for 5 days, to eliminate possible phosphate retained in the cells.

4.2.1 Arsenic and phosphate treatments to microalgae strain

There were 3 independent variables tested which are 3 arsenic concentrations (0.01 mg L^{-1}, 0.10 mg L^{-1}, and 1.00 mg L^{-1}), 2 arsenic species (As (III) and As (V), and 2 phosphate concentrations (0.24 mg L^{-1} and 0.00 mg L^{-1}). Both *Nostoc* and *Chlorella* strains were treated with 3 different arsenic concentrations at 0.01 mg L^{-1}, 0.10 mg L^{-1}, and 1.00 mg L^{-1} of 2 different arsenic species As (III) and As (V). The working concentrations of both As (III) and As (V) were prepared from 10000 mg L^{-1} of the stock solutions (Danish et al., 2013). All treatments were performed using a 2 L Erlenmeyer flask containing 2 L BG-11 medium in 4 different batches. Two sets of the experiment were performed with 0.24 mg L^{-1} phosphate and 2 sets without phosphate. All arsenic mixtures and concentrations were prepared as in Table 5.

Table 5. Arsenic and phosphate concentrations

Treatment	**Arsenic concentrations (mg L^{-1})**	**Phosphate concentrations (mg L^{-1})**
A	0.01 As (III)	0 or 0.24
B	0.10 As (III)	
C	1.00 As (III)	
D	0.01 As (V)	
E	0.10 As (V)	
F	1.00 As (V)	
G	0.01 As (III) + 1.00 As (V)	
H	0.10 As (III) + 0.10 As (V)	
I	1.00 As (III) + 0.01 As (V)	
Control	0	

4.2.2 Microalgae sampling

The typical growth rate of *Nostoc* is 30 days (Spencer et al., 2011) and Chlorella is 7 days (Gitau et al., 2021). Therefore, the sampling frequency for both microalgae strains was decided at 3-day intervals for *Nostoc* and 24-hour intervals for *Chlorella*. Approximately 15 mL of microalgae cultures were collected to identify the growth and bioaccumulation of arsenic in microalgae.

4.2.3 Cellular biomass measurement

A 1.2 µm nylon filter membrane was used for the biomass dry weight measurement of both microalgae cultures. The nylon filter was pre-washed with distilled water to eliminate dust and air bubbles on the filter membrane. The filter membranes were dried at 60 ^{o}C for 24 hours. Filter membranes were then transferred into a desiccator to cool down and the weight of the filter papers was measured at least 3 times until a constant mass was obtained. A 10 ml of culture was collected and filtered using the pre-washed filter membrane. The filter membrane was then dried and re-weight unto a constant mass was obtained (Ratha et al., 2016).

4.2.4 Cellular optical density measurement

Approximately 5 ml of samples are collected every 3-day intervals for *Nostoc* culture, and samples are collected every day for *Chlorella* cultures. The optical density of cyanobacteria i.e. *Nostoc* and green microalgae i.e. *Chlorella* were measured using the UV-vis spectrophotometer 365 (Agilent Technology, California) at the optical densities of 625 nm (Degen et al., 2001) and 680 nm (Hadiyanto et al., 2014) respectively. Distilled water was used as a blank for calibration of the instrument.

4.2.5 Microalgae growth rate determination

To identify the growth rate of both microalgae, specific growth rates of the microalgae were analysed. The specific growth rates were calculated as μ_s, where N_1 and N_2 demoted the cell density at time t_1 and t_2, respectively.

$\mu_s = Ln(N_2)-Ln(N_1)/(t_2-t_1)$

4.2.6 Intracellular arsenic extraction and measurement of arsenic concentration uptake by microalgae

Intracellular arsenic extraction was performed by extracting arsenic inside the microalgae cells, while extracellular arsenic was collected by filtering cells from the sub-samples. Cells were filtered from 50 mL sub-samples using a 1.2 µm nylon membrane filter paper (Bioflow LifeScience, Malaysia). The cells were rinsed with sterilized BG-11 medium and Milli-Q water to remove the remaining arsenic from the cell surface. Vacuum pressure was applied to ensure all solvents were removed. The filtered solvents were captured in a 50 mL falcon tube and retained as extracellular arsenic analysis.

The filter paper with the cells was dissolved with 8 mL of 25% nitric acid in a 50 mL falcon tube. The digestion was left for 30 minutes and microwaved at 90 W for 5 minutes to ensure the digestion was completed. The digest was diluted to 10% nitric acid concentration by adding 20 mL of Milli-Q water. All diluted digests were re-filtered with a new 0.45 µm filter and the solvents were retained as the intracellular arsenic analysis. The intracellular and extracellular arsenic were analysed using an ICP-OES Optima-8000 (Perkin Elmer, USA) to measure the exact arsenic concentration, in comparison to the TruQ reference standard (Perkin Elmer, Massachusetts).

4.2.7 Statistical analysis

All statistical analyses were executed with the GraphPad Prism 9.5.1 tool to analyse results for arsenic uptake concentrations. The Normality and Lognormality tests for the normal distribution of the results were performed with the Shapiro-Wilk test and the P-value was obtained. Two-Way ANOVA analysis to identify the significant differences between treatments, the Hierarchical Cluster Analysis (HCA) to identify the different clusters formed between different treatments using the GraphPad Prism 9 tool, and the Principal Component Analysis (PCA) analysis using the SPSS Statistic 28 tool to measure variance within the variables were performed.

Due to the difference in arsenic treatment concentration, intracellular arsenic was calculated as percentage (%), where C_i showed in intracellular arsenic concentration measured, and C_0 represented the initial arsenic concentration fed.

$$\% = \frac{Ci}{C0} \mathrm{X}100$$

4.2.6 Microalgae surface structural analysis

A drop of microalgae culture was dropped on a cover slip and chemically fixed using 4% glutaraldehyde for 12 hours. The fixed samples were rinsed with PBS buffer and repeated twice. Microalgae samples were dehydrated in several concentrations of ethanol according to the concentration at 30, 50, 75, 85, 95, and 100% for 3 minutes each, and the dehydrated samples were dried in a desiccator overnight (Huang et al., 2013). Gold was selected as the coating material to coat the microalgae sample. The samples were loaded onto the SEM instrument to observe the surface structural changes and SEM-EDX were used to detect arsenic presence on the microalgae surface (Yau et al., 2016).

4.3 Results

This Section will include the results for the growth of both microalgae strains measured through both biomass dry weight and optical density methods. The intracellular arsenic uptake by the microalgae cells and the effect of arsenic on the microalgae structure will be demonstrated in this section too.

4.3.1 Microalgae strain growth

Arsenic affected the growth of both *Nostoc* and *Chlorella* in terms of biomass dry weight and optical density.

4.3.1.1 Arsenic affecting *Nostoc* growth in terms of biomass dry weight

The biomass dry weight of *Nostoc* treated with different arsenic treatments without phosphate and with phosphate is shown in Table 8 ($p = 0.044$). *Nostoc* treated without phosphate showed a lag phase from day 0 to day 9, an exponential phase from day 9 to day 15, a stationary phase from day 15 to day 24, and a decline phase from day 24 to day 30. *Nostoc* showed a higher biomass dry weight treated under all 9 different arsenic treatments compared to the control. For As (III) treatments, *Nostoc* showed a similar biomass for treatment with 0.01 mg L^{-1} and 1.00 mg L^{-1}, higher compared to 0.10 mg L^{-1} during the exponential phase. The biomass remained higher until day 15 for 0.01 mg L^{-1} As (III) compared to other treatments. For As (V) treatments, *Nostoc* showed the highest biomass treated with 0.01 mg L^{-1} As (V), followed by 0.10 mg L^{-1} and 1.00 mg L^{-1} As (V). For mixed arsenic treatments, *Nostoc* showed a similar biomass for treatment under 0.01 mg L^{-1} As (III) with 1.00 mg L^{-1} As (V) and 0.10 mg L^{-1} As (III) and As (V). The biomass for *Nostoc* treated with 1.00 mg L^{-1} As (III) and 0.01 mg L^{-1} As (V) is slightly lower compared to other treatments but showed higher compared to the control.

When subjected to treatments containing 0.24 mg L^{-1} phosphate, the *Nostoc* biomass showed a lag phase from day 0 to day 12, an exponential phase from day 15 to day 18, and a decline phase from day 18 to day 27, and an increase in biomass was showed from day 27 to day 30. *Nostoc* showed a lower biomass dry weight treated under all 9 different arsenic treatments compared to the control during the exponential phase. For As (III) treatments, *Nostoc* showed similar biomass for all As (III) treatments with different concentrations during the exponential phase. However, the *Nostoc* reaches the exponential phase 3 days earlier for treatment with 1.00 mg L^{-1}, followed by 0.01 mg L^{-1} and 0.10 mg L^{-1}. The is a presence of a stationary phase when the exponential phase is later in contrast to the control. For As (V) treatments, *Nostoc* showed the highest biomass treated with 0.10 mg L^{-1} As (V), and the exponential phase was shown from day 12 to day 18, 3 days longer compared to the control. *Nostoc* showed a similar biomass for 0.01 mg L^{-1} and 0.10 mg L^{-1} As (V) treatment. *Nostoc* treated with mixed arsenic treatments showed a similar biomass for all mixed arsenic treatments during the exponential phase, however, the exponential phase for treatment under 0.01 mg L^{-1} As (III) with 1.00 mg L^{-1} As (V) started on day 9 of the treatment.

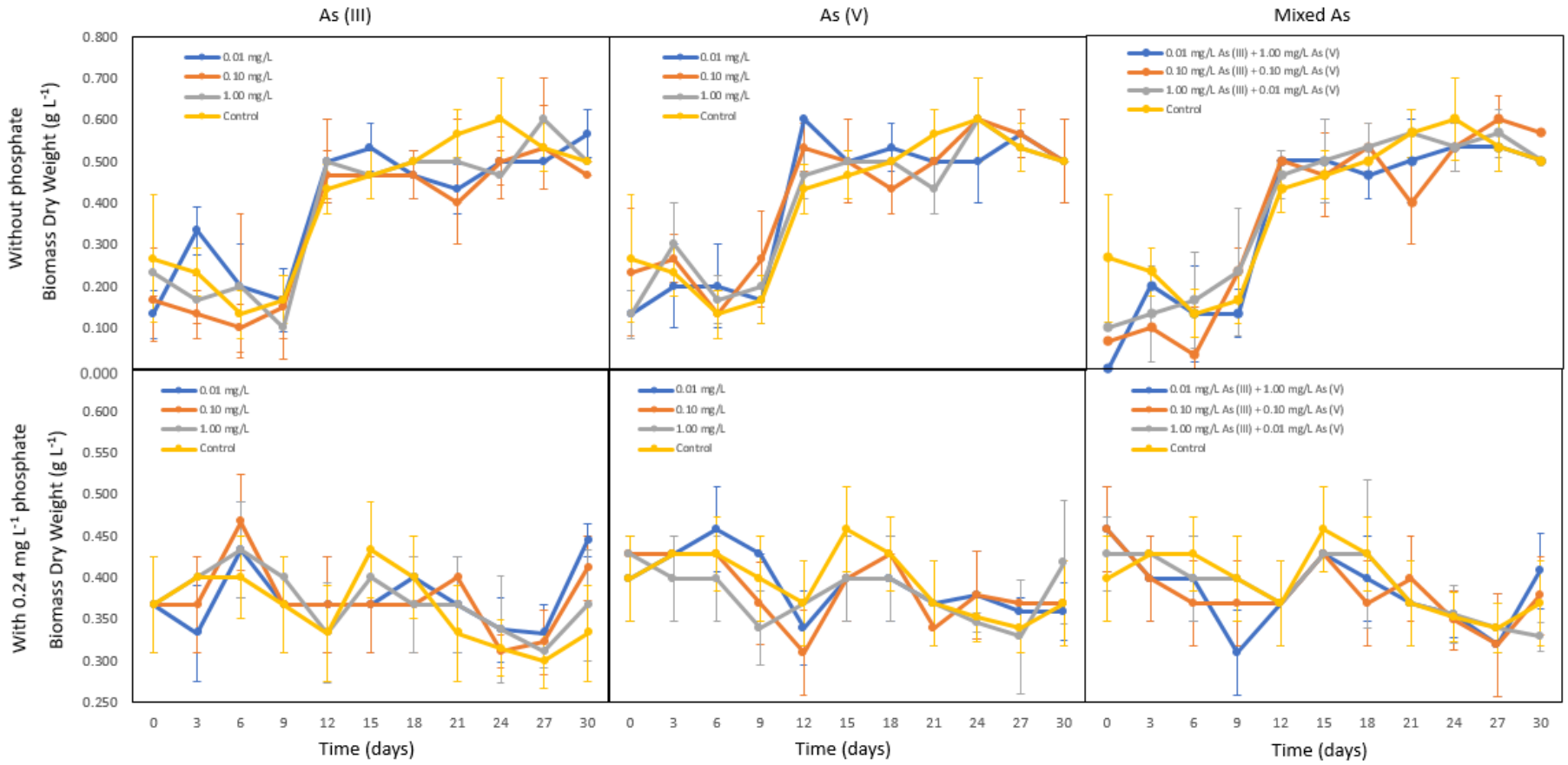

Figure 10. Biomass dry weight of *Nostoc* treated with different arsenic treatment with and without phosphate

4.3.1.2 Arsenic affecting *Chlorella* growth in terms of biomass dry weight

The biomass dry weight of *Chlorella* treated with different arsenic treatments is shown in Table 9 (P = 0.048). *Nostoc* treated without phosphate showed a lag phase from day 0 to day 1, an exponential phase from day 1 to day 5, and a decline phase from day 5 to day 6. *Chlorella* showed a lower biomass dry weight treated under all 9 different arsenic treatments compared to the control. For As (III) treatments, *Chlorella* showed a similar higher biomass during the initial exponential phase, and a similar biomass during the end of the exponential phase for treatment with 1.00 mg L^{-1} compared to the control. *Chlorella* treated with 0.10 mg L^{-1} showed a similar biomass throughout the 7 days of cultivation. The biomass showed an average lower compared to 1.00 mg L^{-1} treatment, followed by 0.01 mg L^{-1} during the initial exponential phase, and the lowest biomass during the end of the exponential phase. For As (V) treatments, *Chlorella* showed the highest biomass treated with 0.10 mg L^{-1} As (V), followed by 0.01 mg L^{-1} and 1.00 mg L^{-1} As (V). The growth patterns were similar but lower compared to the control. Whereas for mixed arsenic treatments, *Chlorella* treated with arsenic showed a shorter exponential phase, where the exponential phase ends on day 4 compared to the control. The biomass for *Chlorella* treated with mixed arsenic treatments was similar and lower compared to the control.

For treatments containing 0.24 mg L^{-1} phosphate, the biomass of *Chlorella* fluctuated throughout the 7 days of treatment. The biomass of *Chlorella* observed for control increased from day 0 to day 1, reduced from day 1 to day 4, remained constant from day 4 to day 5, and declined from day 5 to day 7. For As (III) treatments, *Chlorella* showed similar biomass for 0.01 mg L^{-1} As (III) compared to the control, however, the exponential phase for *Chlorella* treated with 0.01 mg L^{-1} As (III) reached 2 days later compared to the control. For As (V) treatments, *Chlorella* showed the highest biomass treated with 0.10 mg L^{-1} As (V) on day 2, followed by 0.01 mg L^{-1} As (V) on day 4 and the control on day 5. *Chlorella* treated with

1.00 mg L^{-1} As (V) showed an average lower biomass compared to other As (V) treatments and the control. For mixed arsenic treatments, *Chlorella* showed similar biomass for 0.01 mg L^{-1} As (III) with 1.00 mg L^{-1} As (V) on day 5, 0.10 mg L^{-1} As (III) and As (V) compared to the control. Whereas, *Chlorella* showed an average lower biomass when treated with 1.00 mg L^{-1} As (III) with 0.01 mg L^{-1}As (V).

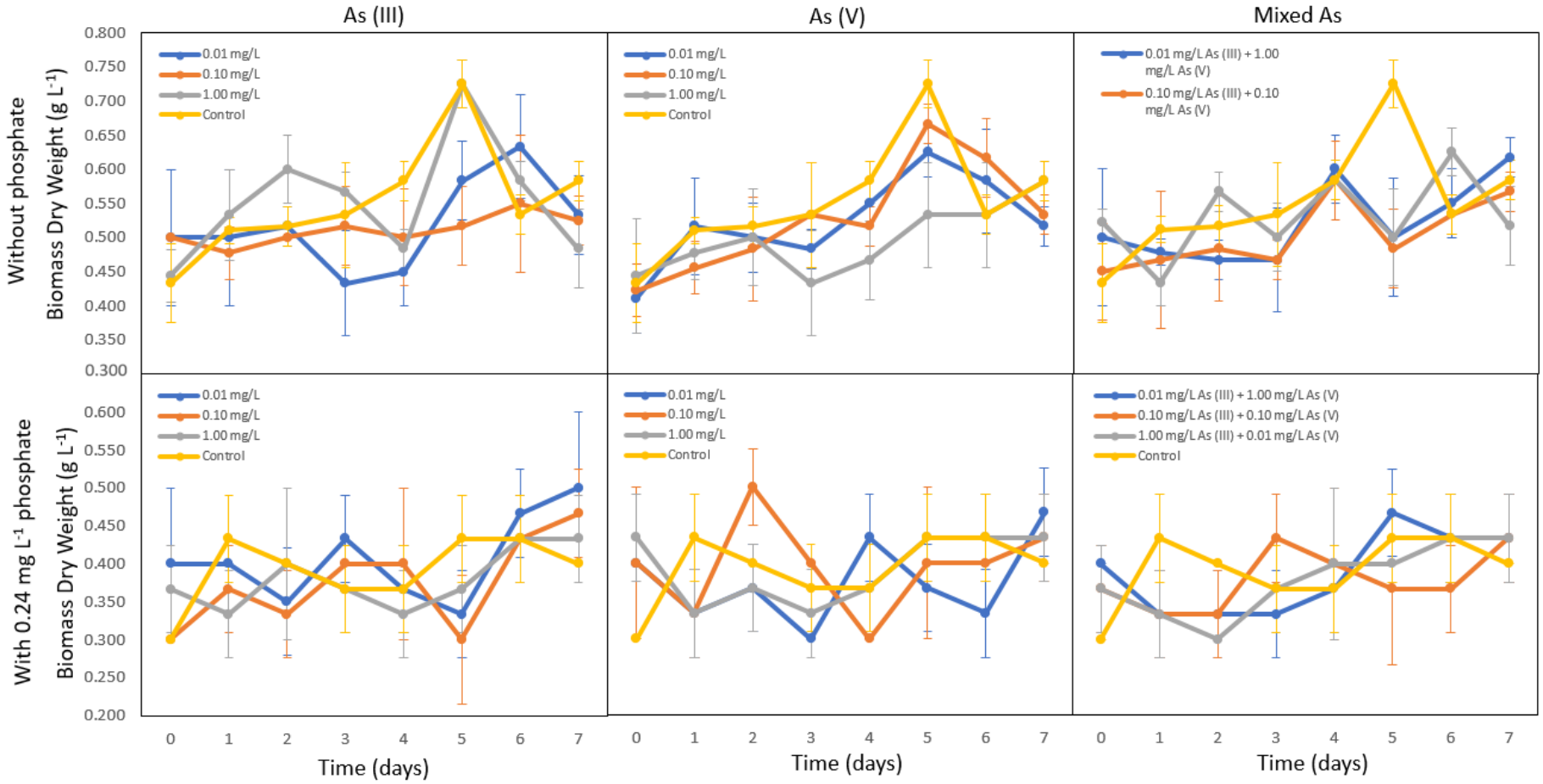

Figure 10. Biomass dry weight of Chlorella treated with different arsenic treatment with and without phosphate

4.3.1.3 Arsenic affecting *Nostoc* growth in terms of optical density

The optical density of *Nostoc* treated with different arsenic treatments is shown in Figure 11 ($p = 0.151$). *Nostoc* treated without phosphate showed a lag phase from day 0 to day 3, an exponential phase from day 3 to day 6, a stationary phase from day 6 to day 27, and a decline phase from day 27 to day 30. For As (III) treatments (Figure 11(A)), *Nostoc* showed a lower optical density compared to the control from day 9 to day 27 with As (III) treatments, except 0.01 mg L^{-1} As (III) treatments with a higher optical density on day 30. The optical density of 0.01 mg L^{-1} and 1.00 mg L^{-1} are similar from day 0 to day 27, which are higher compared to 0.10 mg L^{-1} As (III) treatment. For As (V) treatments (Figure 11(B)), *Nostoc* showed a similar optical density treated with 0.01 mg L^{-1} As (V) compared to the control. Whereas, the optical density of *Nostoc* is similar for treatments under 0.10 mg L^{-1} and 1.00 mg L^{-1} As (V). On average, the optical density of 0.01 mg L^{-1} and control is higher compared to 0.10 mg L^{-1} and 1.00 mg L^{-1}. For mixed arsenic treatments (Figure 11(C)). the optical density of *Nostoc* is similar for treatments with 0.01 mg L^{-1} As (III) with 1.00 mg L^{-1} As (V) compared to the control, whereas the optical density for 0.10 mg L^{-1} As (III) and As (V) is similar to 1.00 mg L^{-1} As (III) and 0.01 mg L^{-1} As (V).

Under treatments with the presence of phosphate, *Nostoc* treated with different arsenic concentrations showed a lag phase from day 0 to day 15, an exponential phase from day 15 to day 21, and a decline phase from day 21 to day 24. The lag phase is longer compared to treatments with phosphate, while the exponential phase is shorter. The optical density of *Nostoc* treated with As (III) (Figure 11(D)), showed the optical density is similar to the control throughout the lag phase. The optical density is higher for treatment with 0.01 mg L^{-1} from day 15 to day 21 compared to the control. Whereas, a similar optical density pattern was shown for 0.10 mg L^{-1} and 1.00 mg L^{-1} treatments throughout 30 days of cultivation, and the optical density increases from day 24 to day 30 for 0.10 mg L^{-1} As (III) treatment. For As (V)

treatments (Figure 11(E)), the *Nostoc* treated with 0.01 mg L^{-1} showed similar optical density compared to the control and showed a higher optical density from day 21 to day 30. *Nostoc* showed a similar optical density for treatment with 0.10 mg L^{-1} and 1.00 mg L^{-1} As (V) treatments, which is also lower compared to 0.01 mg L^{-1} As (V) and control treatments. *Nostoc* treated with mixed arsenic treatments are shown in Figure 11(F). *Nostoc* treated with mixed arsenic showed a lower optical density compared to the control. *Nostoc* showed a similar optical density pattern when treated with 0.10 mg L^{-1} As (III) and As (V) compared to 1.00 mg L^{-1} As (III) with 0.01 mg L^{-1} As (V). Whereas, the optical density of *Nostoc* treated with 1.00 mg L^{-1} As (III) and 0.01 mg L^{-1} As (V) is lower compared to other treatments from day 15 to day 27.

Figure 11a. explained the relationship of *Nostoc* treated with different arsenic concentrations measured through optical density. For clearer labelling and explanation, the 9 arsenic treatments were labelled as:

Labels	Treatments
A	0.01 mg L^{-1} As (III)
B	0.10 mg L^{-1} As (III)
C	1.00 mg L^{-1} As (III)
D	0.01 mg L^{-1} As (V)
E	0.10 mg L^{-1} As (V)
F	1.00 mg L^{-1} As (V)
G	0.01 mg L^{-1} As (III) + 1.00 mg L^{-1} As (V)
H	0.10 mg L^{-1} As (III) + 0.10 mg L^{-1} As (V)
I	1.00 mg L^{-1} As (III) + 0.01 mg L^{-1} As (V)

From the HCA plot result obtained, there are 4 main clusters for the arsenic treatment of *Nostoc* without phosphate. The first cluster consists of treatments D, G, and control, while treatment D is more closely related to the control compared with treatment G. The second cluster consists of treatments C, I, and A, treatment C is more closely related to treatment I compared with treatment A. The third cluster consists of Treatment E, F, and H, treatment E and F are more closely related to each other compared with treatment H. While Treatment B was grouped as the fourth cluster. The first cluster is closely related to the second cluster compared with the third and fourth clusters. For the arsenic treatment with phosphate, there are three main clusters formed. The first cluster consists of treatments B, D, H, I, and control. In this cluster, treatments H and I are closely related to the control, followed by treatments D and B. The second cluster consists of treatments C, G, E, and F. Treatment G is closely related to C, followed by treatments E and F. The third cluster consists of treatment A.

The Loading plot (Figure 11b) showed the relationship between the PCs and the original variables. Different arsenic treatments to *Nostoc* without phosphate showed a positive correlation against PC 1. From the eigenvectors obtained, the control and treatment D showed the highest correlation toward PC 1. Treatments G and H are closely related to the control explained by PC 1, followed by Treatment A > H > I > C > E > F > B. Four treatments which are Treatment A, D, I, and the control showed a negative eigenvector defined by PC 2. For treatments that are positively correlated to PC 2, the sequence of correlation for each treatment against PC 2 from the highest to the least will be treatment G > E > B > F > C > H > control > D > I > A. For arsenic treatments to *Nostoc* with phosphate, all treatments showed a positive value measured by PC 1. Treatment B and I are closely related to the control compared with other treatments, while treatment A has the highest and treatment G has the lowest value measured by PC 1. There are 6 treatments, treatment A, C, D, H, I, and control has a negative value explained by PC 2. Only treatments B, E, F, and G can be explained by PC 2.

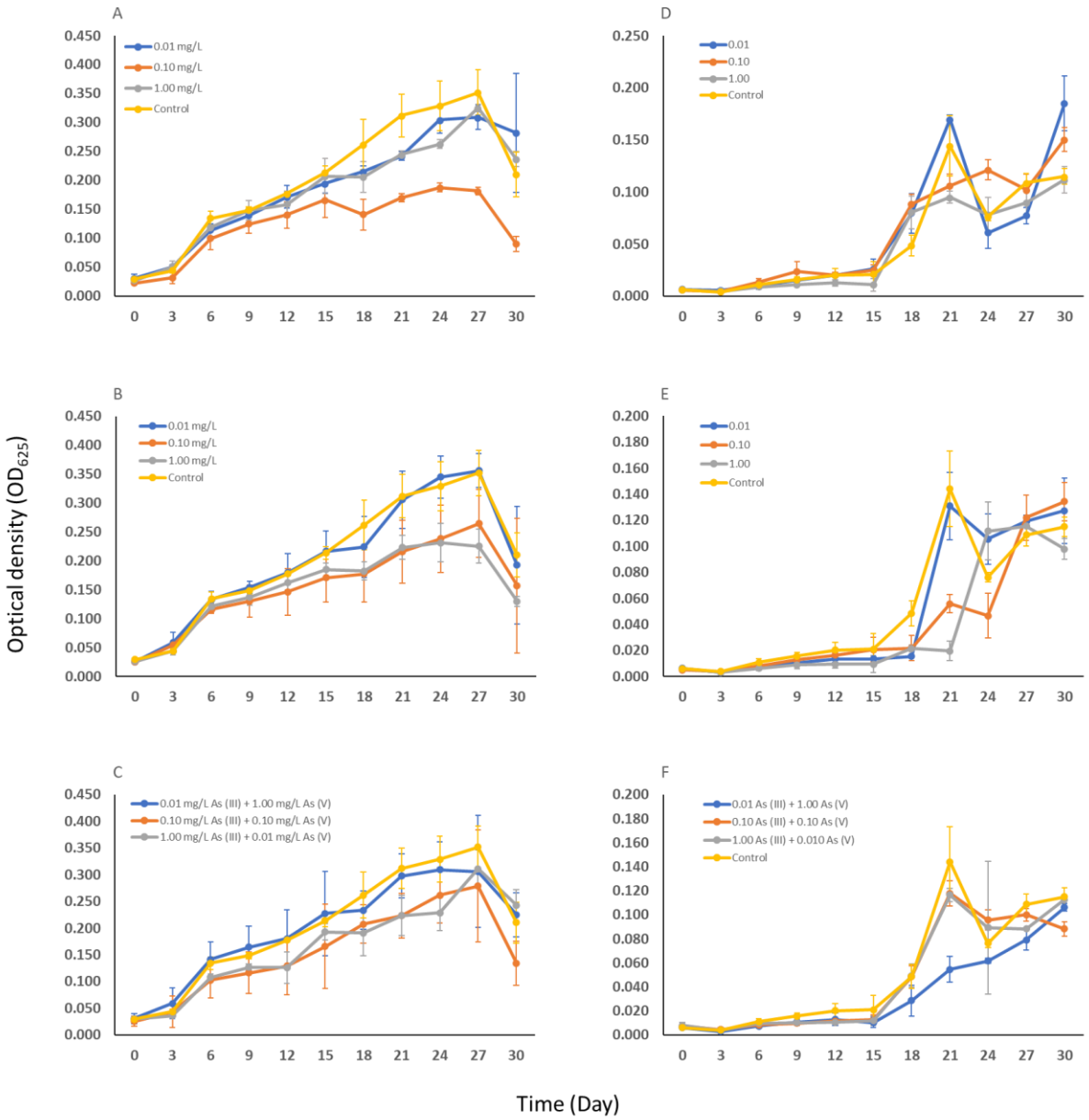

Figure 11. Optical density (OD_{625}) of *Nostoc* without phosphate for As (III) treatments (A), As (V) treatments (B), mixed arsenic treatments (C), and with 0.24 mg L^{-1} phosphate for As (III) treatments (D), As (V) treatments (E), and mixed arsenic treatments (F) (P = 0.151). The initial concentrations treated to the *Nostoc* culture were labelled in the graph.

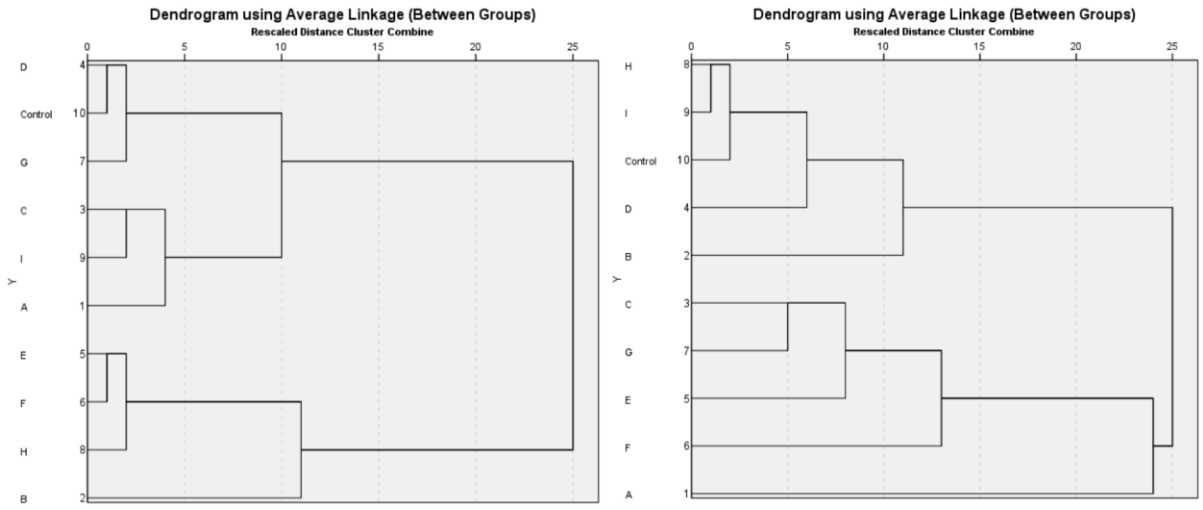

Figure 11a. HCA plot of *Nostoc* treated with different arsenic concentrations and species without phosphate (left) and with phosphate (right) measured through optical density

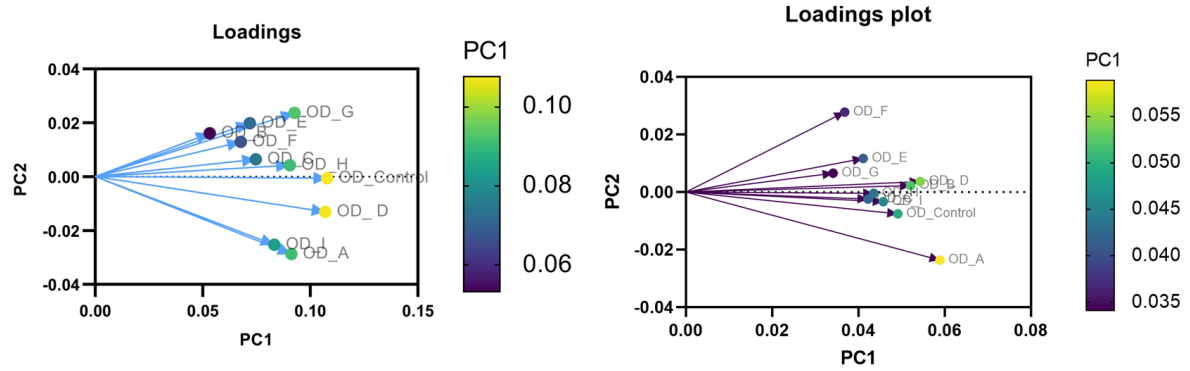

Figure 11b. Loading plot of Nostoc treated with different arsenic treatment without phosphate (left) and with phosphate (right)

4.3.1.4 Arsenic affecting *Chlorella* growth in terms of optical density

The optical density of *Chlorella* treated with different arsenic treatments is shown in Figure 12. *Chlorella* treated without phosphate showed a lag phase from day 0 to day 3, an exponential phase from day 3 to day 4, and a decline phase from day 4 to day 6. *Chlorella* showed a higher optical density treated with different arsenic species and concentrations compared to the control. For As (III) treatments (Figure 12(A)), *Chlorella* treated with arsenic showed a longer exponential phase, from day 3 to day 5 for 0.01 mg L^{-1} and 0.10 mg L^{-1}, whereas the exponential phase for 1.00 mg L^{-1} from day 2 to day 5. The decline phase of *Chlorella* is shorter when treated with different arsenic concentrations, shown from day 5 to day 6. The optical density of *Chlorella* showed the highest for 0.01 mg L^{-1} followed by 1.00 mg L^{-1} and 0.01 mg L^{-1} on the exponential phase. For As (V) treatments (Figure 12(B)), *Nostoc* showed a similar optical density for the exponential phase treated with 0.01 mg L^{-1} As (V) compared to 0.10 mg L^{-1} As (V), however, the exponential phase of *Chlorella* treated with 0.10 mg L^{-1} reaches 1 day earlier. Whereas, the optical density of *Chlorella* under 1.00 mg L^{-1} As (V) is similar to the control, the decline phase showed higher optical density for 1.00 mg L^{-1} As (V). On average, the optical density of 1.00 mg L^{-1} and control is lower compared to 0.10 mg L^{-1} and 1.00 mg L^{-1}, as opposed to the same treatment for *Nostoc*. For mixed arsenic treatments (Figure 12(C)), the optical density of *Chlorella* showed a similar pattern for all treatments compared to the control. *Chlorella* treated under 0.01 mg L^{-1} As (III) with 1.00 mg As (V) showed a higher optical density among 3 different mixed arsenic treatments, followed by 0.10 mg L^{-1} As (III) with As (V), and 1.00 mg As (III) with 0.01 mg L^{-1} As (V).

Under treatments with the presence of phosphate, *Chlorella* showed a lag phase from day 0 to day 3, an exponential phase from day 3 to day 4, and a decline phase from day 4 to day 5. The growth falls into the next curve from day 5 to day 7. Comparing arsenic treatments to the control, *Chlorella* showed a higher optical density without arsenic treatments. For As (III)

treatments (Figure 12(D)), *Chlorella* treated with 1.00 mg L^{-1} showed similar optical density compared to the control, whereas the optical density is lower when treated with 0.01 mg L^{-1} and 0.10 mg L^{-1} As (III). For As (V) treatments (Figure 12(E)), The optical density of *Chlorella* showed higher under 0.01 mg L^{-1} treatment, followed by 1.00 mg L^{-1} and 0.10 mg L^{-1} As (V). for mixed arsenic treatments (Figure 12(F)), higher mixed arsenic treatments which are 0.01 mg L^{-1} As (III) with 0.01 mg L^{-1} As (V) and 1.00 mg L^{-1} As (III) and 0.01 mg L^{-1} As (V) showed a similar optical density compared to the control. Mixed arsenic with 0.10 mg L^{-1} As (III) and As (V) showed a lower optical density compared to other mixed arsenic treatments and the control.

The relationship between arsenic treatments and the optical density of Chlorella is shown in Figure 12a. HCA plot result obtained showed that there are 3 main clusters for the arsenic treatment of Chlorella without phosphate. The first cluster consists of treatments D, E, and G. The second cluster consist of treatment C, control, while the third cluster consists of treatments A, I, B, and F. Treatment C is closely related to the control compared with other treatments and grouped as the second cluster. There are two main clusters shown in the HCA plot for Chlorella treated with different arsenic concentrations with phosphate. The results showed that Treatment E has the most similar outcome compared with the control. The similarity to the control was followed by treatments D, A, and B. Treatments H, I, and F form another cluster and have the least correlation with the control.

Figure 12b. showed the Loading plots of *Chlorella* growth treated with different arsenic concentrations measured through optical density. For arsenic treatments to *Chlorella* without phosphate, all treatments showed a positive value measured by PC 1, only treatments C, E, and control showed a positive value for PC 2, and Treatment A, H, I, and control showed a positive value for PC 3, while Treatment E, F, G, and control showed positive value for PC 4. The eigenvalues for all PC for Loading plots are relatively low, where the positive values for PC 1

are similar to the control except for treatment F and G. All positive values of PC 2 showed no significant difference to the control. Comparing through PC 3 measurement, Treatment A and F are closely related to the control, while Treatment I is least related to the control. PC 4 measurements also showed similar values for treatments E, F, and G compared to the control, while treatment A showed the least relation to the control.

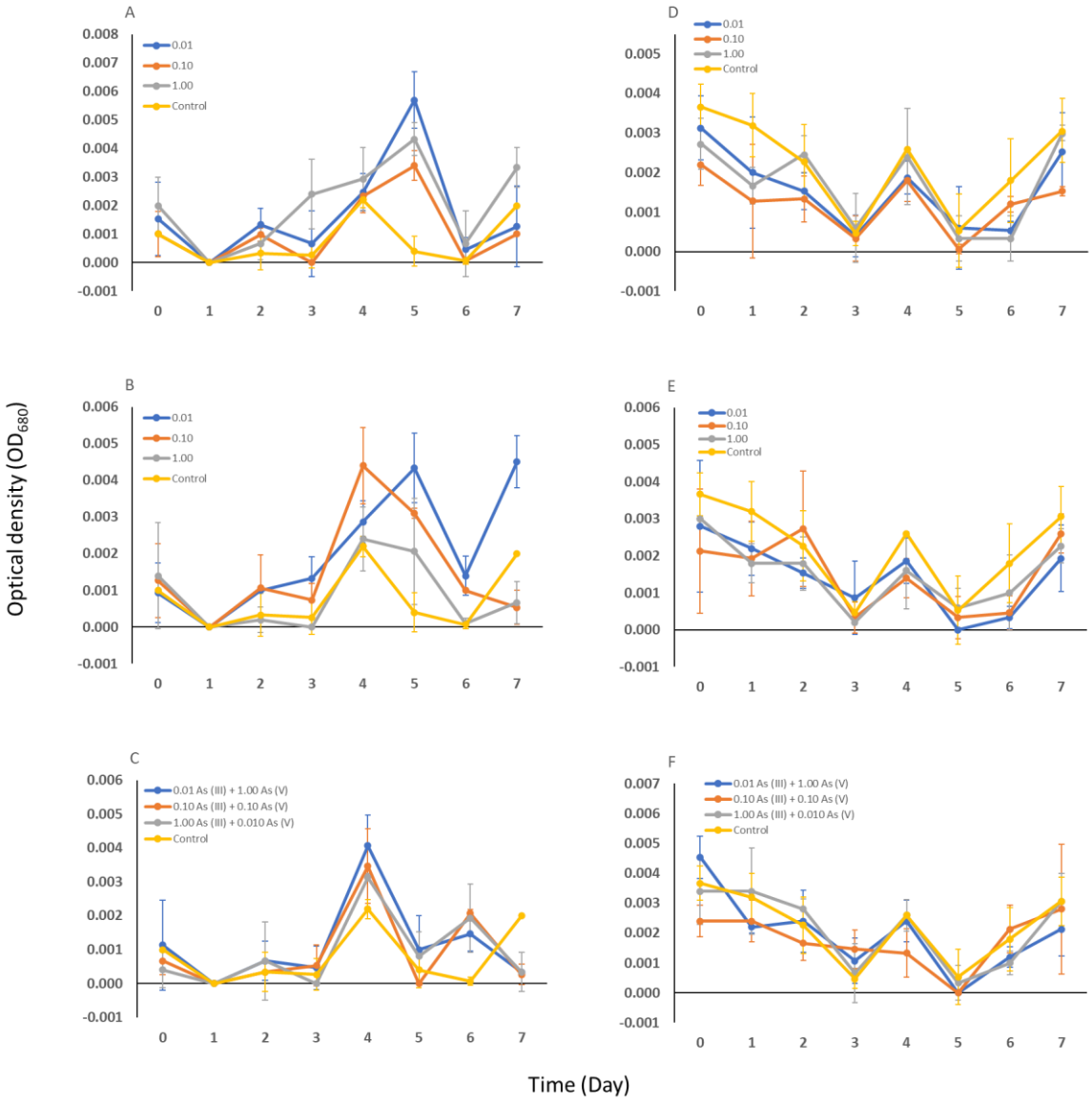

Figure 12. Optical density (OD_{680}) of *Chlorella* without phosphate for As (III) treatments (A), As (V) treatments (B), mixed arsenic treatments (C), and with 0.24 mg L^{-1} phosphate for As (III) treatments (D), As (V) treatments (E), and mixed arsenic treatments (F) ($P < 0.001$). The initial concentrations treated to the *Chlorella* culture were labelled in the graph.

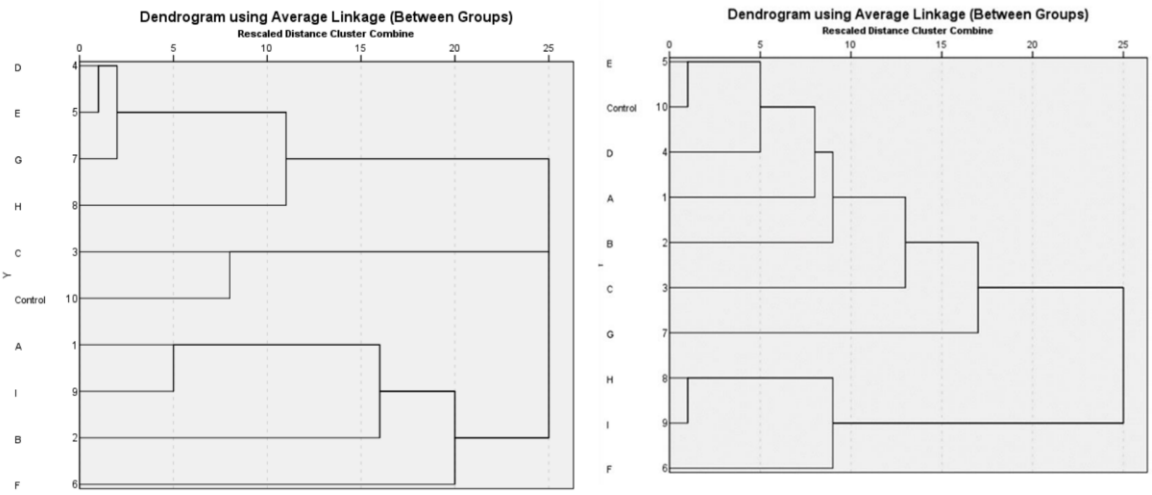

Figure 12a. HCA plot of *Chlorella* treated with different arsenic species and concentrations without phosphate (left) and with phosphate (right) measured through optical density

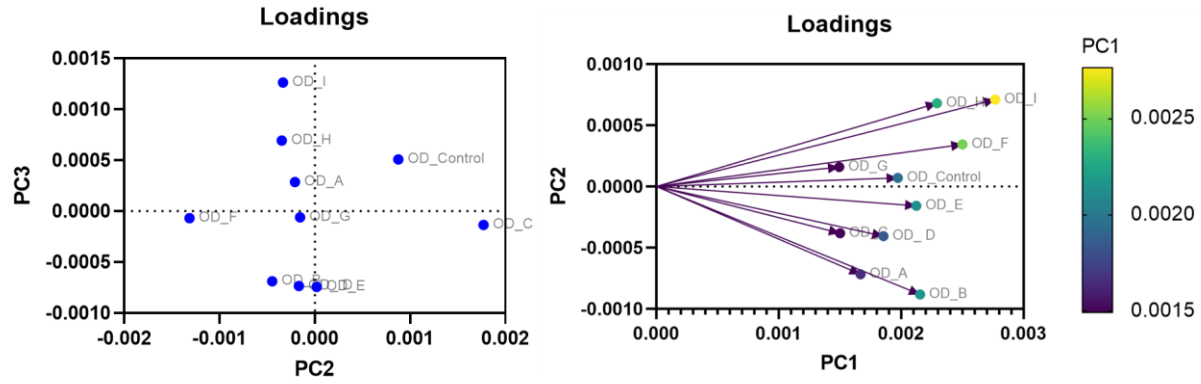

Figure 12b. PCA plot of *Chlorella* treated with different arsenic species and concentrations without phosphate (left) and with phosphate (right)

4.3.1.5 Comparison between *Nostoc* and *Chlorella* growth rate

The specific growth rate (SGR) for both *Nostoc* and *Chlorella* was tabulated in Table 6 and Table 7. From the results obtained, the SGR for *Nostoc* treated with phosphate is approximately 10 times higher compared to treatments without phosphate measured through optical density. Whereas, it showed a different result for biomass dry weight measurement where the SGR of biomass dry weight treated without phosphate is approximately 3 times higher and 2 times higher for *Nostoc* and *Chlorella* respectively compared to treatments with phosphate.

For the optical density measurement, Nostoc showed the highest SGR treated with 0.01 mg L^{-1} As (V) with phosphate, whereas, the 0.10 mg L^{-1} As (III) without phosphate showed the lowest SGR. The mixed arsenic treatment with 0.01 mg L^{-1} As (V) showed the highest SGR value at 0.712 µ while mixed arsenic treatment at 0.10 mg L^{-1} As (III) showed the lowest SGR value at 195 µ when treated with phosphate. For the biomass dry weight measurement without phosphate, 0.10 mg L^{-1} As (III) showed the highest SGR value at 0.649, whereas 0.10 mg L^{-1} As (V) and mixed arsenic at 0.10 mg L^{-1} As (V) and As (III) showed the lowest SGR value at 0.231 µ. Whereas, 0.10 mg L^{-1} As (V) treatment showed the highest SGR at 0.106 µ, while 1.00 mg L^{-1} As (III) and mixed arsenic treatment with 1.00 mg L^{-1} As (III) and 0.01 mg L^{-1} As (V) showed the lowest SGR at 0.61 µ under treatment with phosphate.

Chlorella measured through optical density showed the highest SGR for mixed arsenic treatment 1.00 mg L^{-1} As (V) and 0.10 mg L^{-1} As (III) with phosphate and the lowest SGR value for 0.10 mg L^{-1} As (V) without phosphate. The treatments with phosphate and mixed arsenic with 1.00 mg L^{-1} As (V) and 0.10 mg L^{-1} As (III) showed the highest SGR value at 1.852 µ, whereas 0.01 mg L^{-1} As (III) showed the lowest SGR at 0.511 µ. Whereas, mixed arsenic treatment of 0.10 mg L^{-1} As (III) and As (V) without phosphate showed the highest SGR at 0.649 µ, while 0.10 mg L^{-1} As (III) with phosphate showed only 0.063 µ when measured through the biomass dry weight method.

Table 6: Specific growth rate of *Nostoc* and *Chlorella* measured through optical density

Microalgae strains	Arsenic concentrations (mg L^{-1})		Specific growth rate (μ)	
	As (III)	As (V)	Without phosphate	With Phosphate
Nostoc	0.01	0.00	0.053	0.369
	0.10	0.00	0.029	0.421
	1.00	0.00	0.046	0.663
	0.00	0.01	0.043	0.712
	0.00	0.10	0.035	0.314
	0.00	1.00	0.034	0.579
	0.01	1.00	0.042	0.277
	0.10	0.10	0.059	0.195
	1.00	0.01	0.048	0.382
	0.00	0.00	0.055	0.362
Chlorella	0.01	0.00	0.175	0.511
	0.10	0.00	0.202	0.758
	1.00	0.00	0.225	0.665
	0.00	0.01	0.181	1.050
	0.00	0.10	0.088	0.943
	0.00	1.00	0.238	0.887
	0.01	1.00	0.104	0.904
	0.10	0.10	0.307	1.460
	1.00	0.01	0.330	1.852
	0.00	0.00	0.171	0.990

Table 7: Specific growth rate of *Nostoc* and *Chlorella* measured through biomass dry weight

Microalgae strains	Arsenic concentrations (mg L^{-1})		Specific growth rate (μ)	
	As (III)	As (V)	Without phosphate	With Phosphate
Nostoc	0.01	0.00	0.366	0.069
	0.10	0.00	0.649	0.081
	1.00	0.00	0.536	0.061
	0.00	0.01	0.427	0.067
	0.00	0.10	0.231	0.106
	0.00	1.00	0.282	0.099
	0.01	1.00	0.441	0.102
	0.10	0.10	0.254	0.072
	1.00	0.01	0.231	0.061
	0.00	0.00	0.319	0.087
Chlorella	0.01	0.00	0.260	0.260
	0.10	0.00	0.200	0.063
	1.00	0.00	0.270	0.405
	0.00	0.01	0.129	0.229
	0.00	0.10	0.255	0.255
	0.00	1.00	0.134	0.134
	0.01	1.00	0.366	0.251
	0.10	0.10	0.649	0.223
	1.00	0.01	0.536	0.268
	0.00	0.00	0.427	0.217

4.3.2 Arsenic concentrations uptake by microalgae

The arsenic concentration uptake by both *Nostoc* and *Chlorella* strains showed a difference. *The Nostoc* strain is able to uptake higher arsenic concentrations compared to the *Chlorella* strain.

4.3.2.1 Arsenic Bioaccumulation in *Nostoc*

The arsenic uptake percentage (%) for *Nostoc* is shown in Figure 13. In treatments without phosphate, *Nostoc* uptake the highest arsenic percentage under 0.10 mg L^{-1} As (III) from day 24 to day 27 compared to other arsenic treatments. The arsenic uptake percentage ranged between 2.08% to 19.91% from 0.01 mg L^{-1} As (III) treatment, 9.12% to 100 % from 0.10 mg L^{-1} As (III), and 14.47% to 68.30% from 1.00 mg L^{-1} As (III) (Figure 13(A)). The 0.10 mg L^{-1} treatment showed an average higher arsenic uptake percentage compared to 0.01 mg L^{-1} and 1.00 mg L^{-1} As (III) treatments, whereas 0.01 mg L^{-1} As (III) showed the lowest arsenic uptake percentage. Although the arsenic uptake percentage is highest under 0.10 mg L^{-1} treatment, the arsenic uptake concentration (mg L^{-1}) showed highest for 1.00 mg L^{-1} on day 24 with 0.683 mg L^{-1} as the initial arsenic treated to *Nostoc* is higher. The arsenic uptake percentage ranged between 0 % to 43.42% from 0.01 mg L^{-1} As (V), 0% to 33.35 % from 0.10 mg L^{-1} As (V), and 12.98 % to 29.71 % from 1.00 mg L^{-1} As (V) (Figure 13(B)). On average, the arsenic uptake percentage is highest for 0.01 mg L^{-1} As (V) treatment and minimal arsenic was uptake when *Nostoc* was treated with 0.10 mg L^{-1} As (V) during the initial cultivation period. *Nostoc* uptake higher arsenic percentage when treated with 1.00 mg L^{-1} As (V) at late stages of cultivation. For mixed arsenic treatment, the highest arsenic uptake percentage was measured under treatment with equal As (III) and As (V) ratios. The arsenic uptake percentage ranged between 12.79 % to 32.66% from 0.01 mg L^{-1} As (III) with 1.00 mg L^{-1} As (V), 6.22% to 60.57 % from 0.10 mg L^{-1} As (III) and As (V), and 19.77 % to

43.71 % from 1.00 mg L^{-1} As (III) with 0.01 mg L^{-1} As (V) (Figure 13C). *Nostoc* uptake higher arsenic under 1.00 mg L^{-1} As (III) with 0.01 mg L^{-1} As (V) treatment throughout the cultivation period compared with other mixed arsenic treatments, except day 18 where the highest arsenic uptake percentage under an equal ratio of As (III) and As (V). This result converses with the single arsenic species treatment, as *Nostoc* uptake a higher arsenic percentage under As (III) treatments compared to As (V) treatments.

In treatments with the presence of 0.24 mg L^{-1} phosphate, *Nostoc* uptake arsenic ranged between 0% to 30% from 0.01 mg L^{-1} As (III) treatment, 8% to 37.50% from 0.10 mg L^{-1} As (III), and 0.11% to 37.36% from 1.00 mg L^{-1} As (III) (Figure 13(D)). In contrast to treatments without phosphate, the arsenic uptake percentage range is averagely lower. The *Nostoc* uptakes higher arsenic percentage when treated with 1.00 mg L^{-1} As (III) during initial treatments and reduces gradually up to day 15, then increases gradually until the end of cultivation. Whereas the arsenic uptake by *Nostoc* increases after 9 days of cultivation for 0.10 mg L^{-1} As (III) treatment. The arsenic uptake percentage showed minimal during the initial, mid, and end of the cultivation phase for 0.01 mg L^{-1} As (III). Whereas, arsenic uptake percentage ranged between 0 % to 50.00% from 0.01 mg L^{-1} As (V), 59.27% to 83.85 % from 0.10 mg L^{-1} As (V), and 2.20 % to 66.35 % from 1.00 mg L^{-1} As (V) (Figure 13(E)). The results are different from As (III) where the average arsenic uptake percentage is higher compared to treatments without phosphate. The arsenic uptake percentage showed the highest throughout the 30 days of treatment for 0.10 mg L^{-1} As (V), and the higher arsenic uptake percentage during the initial cultivation phases for 1.00 mg L^{-1} As (V) treatment. The arsenic uptake percentage ranged between 5.69 % to 35.15% from 0.01 mg L^{-1} As (III) with 1.00 mg L^{-1} As (V), 3.64% to 43.98 % from 0.10 mg L^{-1} As (III) and As (V), and 10.45 % to 65.57 % from 1.00 mg L^{-1} As (III) with 0.01 mg L^{-1} As (V) (Figure 13F). The arsenic uptake percentage for 0.01 mg L^{-1} As (III) with 1.00 mg L^{-1} As (V), and 0.10 mg L^{-1} As (III) with As (V) treatment

showed an average lower percentage compared to treatments without phosphate. However, treatments with 1.00 mg L^{-1} As (III) with 0.01 mg L^{-1} As (V) showed a higher arsenic uptake percentage compared to treatments without phosphate.

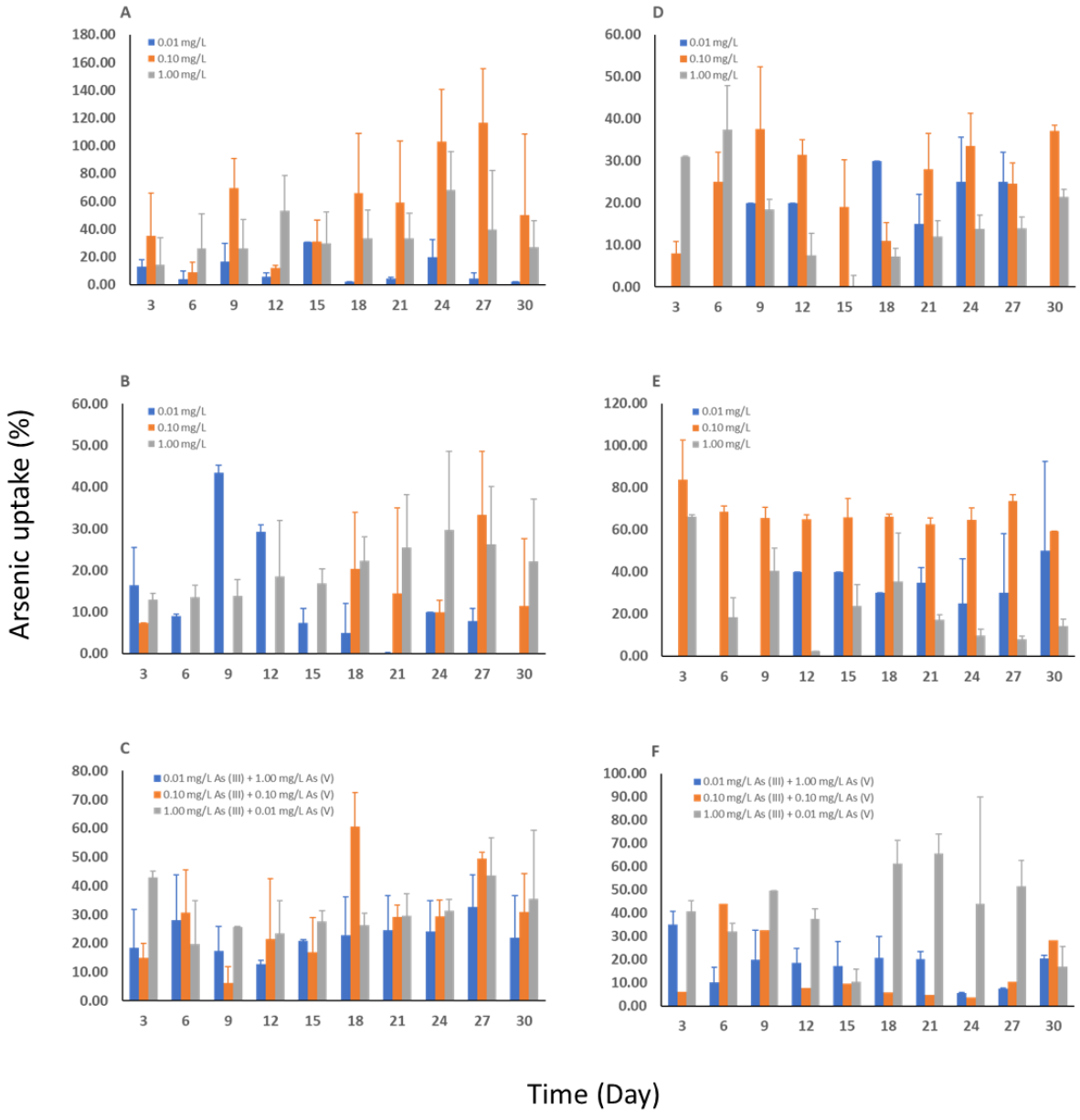

Figure 13. Arsenic uptake (%) of *Nostoc* without phosphate for As (III) treatments (A), As (V) treatments (B), mixed arsenic treatments (C), and with 0.24 mg L^{-1} phosphate for As (III) treatments (D), As (V) treatments (E), and mixed arsenic treatments (F) (P = 0.021). The initial concentrations treated to the *Nostoc* culture were labelled in the graph.

4.3.2.2 Arsenic Bioaccumulation in *Chlorella*

The arsenic uptake percentage (%) for *Chlorella* is shown in Figure 14. In treatments without phosphate, *Chlorella* uptake the highest arsenic percentage under 0.10 mg L^{-1} As (III) on day 1 compared to other arsenic treatments, similar to *Nostoc*. The arsenic uptake percentage ranged between 0 % to 75 % from 0.01 mg L^{-1} As (III) treatment, 0 % to 84.20 % from 0.10 mg L^{-1} As (III), and 2.18 % to 10.29% from 1.00 mg L^{-1} As (III) (Figure 14(A)). The arsenic uptake percentage is higher for 0.10 mg L^{-1} treatment from day 1 to day 4 except day 2, while arsenic uptake is higher for 0.01 mg L^{-1} As (III) for day 2 and day 5 to 7. Compared to *Nostoc*, the arsenic uptake percentage for As (III) treatments without phosphate is averagely lower. The arsenic uptake percentage ranged between 37.11% to 75.00 % from 0.01 mg L^{-1} As (V), 0% to 33.09 % from 0.10 mg L^{-1} As (V), and 0.00 % to 3.31 % from 1.00 mg L^{-1} As (V) (Figure 14(B)). On average, the arsenic uptake percentage by *Chlorella* is minimal for 1.00 mg L^{-1} As (V) treatment, whereas the arsenic uptake percentage is highest for 0.01 mg L^{-1} As (V) treatment throughout 7 days of cultivation. Compared to *Nostoc* treated with the same treatments, the arsenic uptake percentage for *Chlorella* is higher when treated with 0.01 mg L^{-1} As (V) and a lower percentage for 1.00 mg L^{-1} As (V). The arsenic uptake percentages for both microalgae strains were similar for 0.10 mg L^{-1} As (V). For mixed arsenic treatment, the highest arsenic uptake percentage was measured under treatment with equal As (III) and As (V) ratios. The arsenic uptake percentage ranged between 2.92 % to 19.77% from 0.01 mg L^{-1} As (III) with 1.00 mg L^{-1} As (V), 3.19 % to 39.61 % from 0.10 mg L^{-1} As (III) and As (V), and 0.63 % to 39.22 % from 1.00 mg L^{-1} As (III) with 0.01 mg L^{-1} As (V) (Figure 14(C)). *Chlorella* uptake higher arsenic under 0.10 mg L^{-1} As (III) and As (V), and 1.00 mg L^{-1} As (III) with 0.01 mg L^{-1} As (V) treatment during the initial cultivation period. This result showed an

average lower percentage compared to single arsenic species treatments, and *Nostoc* treated with the same mixed arsenic treatments.

In treatments with the presence of 0.24 mg L^{-1} phosphate, *Chlorella* uptake arsenic ranged between 0% to 82.5% from 0.01 mg L^{-1} As (III) treatment, 12.5% to 96.53% from 0.10 mg L^{-1} As (III), and 1.15% to 10.67% from 1.00 mg L^{-1} As (III) (Figure 14(D)). The arsenic uptake percentage range is averagely higher compared to treatments without phosphate and *Nostoc* under the same treatments. The *Chlorella* uptakes higher arsenic percentage when treated with 0.01 mg L^{-1} As (III) during initial cultivation days, and higher arsenic percentage when treated with 1.00 mg L^{-1} As (III) after 3 days of cultivation. Whereas, the arsenic uptake percentage ranged between 25 % to 58.91% from 0.01 mg L^{-1} As (V), 0.00 % to 35.81 % from 0.10 mg L^{-1} As (V), and 1.23 % to 66.25.08 % from 1.00 mg L^{-1} As (V) (Figure 14(E)). The results are different from As (III) where the average arsenic uptake percentage is lower compared to treatments without phosphate. The arsenic uptake percentage showed the highest throughout the 30 days of treatment for 0.01 mg L^{-1} As (V), followed by 0.10 mg L^{-1} and 1.00 mg L^{-1} As (V). The arsenic uptake percentage is minimal for 1.00 mg L^{-1} As (V) throughout the cultivation after the first day. The arsenic uptake percentage ranged between 1.39 % to 30.72% from 0.01 mg L^{-1} As (III) with 1.00 mg L^{-1} As (V), 6.17% to 54.54 % from 0.10 mg L^{-1} As (III) and As (V), and 1.29 % to 35.51 % from 1.00 mg L^{-1} As (III) with 0.01 mg L^{-1} As (V) (Figure 14(F)). The arsenic uptake percentage for all mixed arsenic treatments was low throughout the 7 days of cultivation except on the first day of treatment. The percentage is also low compared to treatments without phosphate and the same treatments to *Nostoc.*

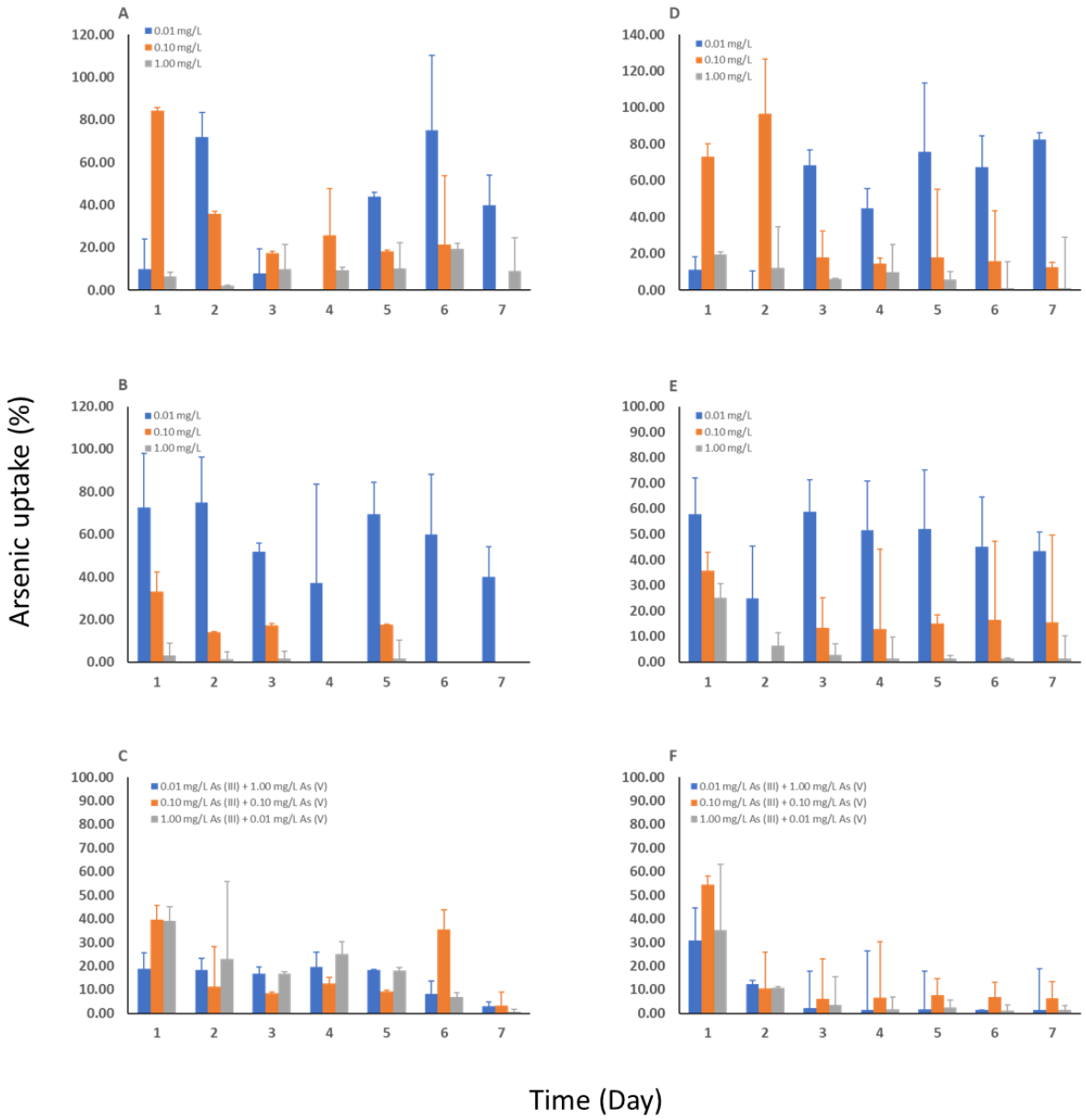

Figure 14. Arsenic uptake (%) of *Chlorella* without phosphate for As (III) treatments (A), As (V) treatments (B), mixed arsenic treatments (C), and with 0.24 mg L^{-1} phosphate for As (III) treatments (D), As (V) treatments (E), and mixed arsenic treatments (F) ($p = 0.038$). The initial concentrations treated to the *Chlorella* culture were labelled in the graph.

4.3.3 Ultrastructural analysis by Scanning Electron Microscopy (SEM)`

Nostoc showed the ability to enhance in terms of growth and uptake and remove the highest arsenic concentration under 1.00 mg L^{-1} As (III) without phosphate condition, the vegetative cell surface was analysed to identify the arsenic concentration adsorb on the cell surface and the effect of arsenic on the structural changes. The ultrastructural surface of *Nostoc* viewed under SEM was illustrated in Figure 15. There are no obvious changes observed in terms of vegetative cell size for both the control and As (III) treated cells. Although there are no differences in terms of vegetative cell size for both treated and control conditions, the vegetative cells with arsenic treatment showed a rougher, highly damaged, and disrupted cell surface (Figure 16) compared to the control cells. The cells showed rougher surfaces with more wrinkles compared to the control cells with smooth surfaces. Besides, the cell shape with arsenic treatment showed damages compared to the round spherical shape of the control cells. Results in Figure 17 showed no arsenic detected on the surface of *Nostoc* for both control and treated cells. Besides arsenic, most of the elements detected on the control cell surface showed a lower concentration in arsenic-treated cells, including carbon, potassium, sodium, etc.

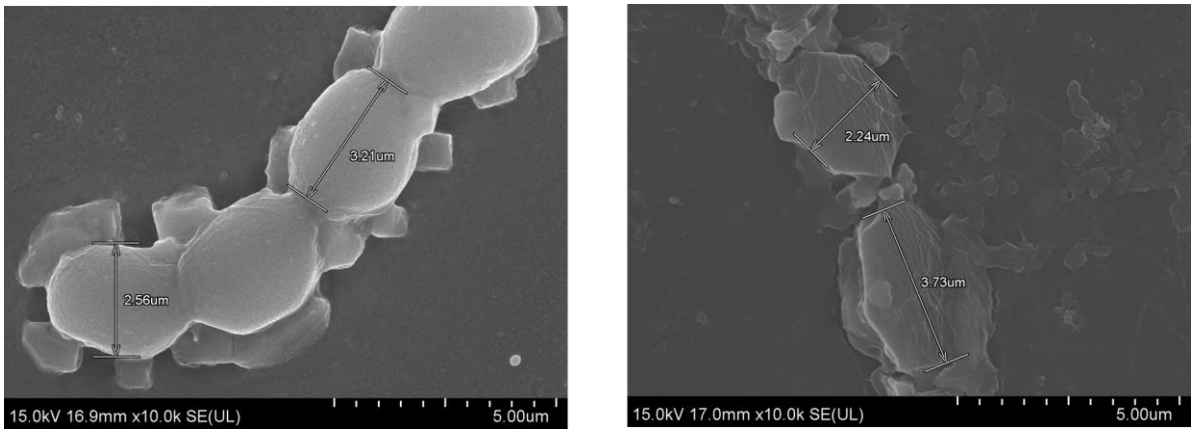

Figure 15. Overall figure of Nostoc under control treatment (left) and 1.00 mg L-1 As (III) treatment (right) viewed under SEM. It was clear that the cell surfaces of the As-treated cells exhibited greater signs of rupture, roughness with rigid textures, and corrugation when compared to the smooth surfaces of the control cells.

Control vegetative cells

As (III) treated vegetative cells

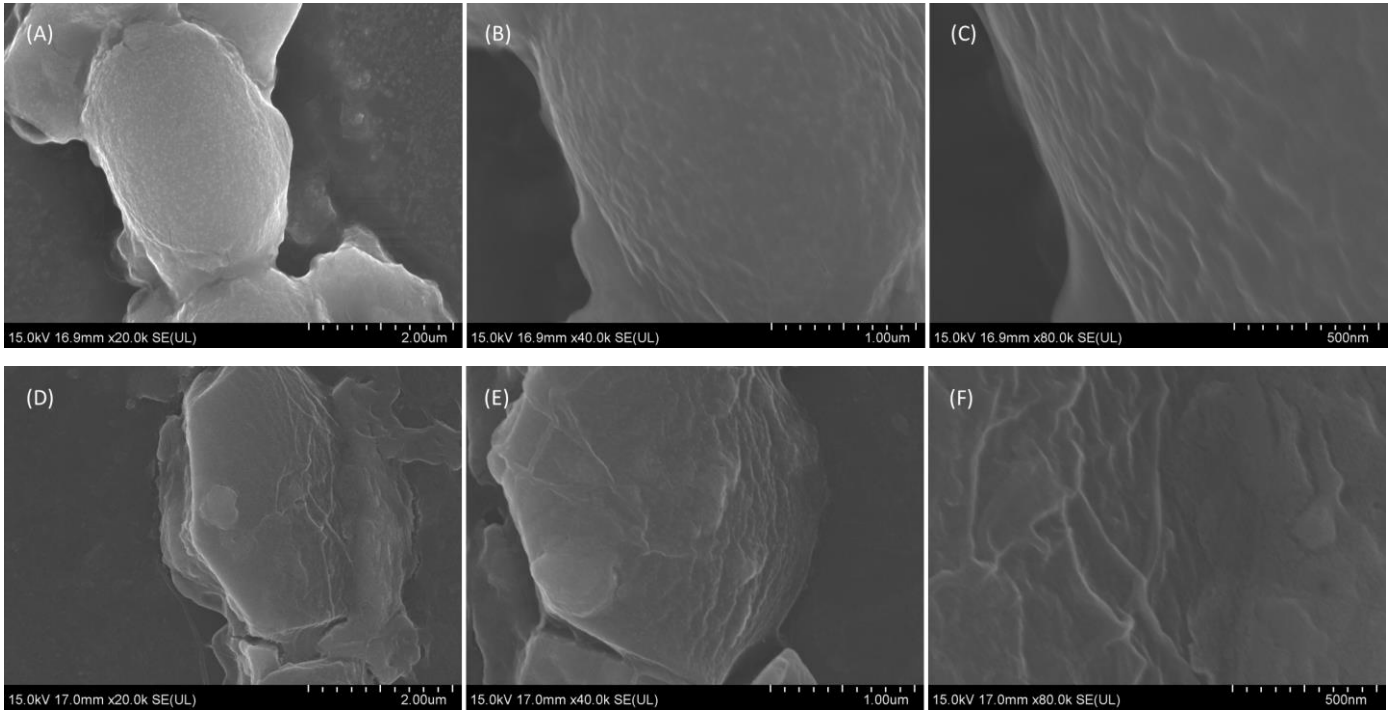

Figure 16. Surface structure of *Nostoc* vegetative cell under control treatment with 20k X magnification (A), 40k X magnification (B), 80k X magnification (C) and 1.00 mg L^{-1} As (III) treatment with 20k X magnification (D), 40k X magnification (E), 80k X magnification (F) viewed under SEM. *Nostoc* treated with 1.00 mg L^{-1} As (III) (D, E, F) showed changes in cell surface structure, with a more ruptured cell surface compared to the control

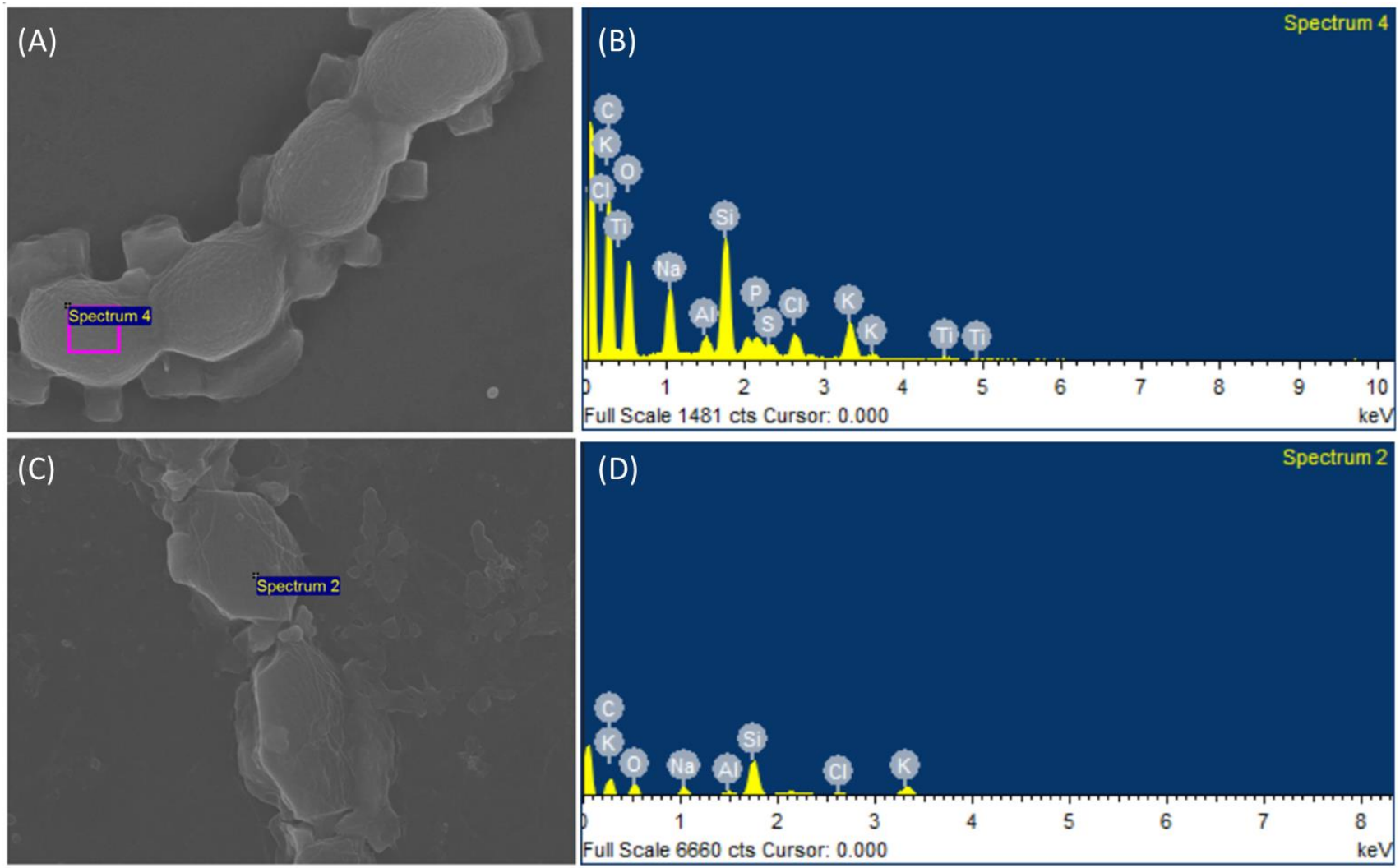

Figure 17. SEM-EDX image and results for *Nostoc* under control (C, D) treatment, and cells treated with 1.00 mg L^{-1} As (III) (C, D). Both control and treated cells do not show the presence of arsenic in the SEM-EDX result

4.4 Discussion

4.4.1 Effect of phosphate on the microalgae lag phase

Phosphate is an important element required for the growth of microalgae. It is listed as the macronutrient in the composition of BG-11 medium required for the *Nostoc* and *Chlorella* growth (Chapter 3). The overall results in Section 4.3 demonstrated that both *Nostoc* and *Chlorella* showed fluctuations in the biomass and a longer lag phase measured through the optical density compared to treatments without phosphate. The possible reason may be due to the pre-cultivation of both microalgae strains before the arsenic treatment test. Both microalgae strains were pre-cultivated for 5 days in advance in the BG-11 medium without phosphate to eliminate phosphate from the cells (Lavrinovičs et al., 2020). The pre-cultivation may lead to both strains being adapted to conditions without phosphate. As the phosphate concentration required to maintain the microalgae growth range from 0.001g L^{-1} to 0.179 g L^{-1} (Yaakob et al., 2021), the phosphate remained in the cells after 5 days of pre-cultivation may fall within this range and supported the growth of microalgae cells. Hence, microalgae cells treated without phosphate and arsenic (the control treatment) can continue their growth throughout the cultivation period. The additional 0.24 mg L^{-1} may disrupt the adaptation of the microalgae cells to the phosphate-depleted conditions. This leads to a period that will be required for the microalgae cells to re-adapt to conditions with the presence of phosphate (Ramírez-Romero et al., 2023). Hence, the lag phase was prolonged for treatments with the addition of phosphate and fluctuation was observed in the biomass of both microalgae strains.

4.4.2 Biomass dry weight result moderately correlate to the optical density result

Optical density is a simple but indirect method of measuring the growth (Griffiths et al., 2011) of microalgae, which indicates the light absorption of the microalgae cells. Whereas, biomass dry weight measurement is a method which requires a longer period to identify the growth of microalgae. Past studies (Jena et al., 2012; Masojídek et al., 2011) demonstrated that biomass and optical density are highly correlated with R^2 value larger than 0.99. This indicates that more than 99% of the optical density variation can be explained by the variation in biomass dry weight. However, our results demonstrated a moderate correlation (r^2 = 0.51, p-value < 0.005) between the biomass dry weight to the optical density of the microalgae cells. The *Nostoc* biomass treated without phosphate showed an exponential phase or a drastic increase from day 9 to day 12, however, the optical density increased gradually from day 6 to day 27. Whereas, the biomass of *Nostoc* treatment with 0.24 mg L^{-1} phosphate reaches the exponential phase from day 12 to day 15, however, the optical density showed the exponential phase from day 15 to day 21. This indicated that the exponential phase for *Nostoc* measured through biomass dry weight reaches the exponential phase earlier compared to optical density measurement. This situation differs in *Chlorella* strains, where the biomass dry weight reaches the peak 1 day later compared to the measurement of chlorophyll content when phosphate is lacking in the cultivation. Under treatments with 0.24 mg L^{-1} phosphate, the biomass dry weight fluctuated throughout the growth phases, but the optical density showed a similar pattern compared to treatments without phosphate.

This indicates that the biomass dry weight could not explain most of the changes in the optical density, as both measurements are moderately correlated with each other. The reason behind the moderate correlation between both measurement methods is that the biomass dry weight is measured as the total cell mass, including both viable and dead cells (Wang, n.d.). The fluctuation in the biomass of microalgae cells may be due to the dead cells being counted in

the total biomass. Dead cells were counted in the total biomass and can retain or reduce the biomass through apoptosis or cell shrinkage. As there will be some cells able to adapt to the new cultivation condition, the viable cells will increase the biomass at the same period. The changes in cell viable and cell dead ratio are hypothesized to cause the fluctuation in the cell biomass dry weight. The second reason where biomass dry weight and optical density moderately correlate may be due to the changes in cell structure affected the optical density value (Ross, 2014). The optical density measurement measured the density of microalgae cells in the medium (Beal et al., 2020). However, the chlorophyll content or pigment produced by the cell, and the cell structure, morphology, and size changes throughout the cultivation will affect the optical density measurement (Chioccioli et al., 2014). The increase in viable cells that produce pigments or increase the cell size increased the optical density but the cell biomass remained consistent. Another possible reason could be due to a delay occurring between chlorophyll and cell growth. Chlorophyll is significant for the microalgae growth. It supports oxygenic photosynthesis which absorbs light and performs photosynthesis to derive energy for metabolism (Silva & Lombardi, 2020). The increase in optical density earlier compared to the increase in biomass may be due to the chlorophyll concentration in the microalgae cells increase, thus the performance of the metabolic process will take time to further increase the biomass of the microalgae. A time period was required for the photosynthesis and metabolism process leading to a delay in the increase of biomass observed.

4.4.3 Arsenic enhances the biomass dry weight of *Nostoc* with the absence of phosphate

Results in Section 4.3.1 showed that arsenic can increase the biomass of the *Nostoc* strain when there is a lack of phosphate. The lack of phosphate condition enhances biomass drastically, but the optical density increases gradually. Although the optical density is lower compared to the control, treatments at 0.01 mg L^{-1} As (V) and 1.00 mg L^{-1} As (III) with 0.01 mg L^{-1} As (V) showed similar optical density to the control. All microalgae strains continue their growth throughout the 30 days of cultivation period indicating that they can survive under all 9 different arsenic treatments. Among the 9 different treatments, treatment with a higher concentration which is 1.00 mg L^{-1} for single arsenic species and a total of 1.01 mg L^{-1} for mixed arsenic species treatment, *Nostoc* showed the highest biomass when it was treated with 1.00 mg L^{-1} As (III). Under treatments with the presence of phosphate, *Nostoc* biomass fluctuated indicating that the adaptation of *Nostoc* to the new medium occurs during the lag phase. The biomass of the *Nostoc* treated with arsenic with the presence of phosphate showed a lower growth compared to the control. This indicates that phosphate does not aid the adaptation of microalgae when there is a presence of arsenic, but also reduces the growth in terms of total biomass. The As (III) enhances the *Nostoc* biomass compared ($P < 0.05$) to the control under treatment when phosphate is lacking in the medium. This suggests that phosphate reduces the As (III) impact on the *Nostoc* biomass. In phosphate-depleted conditions, *Nostoc* cells utilise As (III) as a nutrient source (Knauer & Hemond, 2000), and a high phosphate concentration does not protect cells from arsenic toxicity (Knauer & Hemond, 2000). Only 0.01 mg L^{-1} As (III) improves the optical density of *Nostoc* with the presence of phosphate, which also indicates that phosphate does not enhance the optical density of *Nostoc* treated with arsenic. The overall comparison of the growth of *Nostoc* strains concluded that arsenic can increase the biomass of *Nostoc* when there is a lack of phosphate where 1.00 mg L^{-1} As (III) is the highest arsenic concentration treated to *Nostoc* which improved the biomass.

4.4.4 Arsenic improves the growth of *Chlorella* in the absence of phosphate

Results in Section 4.3.1 showed that arsenic reduces the biomass of the *Chlorella* strain when there is a lack of phosphate, and fluctuates the biomass of *Chlorella* throughout the 7 days of cultivation period. Only 1.00 mg L^{-1} As (III) treatment improves *Chlorella* biomass during the initial exponential phase and showed similar biomass during the end of the exponential phase, indicating that this treatment can improve or maintain the *Chlorella* growth. Although the biomass of *Chlorella* increases in different days compared to the control when there is a presence of phosphate, the total biomass of *Chlorella* is still lower compared to the biomass of *Chlorella* treated without phosphate. This indicates that arsenic could not improve the biomass of *Chlorella* for both the presence and absence of phosphate, but only maintain the biomass in both conditions. The optical density of *Chlorella* for conditions with and without phosphate showed a similar pattern and similar exponential phases, indicating that *Chlorella* can adapt to conditions with additional phosphate in a shorter time, in comparison to *Nostoc* strain which showed a significant difference between both conditions. Although the biomass of *Chlorella* still fluctuated, the improvement in growth indicated that *Chlorella* can adapt to the supplied condition. The optical density of *Chlorella* was higher compared to the control when phosphate was lacking, indicating that arsenic can improve the optical density of *Chlorella*. However, this is opposed to conditions with the addition of phosphate, where the optical density was presented in a similar pattern but the value is lower compared to the control. Among 9 different treatments, 0.01 mg L^{-1} As (III) improves optical density the highest, followed by 1.00 mg L^{-1} As (III). Overall, arsenic could not improve the biomass of *Chlorella* but increased the optical density for all 9 treatments. *Chlorella* improves growth better with single As (III) treatment, compared to single As (V) and mixed arsenic treatments.

4.4.5 Arsenic concentration affected the growth of microalgae

Arsenic affecting the microalgae growth was hypothesized to be inversely proportional to the supplied arsenic concentration, where higher arsenic concentration reduces the growth higher compared to the lower arsenic concentrations. However, these results differ from our findings, where some of our results revealed that higher arsenic concentration improves the growth better, while the mid arsenic concentration (0.10 mg L^{-1}) performed lowest in terms of growth. This can be observed when 1.00 mg L^{-1} (highest arsenic concentration) showed a higher or similar biomass and optical density compared to 0.01 mg L^{-1} (lowest arsenic concentration) As (III), while 0.10 mg L^{-1} (mid arsenic concentration) showed significantly lower growth. This outcome was found under As (III) treatments for both *Nostoc* and *Chlorella* cells without phosphate and is unexpected as past research demonstrated growth results are inversely proportional to the arsenic concentrations (Bahar et al., 2016; Wang et al., 2015). These results suggest that microalgae growth is not related to the concentration of arsenic supplied, similar to Das et al. (2023) which stated that *Diacronema lutheri* growth is irrespective of the arsenic concentration as it combats the effect of arsenic stress. Several reasons may explain on the performance of 0.10 mg L^{-1} concentration is lower, (1) 0.10 mg L^{-1} concentration is toxic to microalgae which reduces the biomass of microalgae. A lower concentration of 0.01 mg L^{-1} is not toxic to microalgae cells which does not affect the microalgae growth. (2) 1.00 mg L^{-1} arsenic concentration causes harm to microalgae cells and is sufficient to activate the defence mechanism of the cells. As the defence mechanism of microalgae cells was activated, the toxicity of arsenic was reduced. A lower arsenic concentration might harm the cell and is insufficient to activate the defence mechanism. (3) Low arsenic concentration which does not cause harm to the microalgae may act as a nutrient to the microalgae and improve their growth compared to the mid arsenic concentration. As (V) was hypothesized to substitute in phosphorylation reactions including ATP production, however, the products were unstable and

dissociated rapidly (Yan et al., 2019). Miazek et al., (2015) stated that Cyanobacteria *Nostoc minutum* improved its growth under the presence of 1g L^{-1} arsenic. According to Sakai et al. (2017), 0.1 mg L^{-1} of arsenic was reported in the freshwater of Malaysia. This indicated that microalgae may not be able to improve its growth under low arsenic concentration conditions in Malaysia. Whereas, areas with high microalgae bloom may indicate there is a higher arsenic contamination.

4.4.6 *Nostoc* uptakes higher arsenic concentration compared to *Chlorella*

The overall result demonstrated in Section 4.3.2 clearly showed that *Nostoc* uptakes higher arsenic percentage throughout the cultivation period compared to *Chlorella*. *Nostoc* uptake higher arsenic percentage under As (III) treatment without phosphate and As (V) treatments with the presence of phosphate. These results were fully opposed to the results stated by Zhu et al. (2020), where the cyanobacteria accumulated higher As (III) when phosphate was present compared to As (V). This can be explained when both phosphate and As (V) share a similar structure, and As (V) enters microalgae cells through the phosphate uptake system (Ferrari et al., 2013). Another possible reason phosphate enhances arsenic uptake by *Nostoc* under As (V) treatments could be due to the phosphate concentration used in our study was insufficient to compete with As (V), as the initial phosphate concentration supplied will affect the bioaccumulation concentration of arsenic in microalgae (Bahar et al., 2016). Results stated by Bahar et al. (2016) mentioned that the As (V) uptake is higher compared with As (III) with a lower initial phosphate concentration compared to a higher phosphate concentration. Besides, the presence of phosphate increased the rate of the phosphate channel in the uptake of both phosphate and As (V). The existence of high and low-affinity phosphate transport systems, Pst (Martín & Liras, 2021), and 2 clusters of genes for phosphate transporter on *Nostoc* sp. PCC 7120 genome (Miyashita et al., 2015). Although the characterization of As (V) uptake is not

identified yet, Wang et al. (2015) stated that the channels might be capable of discriminating between As (V) and phosphate. Martín and LirAs (2021) stated that As (V) is toxic at concentrations above 10 mM to bacteria *Streptomyces griseus*, and some mutants resist As (V) up to 100 mM. The mutants are imparted in phosphate transporter, which may lead to higher arsenic concentration uptake with 1.00 mg L^{-1} As (V) treatment. *Nostoc* uptake of higher arsenic concentration treated with As (III) under phosphate-depleted conditions may be due to As (III) entering *Nostoc* via the aquaglyceroporins (Arora et al., 2018). Entering cells through aquaglyceroporins is the result of a concentration gradient, by diffusion (Miyashita et al., 2015), which leads to ease and higher efficiency in arsenic uptake. Currently, there is no article found that relates the presence of phosphate to As (III) uptake by microalgae.

Whereas, *Chlorella* uptake higher arsenic concentrations for low arsenic concentrations under single arsenic species treatment. The *Chlorella* only uptake a higher arsenic concentration during initial cultivation days, but the arsenic uptake is minimal throughout the cultivation period. These results indicate that *Chlorella* could not uptake arsenic into its cells for a longer period. The higher arsenic uptake during the initial days was limited to only 0.10 mg L^{-1} concentration, which may be due to the arsenic being captured into the cells through aquaglyceroporins, and excreted out from the cell (Garbinski et al., 2019). The defence mechanism of *Chlorella* towards the 0.10 mg L^{-1} arsenic was activated and further reduced arsenic uptake into the microalgae cell (Wang et al., 2015). As only 0.01 mg L^{-1} of arsenic concentration were uptake throughout the cultivation period, this concentration may not be harmful to the *Chlorella*. *Chlorella* uptake low arsenic percentage when treated with mixed arsenic treatment conditions for both with and without phosphate. The possible reason is the concentration of mixed arsenic (ranging from 0.2 mg L^{-1} to 1.01 mg L^{-1}) is too high which could not be uptake by *Chlorella*. Another reason is *Chlorella* cannot uptake arsenic when there is the presence of different arsenic species in the medium.

Overall, *Nostoc* performed better in terms of arsenic uptake compared to *Chlorella* cells. *Nostoc* uptake the highest arsenic concentration under 1.00 mg L^{-1} As (III) treatment with a lack of phosphate which also improved its growth under this treatment.

4.4.7 Effect of arsenic on the microalgae cell surface

There are no differences in terms of vegetative cell size (Figure 15) of *Nostoc* cells for both control and treated cells indicating that 1.00 mg L^{-1} As (III) did not alter the cell size. Arsenic concentration was not identified on the surface of *Nostoc* cells for both control and treated cells, indicating that As (III) may not adsorb on the *Nostoc* cell surface. This differs from the statement by Podder and Majumder (2015) and Arora et al. (2018) that arsenic was detected through SEM-EDX. However, the arsenic concentrations used for microalgae arsenic treatments in these papers were higher (50 to 2000 mg L^{-1} and 500 mg L^{-1} respectively) compared to the highest treatments performed under this project (1.00 mg L^{-1}), which may indicate that the arsenic does adsorb on cell *Nostoc* cell surface but the concentration is lower than the detection limit of the SEM-EDX instrument.

Nevertheless, it was clear to see that the surface changes stated in Section 4.3.3 showed that As (III) treatment causes damage to the cell's surface morphology. This result is similar to Arora et al. (2018) and Podder and Majumder (2015), where *Scenedesmus* and *Chlorella pyrenoidosa* cell surfaces appeared to be more ruptured, rigid textures, and corrugated compared to the control cells which showed smooth structure. The changes in surface structure could be due to the arsenic exerting oxidative stress that damages the microalgae lipids (Xiao et al., 2022), which is the component that forms the microalgae membrane (Poulhazan et al., 2020). Besides, the accumulation of arsenic on the cell wall causes the surface to be coarser compared to cells without arsenic treatment (Podder & Majumder, 2015).

Although the results in Sections 4.3.1 and 4.3.2 prove that As (III) improves the *Nostoc* growth and arsenic uptake, damage was observed on the cell surface indicating that *Nostoc* may not uptake arsenic or continue its growth for a longer period. Long-term observation of the cell surface structure will be required to identify if the damage was irreversible, the period that the cells can improve or maintain their growth, and the uptake of arsenic.

4.5 Conclusion

In this Chapter, it is concluded that the results have proven the optical density of microalgae is moderately correlated to the biomass dry weight. Besides, the addition of phosphate after pre-treatment will prolong the lag phase of the microalgae or cause fluctuation in the growth, as microalgae require a longer period to adapt to the new cultivation condition. The adaptation of *Chlorella* on phosphate supplied condition is shorter compared to *Nostoc* in terms of optical density measurement. Furthermore, As (III) at higher concentration enhances the biomass and arsenic uptake of *Nostoc* when there is a lack of phosphate. The phosphate supplied to the microalgae does not reduce the effect of As (V), indicating that the microalgae may be able to differentiate As (V) and phosphate. Lastly, there may be other mechanisms or uptake pathways of As (III) involving phosphate as phosphate was proven to affect As (III) uptake and entering the microalgae cells.

CHAPTER 5

METABOLIC PATHWAY AND SPECIFIC GENE EXPRESSION ANALYSIS OF *NOSTOC* MUM003 STRAIN IN RESPONSE TO ARSENIC TOLERANCE

5.1 Introduction

Nostoc is a cyanobacteria group under the family Nostocaceae. Studies have proven that *Nostoc* can uptake and metabolize or reduce the toxicity of arsenic. Research outcomes from Chapter 4 clearly discuss the effect of different species and concentrations on microalgae growth and arsenic uptake. In this Chapter, the treatment which is 1.00 mg L^{-1} As (III) under phosphate-depleted conditions was further studied to understand the molecular mechanism of *Nostoc* related to arsenic.

5.1.1 Arsenic enters *Nostoc* cells via transporter and diffusion

According to Ramanan et al. (2000), As (V) enters the cyanobacterial cells through the phosphate transporters. As both phosphate and As (V) share the same transport channel, high phosphate concentration conditions will lead to competitive binding to the active site of ArsC and the phosphate transport system (Zhang et al., 2014). The As (V) located inside the cell will be reduced to As (III) by the ArsC enzyme and extruded to the extracellular through the ArsB. Whereas, As (III) is taken up by the cells through diffusion, and will bind to cysteine-rich compounds to reduce its toxicity. Besides redox reaction and complexation, inorganic arsenic was methylated and formed organoarsenicals which involves methylation with *S*-adenosylmethionine (SAM). The methylated arsenic species were MA(V), DMA(V), trimethylarsine, and oxo-arsenosugars. This methylation process is also the detoxification mechanism of arsenic found in cyanobacteria (Ramanan et al., 2000). According to Ramanan

et al. (2000), cyanobacteria possess a main difference compared to other algae where they are lacking with organelles such as vacuoles to sequester As (III)-thiol conjugates.

5.1.2 Other arsenic-related genes

There are several genes involved in arsenic bioremediation. Rosen (2002) stated that As (III) can be uptake through the homolog of GLpF by *Escherichia coli* and *Saccharomyces cerevisiae*, which is also a metalloid transporter. The transporters for As (III) are Acr3p and Ycf1p. The AQP7 and AQP9 cRNA will increase the transportation of As (III), which suggests that only some of the aquaglyceroporins transport As (III) (Rosen, 2002).

The *Ars* genes also show their importance in the detoxification of arsenic in certain bacteria species. The chromosome or plasmid of bacteria consists of the *ars* operons. They mainly confer the inorganic arsenic detoxification and are correlated with other arsenic-related genes to reduce the toxicity of organoarsenicals (Yan et al., 2019). *Ars* genes comprise 3 genes i.e. arsB, arsH (unknown protein), and arsC, in the form of *arsBHC* operon activated by ArsR. The arsB and arsC genes are found in various sequenced cyanobacteria including *Synechocystis* sp. PCC 6803, *Synechococcus* sp. PCC 7942, and *Anabaena variabilis* (Miyashita et al., 2015). The *arsC* encodes for the reduction of As (V) (Zhang et al., 2014), with two *arsC* genes, arsl1 and arsl2 encoding for As (V) reductase (Miyashita et al., 2015), while the *acr3* gene encodes for As (III) efflux pump (Zhang et al., 2014). There is also a cluster of 4 genes i.e. ars1102 (arsB), all1103 (arsR), alr1104 (hypothetical protein) and alr1105 (As(V) reductase). The arsB homolog and alr1097 (multidrug efflux protein) were identified as the upstream of ars1102, which plays a role in multiple processes i.e. detoxification, survival, and expression under arsenic stress conditions (Miyashita et al., 2015). Besides the *Ars* gene, the *arx* gene was also found involved in the As (III) oxidation system through combination with nitrate respiration or

integration with the electron transport chain of anoxygenic photosynthesis reaction (Andres & Bertin, 2016). As (III) extruded from the cell utilizing two mechanisms, the carrier-mediated efflux via As (III) carrier protein, and the membrane-bound protein (Miyashita et al., 2015), As (III)-translocating ATPase (ArsB) (Rosen, 2002).

The current deficiency in understanding the arsenic-related pathways of microalgae underscores a critical knowledge gap that needs to be addressed for comprehensive insights into the role of microalgae in arsenic bioremediation. This chapter aims to identify arsenic-related genes within in *Nostoc* whole genome sequence and identify the regulation of arsenic-related genes.

5.2 Methodology

Based on results reported in Chapter 4, *Nostoc* showed an improvement in terms of growth and arsenic uptake treated under 1.00 mg L^{-1} As (III) without phosphate for a period of 24 days. Hence, the same treatment was performed in this Chapter to reveal further the possible detoxification mechanism that occurred in the *Nostoc* strain.

5.2.1 Working cultures

The working strain for *Nostoc* cultivated for 14 days was collected and pre-cultivated in BG-11 medium without phosphate for 5 days to eliminate possible phosphate retained in the cells. A 1.00 mg L^{-1} As (III) concentration added to the *Nostoc* cultures in fresh BG-11 medium without phosphate were cultivated for 24 days in a 2 L Erlenmeyer flask. Duplicates for both treated and control cultures were prepared for the analysis (Danish et al., 2013).

5.2.2 RNA extraction using the kit method vs Trizol method

After 24 days of cultivation, 1 L of the *Nostoc* cultures for each flask were collected for RNA extraction. Two different RNA extraction methods involving ZymoBIOMICS RNA Miniprep Kit (Zymo Research, United States) and Tri-RNA reagent (Favorgen, Austria) were performed to compare the efficiency of the extraction method. Both methods were performed according to the manufacturer's protocol.

For the RNA extraction method involving an RNA extraction kit, the reagents and steps involved are as below:

a. A 750 µL of DNA/RNA Shield was added to approximately 100 mg of *Nostoc* sample in a ZR BashingBead Lysis Tube and cap tightly.
b. The cell lysis was performed through mechanical homogenization in a high-speed bead beater for 5 minutes
c. A 400 µL of the supernatant was transferred to a nuclease-free tube
d. A 400 µL of RNA Lysis Buffer was added to the supernatant and mixed well
e. Another 800 µL of 95% ethanol was added to the lysis buffer and mixed well
f. The mixtures were transferred into the Zymo-Spin IIICG Column in a collection tube and centrifuged at 10000 xg for 30 seconds. The flow-through were discarded
g. A 400 µL RNA Prep Buffer was added to the column and centrifuge. The flow-through were discarded. This step was repeated once with the same volume of RNA Wash Buffer
h. The column was transferred to a nuclease-free tube
i. A 85 µL ZymoBIOMICS DNase/RNase-Free water was added to the column matrix and centrifuged at 10000 xg for 30 seconds
j. A 10 µL of DNA Digestion buffer and 5 µL of DNase I was added and mixed through inversion. This mixture was incubated at room temperature for 15 minutes
k. A 200 µL RNA Lysis buffer was added to the sample and mixed. The mixture was added with 300 µL of 95% ethanol and mixed thoroughly
l. All mixtures were transferred to a new Zymo-Spin IIICG Column in a collection tube and centrifuged at 10000 xg for 30 minutes. The flow-through was discarded
m. A 400 µL RNA Prep buffer was added to the column and centrifuged at 10000 xg for 30 seconds, and the flow-through was discarded. This step was repeated with 700 µL of RNA wash buffer

n. Another 400 µL of RNA Wash buffer was added and centrifuged at 10000 xg for 1 minute
o. A 100 µL ZymoBIOMICS DNase/RNase-free water was added to the column and centrifuge at 16000 xg for 3 minutes.

For the RNA extraction method using Tri-RNA reagent, the reagents and methods were performed as follows:

a. A 1 mL of Tri-RNA Reagent was added to approximately 100 mg of *Nostoc* cells.
b. The *Nostoc* tissues were homogenized using a glass-Teflon. The homogenates incubate for 5 minutes at room temperature
c. A 0.2 mL of chloroform was added to the homogenate and mixed vigorously, followed by centrifugation at 12000 rpm for 3 minutes to separate the phase
d. The clear upper aqueous phase containing RNA was carefully transferred to a clean tube
e. 1X volume of the isopropanol was added, and the samples were vortexed, and incubated at room temperature for 10 minutes. Incubated samples were centrifuged at 12000 rpm for 15 minutes
f. The supernatants were discarded and the RNA pellet was washed with 0.5 mL ice-cold 70% ethanol
g. The washed samples were centrifuged for 1 minute and the supernatants were removed carefully
h. A brief spin was performed to ensure that the RNA pellet was precipitated and residue supernatant was carefully removed
i. The dried RNA pellet was resuspended in 50 µL of TE buffer

5.2.3 RNA concentration, purity, and integrity analysis

The concentration and absorbance of RNA were checked through the NanoDrop spectrophotometer (Thermo Fisher Scientific, Malaysia), and the elution buffer for RNA extraction was used as a blank for calibration. The purity and integrity of the RNA were analysed using gel electrophoresis method. The gel was prepared using 1% agarose gel (Vivantis Technologies, Malaysia) and TBE buffer (Apical Scientific, Malaysia). Before loading the RNA into the gel, the RNA was heated at 90 ^{o}C for 1 minute and cooled on ice for 1 minute to minimize the formation of the secondary structure. A 1 µL of 6X Loading dye (SMOBIO Technology, Taiwan) was then added to the RNA to allow tracking of the sample. The 10 kb ladder (SMOBIO Technology, Taiwan) was loaded to the same gel as the reference of the RNA size (Rivera, 2023). The gel was run at 100 W for 35 minutes and loaded onto the UV tray and observed under the GelDocEZ instrument (BioRad, California)

5.2.4 Predicting RNA related pathway

The Whole Genome Sequence (WGS) of *Nostoc* (PRJNA1069320) was assembled and annotated through the Galaxy tool (https://usegalaxy.org/). The proteins, RNA, genes, and compounds presented in the *Nostoc* genome were predicted using the standalone Biocyc Pathway tool v27.0 (https://biocyc.org/). To identify the overview pathways presented in *Nostoc*, the database of the *Nostoc* was first built using the PathoLogic function with the annotated gene bank and fna file downloaded from the Galaxy tool result. The arsenic-related genes and pathways were viewed from the overview figure or the compound search bar.

5.2.5 Primer design

Arsenic-related genes were identified and primers were designed to identify the regulation of the targeted genes. The sequence from the FastA file in the nucleic acid sequence was selected and the Primer3Plus tool (https://www.bioinformatics.nl/cgi-bin/primer3plus/primer3plus.cgi) was used to design all targeted primers. Designed primers were purchased from Apical Scientific (Malaysia).

5.2.6 PCR analysis

To identify the regulation of the targeted genes, PCR analysis was performed to check for the presence of the bands. The cDNA required for PCR was synthesized using the OneScript Hot cDNA synthesis kit (ABM, United States) according to the manufacturer's protocol. A 2 µL of RNA was added to a mixture of 4 µL 5X RT Buffer, 1 µL dNTP, 1 µL of forward and reverse primer each, 1 µL of OneScript Hot RTase, and 10 µL of nuclease-free distilled water. The mixture was incubated for 15 minutes at 60 ^{o}C followed by 85 ^{o}C for 5 minutes and kept on ice. The PCR sample for analysis was prepared using the REDiant II PCR Master Mix (Apical Scientific, Malaysia) according to the manufacturer's protocol. A 1 µL of cDNA sample synthesized was added to a mixture of 25 µL of REDiant 2X PCR Master Mix, 1 µL of forward and reverse primer each, and 22 µL of nuclease-free distilled water. The PCR mixtures were amplified under conditions of initial denaturation at 95^{o}C for 3 minutes, denaturation at 95^{o}C for 1 minute, annealing at 63^{o}C (depending on the primer set) for 1 minute, extension at 72^{o}C for 2 minutes (depending on the primer length), and a final extension at 72 ^{o}C for 10 minutes. The denaturation to extension step was repeated for 35 cycles. All PCR products were run through 1% agarose gel electrophoresis.

5.3 Results

In this section, the RNA extraction using the kit method and Trizol method will be compared to indicate the method which is more suitable for microalgae. Additionally, the primer designed from the *Nostoc* whole genome sequence and the genes expressed from the RNA will be discussed in this section.

5.3.1 RNA concentration and purity

The RNA of *Nostoc* was first extracted using the kit method and the results were shown in Table 8. Unfortunately, the RNA concentration is much lower than required and the absorbance of the RNA exceeds the range required for RNA quality. The highest RNA extracted using the kit method is only 149.0 ng μL^{-1}, while the A260/230 did not fall within the required range which is 2.0-2.2.

The *Nostoc* RNA was then extracted using the Trizol method (Table 9). A higher RNA concentration ranging from 983.2 ng μL^{-1} to 2410.3 ng μL^{-1} was extracted. However, most of the absorbances of A260/280 and A260/230 exceed the required range. A DNase treatment was performed to eliminate gDNA contamination during the RNA extraction. The remaining RNA concentration ranged from 256.2 ng μL^{-1} to 853.1 ng μL^{-1}, where all RNA samples reduced in concentration. All absorbance on A260/280 increased but exceeded 2.0, and all A260/230 improved and fell within the acceptable range

Table 8. Microalgae RNA extraction using the kit method

Treatments	RNA concentration (ng/µL)	A260/280	S260/230
Control	63.3	1.88	0.85
	47.0	1.81	0.90
1.00 mg L^{-1} As (III)	149.0	2.11	1.08
	78.2	2.16	2.10

*Minimum requirement for RNA sequencing is ≥100 ng/µL for ≥ 20 µL, A260/280 ranged between 1.8-2.0, A260/230 ranged between 2.0-2.2

Table 9. Microalgae RNA extraction using the Trizol method

Treatments	RNA concentration (ng/µL)	A260/280	A260/230
Before DNase treatment			
Control	983.2	1.57	0.62
	1915.2	1.83	0.55
1.00 mg L^{-1} As (III)	1483.8	1.98	1.22
	2410.3	1.81	0.51
After DNase treatment			
Control	630.3	2.12	1.91
	512.9	2.09	1.95
1.00 mg L^{-1} As (III)	256.2	2.10	1.97
	853.1	2.15	1.99

*Minimum requirement for RNA sequencing is ≥100 ng/µL for ≥ 20 µL, A260/280 ranged between 1.8-2.0, A260/230 ranged between 2.0-2.2

5.3.2 RNA purity and integrity

The RNA of *Nostoc* stock culture cells were extracted using the Trizol method to identify the suitability of the extraction method. The RNA was examined with gel electrophoresis (Figure 18). All RNA from the stock culture showed clear bands but gDNA was identified. This indicates that the Trizol method is suitable for RNA extraction, however, there is a need for DNase treatment to eliminate DNA contamination from the RNA.

The RNA of *Nostoc* cells treated with control and As (III) treatments were extracted using the exact method as for the stock culture and the RNA were examined with gel electrophoresis (Figure 19). Both the control and treated *Nostoc* RNA showed faint bands compared to the stock culture. Another cultivation was performed to compare the stock cultures, control treatment, and As (III) treatments for 24 days, and all extraction and gel electrophoresis for the cultures were run simultaneously to identify the differences between these treatments. The stock culture (labelled as X1 and X2) showed clear bands, while both control and treated *Nostoc* RNA showed fully degraded 23s and 16s rRNA.

The RNA extracted using the kit is shown in Figure 20. The RNA extracted using the kit method showed a more intact band compared to the Trizol method. Besides, DNA contamination was fully eliminated from the RNA.

The selection of suitable extraction methods plays a vital role in obtaining high-quality RNA, influencing the subsequent analysis. Optimal RNA quality and concentration enhance the efficacy of ensuring downstream processes such as PCR analysis or sequencing. Working with subpar RNA may compromise the proceeding applications characterized by labour-intensive processes, extended time requirements, low-quality results, and heightened expenses.

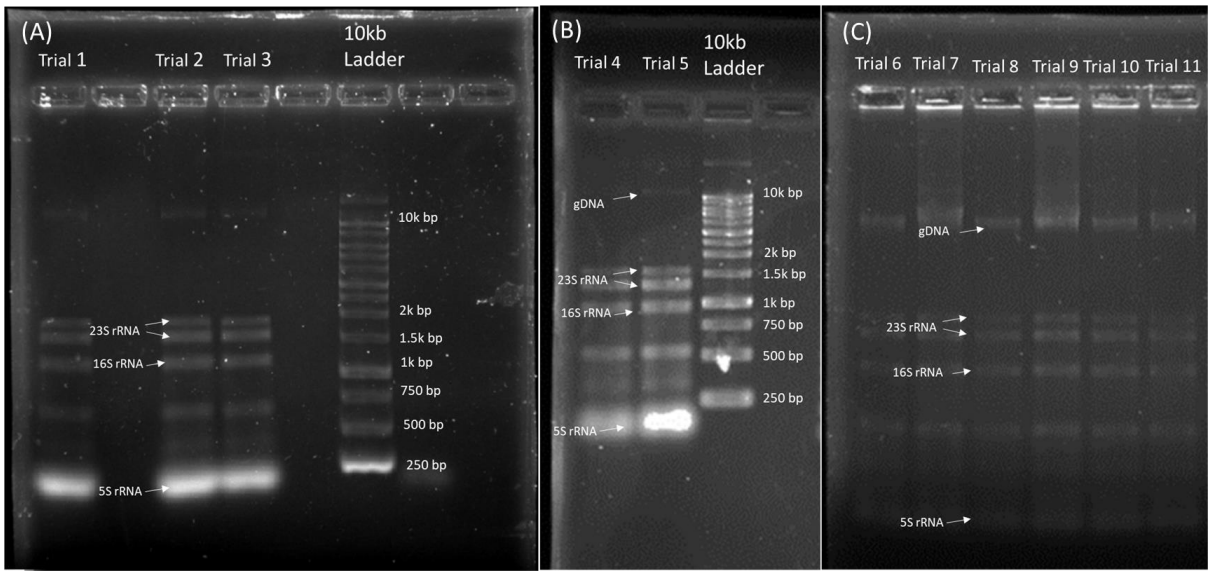

Figure 18. RNA of *Nostoc* stock samples performed without any treatments. All RNA showed a clear and sharp band.

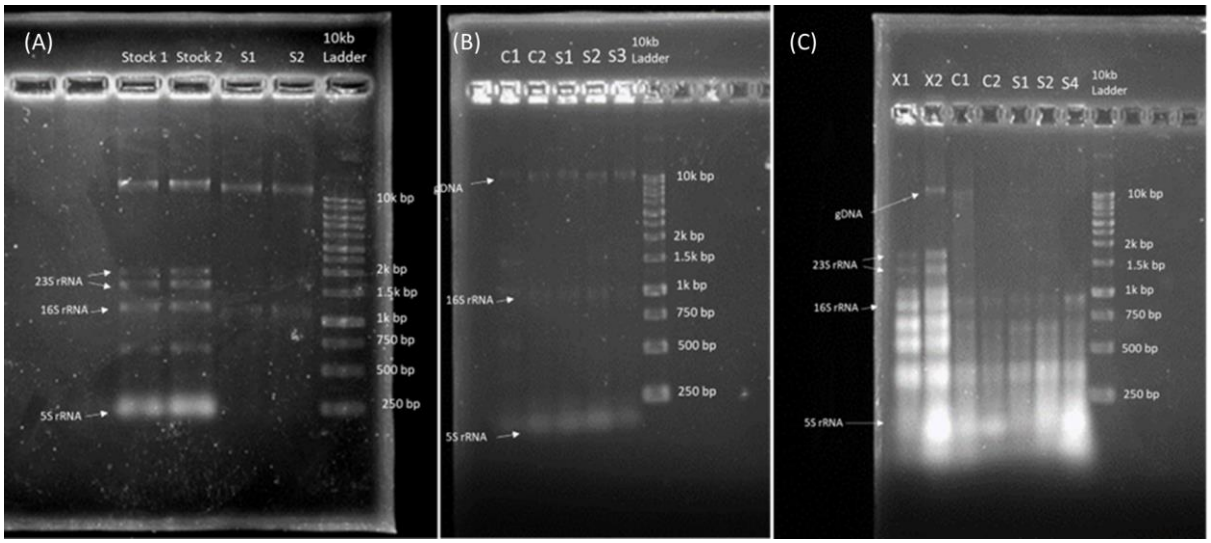

Figure 19. RNA of *Nostoc* samples for stock culture and As (III) treated samples (A) Controlled samples and As (III) treated samples (B), normal cultivation conditions, controlled samples, and As (III) treated samples (C). All control and As (III) treated samples showed faint bands compared to stock samples and 16s and 23s rRNA were nearly invisible.

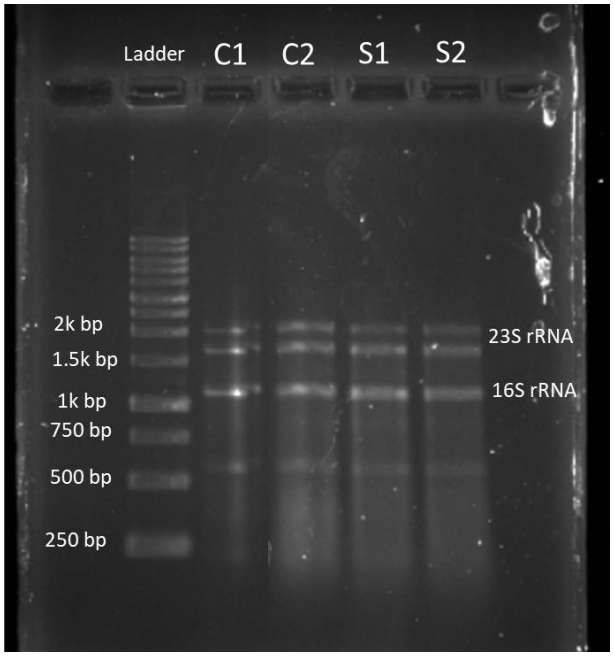

Figure 20. RNA of *Nostoc* samples for Controlled samples (C1 and C2) and As (III) treated samples (S1 and S2). All samples showed clear 16s and 23s rRNA.

5.3.3 Predicted pathways involving As (III) metabolism in *Nostoc*

From the results generated through the Pathway tool, *Nostoc* consists of multiple compounds related to As (III). The main compounds or enzymes found in the *Nostoc* related to As (III) were arsenical pump-driving ATPase (arsA), arsenite metallochaperone (ArsD) complex, arsenic triglutathione, arsenite methyltransferase (arsM), and methylarsonous acid.

Additionally, there are 3 main pathways found in the *Nostoc* whole genome sequence. The arsenical pump-driving ATPase (arsA) transporter shown in Figure 21 exports arsenic out from the cell through the reduction of ATP. Besides, the arsenite-[ArsD arsenite metallochaperone] complex (Figure 23) was also identified as another transporter which is similar to arsA transporter where it also utilizes the ATP to excrete arsenic from the cell. Arsenic triglutathione was also found in the *Nostoc* cells where it methylates the arsenite through the addition of reduced thioredoxin and binds to *S*-adenosyl-L-methionine (SAM) to reduce the As (III) toxicity.

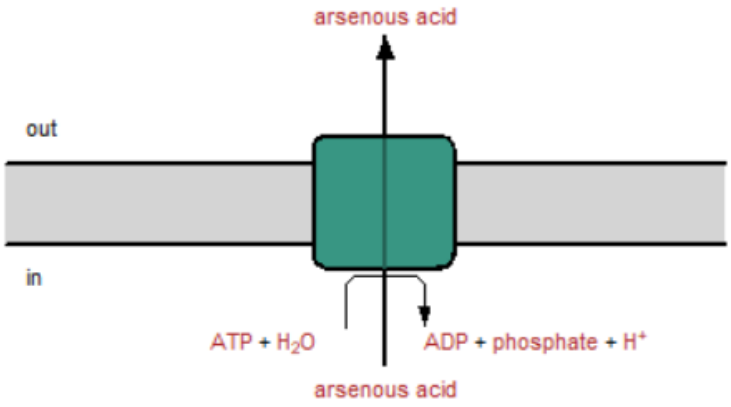

Figure 21. Arsenical pump-driving ATPase (arsA) transporter

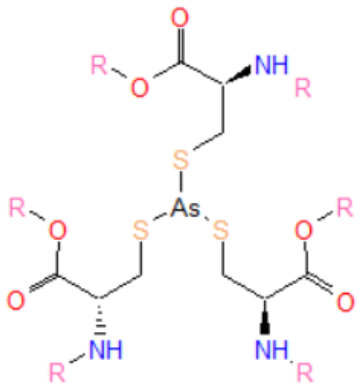

Figure 22. The chemical structure of Arsenite metallochaperone complex (ArsD)

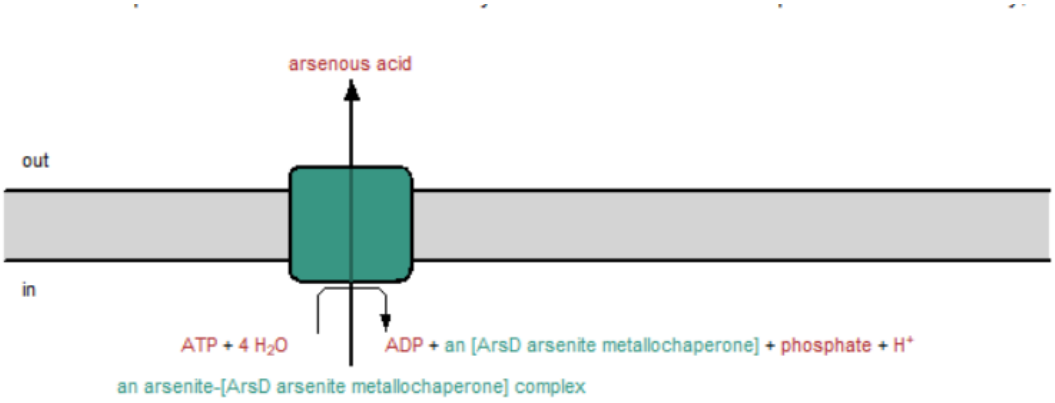

Figure 23. ArsD with As (III) excrete arsenous acid through ArsA transporter

5.3.4 Primer design

Six primers were designed to identify the possible genes regulated by *Nostoc* when treated with As (III) for 24 days. The primers are selected as stated in Table 10 according to the possible pathways predicted from the Whole genome sequence. A housekeeping gene was designed based on the 16s rRNA as the reference primer to identify the expression of genes as this gene will express under both normal and pathophysiological conditions. Past research (Khuntia et al., 2014) has shown As (III) oxidized to As (V) and reduces arsenic toxicity. Hence, the Acr3 gene was designed to identify the presence of As (V) in the cells. The ArsA and ArsB which belongs to the Ars pathway were selected to identify which transporter was utilized by *Nostoc* to excrete As (III) from the cell. The arsenite methyltransferase gene was targeted to identify the methylation process of As (III) in the cells. Whereas, the GST gene was designed to identify the synthesis of GSH for the As (III) detoxification through the formation of arsenic triglutathione.

Table 10. Details of primer sets designed

Primer set	Gene	Gene size (bp)	Function	Primer sequence	Justification behind gene selection
1	16S rRNA	537	Housekeeping gene	F: TGTCGTCGTCTATCACAACC R: CCGATGCGTCCACCACTT	As a reference primer to identify the expression of genes from the RNA
2	Arsenical resistance protein, Acr3	558	Arsenate mycothiol formation	F: GGTGAAGCCGTTTTCCATGG R: CGATTGAGCAGGTAGGCGAT	To identify the formation of As (V) through oxidation in the *Nostoc* cell
3	Arsenical pump-driving ATPase, ArsA	304	Arsenite extrusion pump	F: CGATGATGCAGCTCCAGGAT R: ACAAGGGCGAGCAGTTTCTC	To identify the pathway of As (III) removal
4	Arsenical pump membrane protein, ArsB	526	Arsenite extrusion pump	F: CCATACTGGACCTTGGTTCG R: CCGCAGGTAATCATCCAACT	To identify the pathway of As (III) removal
5	Arsenite methyltransferase	531	Methylation of Arsenite	F: TGTCGAACCTCGTCAACATC R: GGCCATAGACGACCAGGTA	To identify As (III) methylation process
6	Glutathione-S-transferase, GST	230	Production of GSH	F: GCCTGTCAGCAGAAGAGTGA R: GGCCTGATAGTTCAGGACCA	To identify the synthesis of GSH

5.3.5 Presence of gene expression

All 6 sets of primers were run with PCR analysis to identify the expression of genes and predict the possible pathways of As (III) metabolism in the *Nostoc*. The results illustrated that all RNA samples (both treated and control) showed a clear band for the housekeeping gene (Figure 24). This indicates that the gene regulated were expressed and the housekeeping gene is suitable as the reference point for expression level analysis. Among multiple arsenic-related genes and the GST gene, only the arsenite methyltransferase gene (Figure 25) showed a faint band in the gel. This suggests that a methylation process occurs in the *Nostoc* cell to reduce the As (III) toxicity compared to extrusion through the Ars transporter or binding to glutathione.

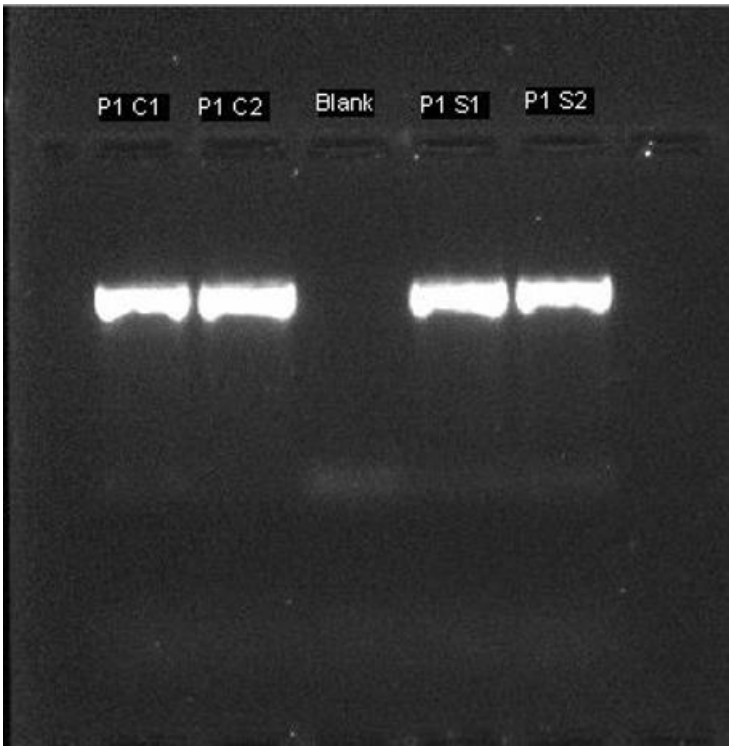

Figure 24. All treatments and controls showed clear bring bands for the first primer sets (housekeeping gene). P1C1 and P1C2 represent the control samples, whereas P1S1 and P2S2 represent the treated samples.

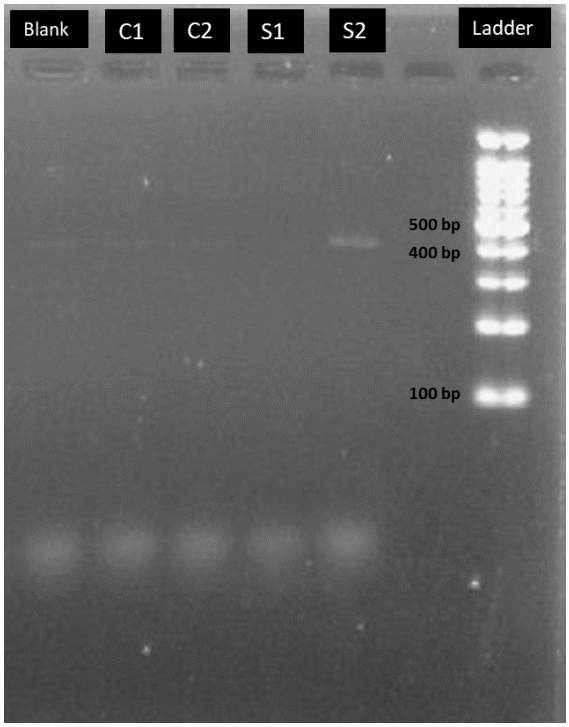

Figure 25. PCR gel electrophoresis image for Primer 5 (Arsenite methyltransferase)

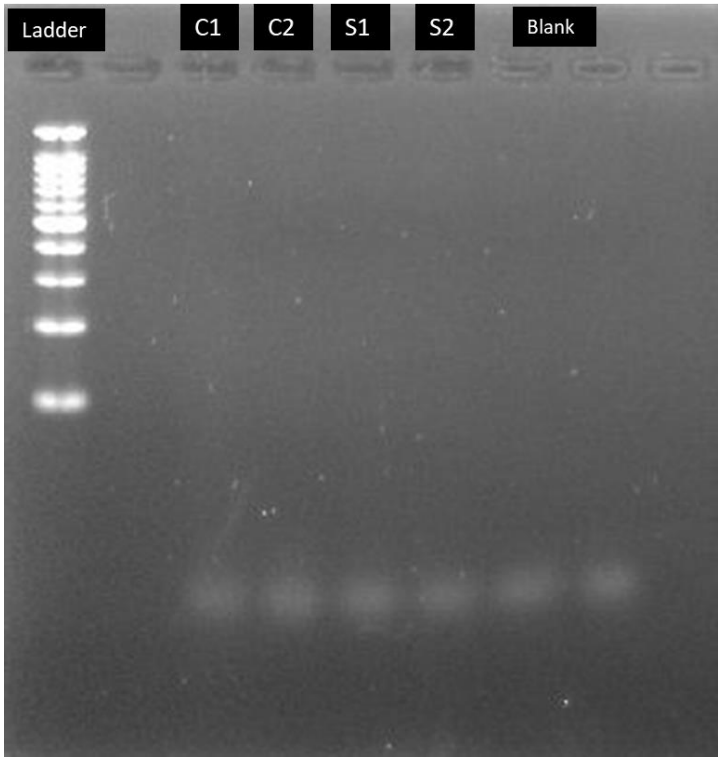

Figure 26. PCR results for primer sets without bands. The Primer set for Acr3, ArsA, ArsB, and GST does not show any bands, indicating that the *Nostoc* does not regulate these genes.

5.4 Discussion

Results in Chapter 4 showed that 1.00 mg L^{-1} As (III) treatment without phosphate increases the growth of *Nostoc* and arsenic uptake compared to the control and other treatments. Under this treatment, cultivation on the 24th day showed the highest arsenic uptake. Hence, the possible metabolic reaction of As (III) uptake by *Nostoc* will be discussed in the following discussion section.

5.4.1 The kit method is more suitable for RNA extraction but a higher initial sample volume is required

Results in Section 5.3 showed that the RNA concentration extracted with the Trizol reagent was higher compared to the kit extraction method. This is similar to Poong et al. (2017), where the RNA concentrations extracted using the Trizol method are higher (ranges from 5.42 to 6.07 ng μL^{-1}), and extraction using the kit method showed concentrations below the detection limit measured using the Qubit instrument. This is due to the RNA being trapped in the column used in the kit causing leftover RNA could not be collected as the final product. Although the Trizol method showed RNA with higher concentration, DNA contamination was found in the RNA sample. An additional DNase treatment will be required to eliminate the DNA contamination, which will highly reduce the RNA concentration. Besides, in some treatments, DNA could not be fully removed from the RNA. As the presence of DNA will interrupt the downstream process, a repetition of DNase treatment will be required which increases the risk of RNA degradation. All samples extracted using the kit method showed a clear RNA without DNA contamination. Hence, the Trizol method will be more suitable if the quantity of the initial sample volume is low, however, the kit method will be preferred to obtain the pure RNA.

5.4.2 Carbohydrate carryover reduces the RNA absorbance

The requirement of RNA sequencing is where the absorbance of A260/280 ranged between 1.8-2.0, whereas, the absorbance for A260/230 ranged between 2.0-2.2. It is clearly seen that RNA extracted using both the kit method and the Trizol method showed the absorbance at A260/230 significantly lower compared to the required value. According to Thermo Fisher Scientific, the occurrence of a low A260/230 ratio may be due to the carbohydrate carryover from the sample. This situation often occurs in plant samples, hence, microalgae which share similar characteristics to plants may encounter a similar problem. Apart from carbohydrate carryover, the phenol or guanidine leftover from the RNA extraction and glycogen used for precipitation may also lead to a poor A260/230 ratio. Thanh et al., (2009) reported that the RNA extraction of *Ankistrodesmus convolutes* using phenol and chloroform resulted in clear but slightly smear RNA bands the A260/280 absorbance is within 1.79 to 1.86 in an acceptable range however, the A60/230 which explained the purity of RNA was not discussed. The RNA extraction for *Chlorella* species using 0.1% diethyl pyrocarbonate, Trizol method with the additional sodium chloride or potassium acetate, and using the PureLink RNA mini standard kit were performed to compare the efficiency of the methods (Poong et al., 2017). The overall outcome stated that the Trizol method with the addition of potassium acetate and liquid nitrogen for the sample preparation showed the highest yield. Whereas, the method without liquid nitrogen and the kit method showed a significantly low yield. The methods involving Trizol showed an optimal A260/280 absorbance, ranging from 1.73 to 1.95, however, the absorbance for the kit method is significantly lower which is at 1.36. All methods for the RNA extraction showed the A260/230 ratio exceeded the required range. The absorbance for the Trizol method without liquid nitrogen ranges between 0.5 to 0.23, and the same method included performed with liquid nitrogen are 1.56, 2.40, and 2.45. Whereas, the absorbance for the kit method is 0.19. These results showed similarities to this project, where both the reagent

method and kit method could not provide an optimal absorbance for the RNA measured at A260/230.

5.4.3 Arsenic-related pathways in *Nostoc*

The 3 main arsenic-related pathways analysed from the *Nostoc* whole genome sequence were arsA transporter, arsD transporter, and arsenite methylation.

5.4.3.1 Arsenical pump-driving ATPase (arsA)

According to Jekel and Amy (2006), the predominant arsenic species found in the natural water sources is As (III), which is also stated as arsenous acid, arsenite. Whereas, another oxidation state is As (V), which is also known as arsenic acid, arsenate. Arsenical pump-driving ATPase (arsA) is a transporter belonging to the Ars family. This enzyme contains 2 subunits, which form the channel part and the ATP binding site. As (III) was removed from the cell cytoplasm through the arsenite efflux pump in the Nostoc cell.

5.4.3.2 Arsenite metallochaperone complex (arsD)

ArsD metallochaperone (Figure 28) is a protein which involved in the detoxification of arsenic. It transfers the As (III) to the Ars efflux pump i.e. ArsA and ArsB. The ArsA and ArsB showed similar functions which excrete As (III) from the cell. The main difference is the involvement of ArsD, where As (III) can be excreted with and without ArsD through the ArsA transporter, whereas, ArsD is required to excrete arsenous acid through the ArsB transporter. According to Lin et al (2022), ArsD improves the binding of As (III) to ArsA, hence increasing the affinity and arsenic extrusion when As (III) is at a lower concentration. ArsD is involved in the arsA transporter reaction, where this reaction also utilizes the ATP and forms ADP to excrete

arsenous acid from the cell. Besides of ArsA transporter, ArsD also reacts with arsenic triglutathione to form ArsD complex and glutathione

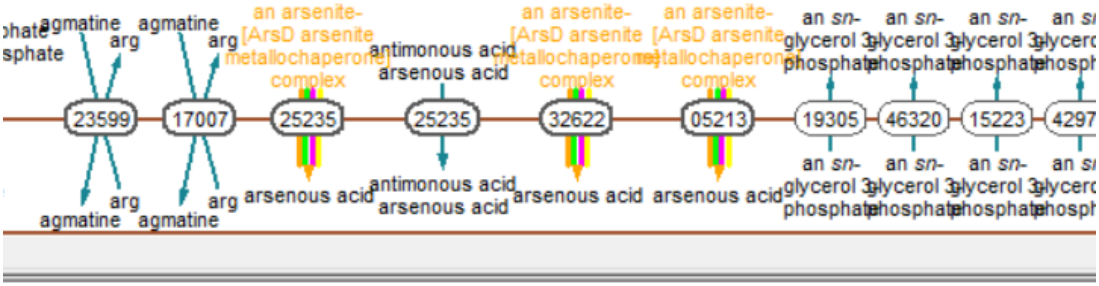

Figure 27. The overview of ArsA transporter without ArsD (25235) and with ArsD (32622)

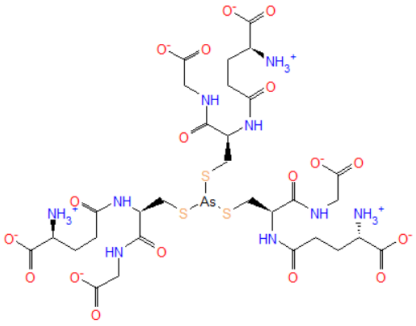

Figure 28. Chemical structure of arsenic triglutathione

5.4.3.3. Arsenite methyltransferase (ArsM) and arsenic triglutathione

Arsenite methyltransferase is a protein that catalyses methylation of As (III) to S-adenosyl-L-methionine (SAM). It binds As (III) to three thiols to form arsenic triglutathione. Arsenic triglutathione is an organic thioarsenocal compound formed by arsenous acid with 3 glutathione. The formation of arsenic triglutathione from arsenous acid and glutathione is reversible with the addition of arsenite methyltransferase. Arsenic triglutathione involves in the methylation of arsenite through the addition of reduced thioredoxin and binds to S-adenosyl-L-methionine (SAM). It forms the pentavalent methylarsonate and is further reduced to an enzyme-bound methylarsonous acid by electrons from thioredoxin. The enzyme

will undergo methylation forming pentavalent cacodylate intermediate and reduced to dimethylarsinous acid. The products of the methylation process were trimethylarsane (TMAs), methylarsonous acid, dimethylarsinous acid (DMAs), and arsenite methyltransferase.

5.4.4 Arsenite methylated in *Nostoc* after 24 days of cultivation without the presence of phosphate

The results in Section 5.3.3 overall summarized the possible pathway of *Nostoc* in reducing the toxicity of As (III). The 3 main pathways involved are (1) removal of As (III) to the extracellular utilizing ArsA and/or ArsB transporter with or without arsenite metallochaperone (ArsD), (2) Methylation of As (III) through binding to S-adenosyl-L-methionine (SAM) to form methylated arsenic which has lower toxicity, and (3) formation of arsenic triglutathione through binding of As (III) to glutathione to lower the toxicity of As (III) to the *Nostoc* cell.

Among the 3 different pathways involved, the Ars transporters require the utilization of ATP to extrude arsenous acid. The *Nostoc* was starved with phosphate for 5 days in advance and removed from the BG-11 medium during the treatment period. Hence, lack of phosphate in the *Nostoc* cell may minimize the formation of ATP, thus leading to the Ars pathway was not regulated on day 24 cultivation with the presence of As (III).

The pathways involving methylation and GSH do not involve phosphate in the reaction. GSH plays multiple roles in the detoxification of stress-inducing factors, i.e. reactive oxidative species (ROS), peroxides, and heavy metals (Jozefczak et al., 2012). The results shown in Section 5.3.4 demonstrated that As (III) may undergo a methylation process for detoxification instead of binding to GSH. This may due to the formation of GSH is not being sufficient to support all detoxification processes, leading to a competition of GSH in those reactions, hence, the methylation process occurred to reduce the toxicity of As (III) in *Nostoc*. Besides, the formation of arsenic triglutathione occurred before the methylation process. As the RNA

extraction was performed on day 24, the binding of As (III) to GSH may have occurred earlier, whereas the methylation process occurred during the culture collection period. The arsenic concentration showed higher (Chapter 4) on day 24 compared to the initial cultivation period may be due to the ATP required for the Ars transporter being utilized during the initial cultivation period. As ATP was reduced and lacking during the late stages of cultivation, the extrusion through the Ars transporter could not be performed thus reducing the arsenic removal rate (*Oxidative Phosphorylation*, n.d.) from the *Nostoc* cells and leading to high arsenic concentration detected in the cell. This formed a new hypothesis where phosphate affected the arsenic accumulation concentration in the *Nostoc* cell by inhibiting the As (III) extrusion pathway which required ATP.

5.5 Conclusion

In this Chapter, it is concluded that there are 3 main arsenic-related pathways to reduce the arsenic toxicity in *Nostoc*. The 3 main pathways were direct extrusion of the As (III), As (III) methylation to SAM, and binding As (III) to GSH to form complexes. *Nostoc* MUM003 strain reduces the arsenic toxicity through the methylation process after treat with As (III) without phosphate for 24 days. The pathways associated with arsenic may exhibit reduced effectiveness in the absence of phosphate conditions, providing a new hypothesis on the effect of phosphate on intracellular arsenic concentration when *Nostoc* was treated with As (III). The As (III) extrusion pathways required ATP to release arsenic from the cell, hence this pathway fails to regulate under phosphate-depleted conditions, further leading to higher arsenic concentrations accumulated in the cells.

CHAPTER 6

SUMMARY, GENERAL CONCLUSION, AND FUTURE RECOMMENDATIONS

6.1 Thesis Summary

Arsenic is a toxic compound detected in freshwater systems. Toxic arsenic removal is crucial as the freshwater system is a potential drinking water source for human needs. In Chapter 1 (Introduction), the importance of the ex-mining lakes as freshwater sources was mentioned and the health consequences of arsenic consumption were discussed. Past studies in Chapter 2 also stated the potential of microalgae as an arsenic bioremediation candidate compared to other aquatic organisms. Thus, we aim to compare the cell growth, physiological, and genomic response of two selected microalgae strains *Nostoc* and *Chlorella* in response to arsenic exposure. The project was separated into 2 different stages with 2 objectives which were:

a. To investigate the response of the selected *Nostoc* strain and *Chlorella* strain under increasing arsenic and phosphate concentration, in terms of microalgae growth, adsorption and accumulation of arsenic
b. To identify the gene expression of the microalgae strain that accumulates the highest arsenic concentration

In Chapter 3, the general methodology to achieve these objectives was listed. The isolation of axenic culture from the single colony, cultivation of both microalgae strains in BG-11 medium, and the culture maintenance method were stated.

In Chapter 4, to answer the first objective, both microalgae cultures pre-cultivated with phosphate were treated with 9 different arsenic treatments with and without the addition of phosphate. The growth of both microalgae strains was measured through biomass dry weight and optical density methods. The biomass dry weight method was performed by drying the

microalgae culture on the filter paper, whereas the optical density was measured using the spectrophotometry instrument. To identify the arsenic uptake in microalgae cells, the intracellular arsenic concentration was extracted and measured using the ICP-OES instrument. The arsenic adsorb on the microalgae surface and surface structural changes of the microalgae were measured and observed using the SEM instrument. The overall result for this chapter concludes that *Nostoc* is the more suitable arsenic bioremediation candidate compared to *Chlorella*. This is due to *Nostoc* can survive under all arsenic treatment conditions, and uptake the highest arsenic concentration when treated with high As (III) concentration. Although As (III) treatment causes rupture on the *Nostoc* cell surface, the mechanism behind the high arsenic uptake concentration is still worthy of further study. The *Nostoc* strain treated with 1.00 mg L^{-1} As (III) with a lack of phosphate for a period of 24 days was selected to proceed to the second objective.

In Chapter 5, aligned with the results from the first research question, we treated *Nostoc* with 1.00 mg L^{-1} As (III) without phosphate. Culture collections were performed on the 24^{th} day. The RNA extraction was performed using two different methods which are the kit and Trizol method to compare the advantages of both methods. To identify the pathways of As (III) metabolization in the *Nostoc* strain, the prediction of As (III) related pathway was performed using BioCyc Pathway tools based on the whole genome sequence of the *Nostoc* strain. Six different genes related to arsenic were selected and primers for PCR analysis were designed to identify the possible pathway that occurs in *Nostoc* after 24 days of cultivation. The overall result for this Chapter concludes that the kit method is a more suitable extraction method compared with the Trizol method, however, a higher initial sample volume will be required.

There were multiple pathways related to As (III) predicted from the *Nostoc* whole genome sequence. The 3 main pathways were direct extrusion of As (III) to the extracellular, As (III) methylation, and binds As (III) to GSH. In this study, the PCR analysis results hypothesized

that *Nostoc* undergo the methylation process to reduce the arsenic toxicity during the treatment period. Moreover, the direct extrusion process of arsenic from the cells does not occur may be due to the lack of phosphate condition. The reduction of arsenic toxicity through methylation and the arsenic does not extrude from the cells leads to higher arsenic concentration accumulated in the *Nostoc* cells.

Overall, our research concluded that the *Nostoc* MUM003 strain is a more suitable arsenic bioremediation candidate compared to the *Chlorella* MUM002 strain. As (III) increases the *Nostoc* growth and *Nostoc* can uptake arsenic from the medium. Additionally, the methylation process occurs in *Nostoc* to reduce the toxicity of arsenic in its cells. The finding on arsenic-related pathways advances the current understanding of the arsenic detoxification pathway in cyanobacteria, by providing an alternative hypothesis about how phosphate affects the As (III) accumulation in the *Nostoc* cells.

6.2 Future Recommendations

There are some future works recommended to be studied for further understanding of mechanisms behind arsenic bioremediation and standardization of protocols and methods.

Optimization of RNA extraction methods for microalgae is crucial to facilitate future extraction processes. The current existing commercial RNA extraction kit lacks specificity for microalgae RNA, and the RNA quality often falls beyond the required range. This raised the question of whether the usage of bacteria or plant kits is more suitable. The current commercial kit which is more suitable will be the plant-based kit. However, modifications of the standard protocol are necessary to achieve optimal RNA quality.

It is recommended to assess the tolerance of microalgae strains in actual arsenic-contaminated environments. Discrepancies between the laboratory conditions and the actual environment frequently arise due to variations in the conditions and symbiotic interactions with other organisms. Therefore, monitoring the microalgae strains in the ex-mining lakes or arsenic-contaminated freshwater is suggested to understand their tolerance and efficiency in arsenic removal from nature.

References

Abdullah, M. I. C., Md Sah, A. S. R., & Haris, H. (2020). Geoaccumulation Index and Enrichment Factor of Arsenic in Surface Sediment of Bukit Merah Reservoir, Malaysia. *Tropical Life Sciences Research*, *31*(3), 109–125. https://doi.org/10.21315/TLSR2020.31.3.8

Ahmad, S., Kothari, R., Shankarayan, R., & Tyagi, V. V. (2020). Temperature dependent morphological changes on algal growth and cell surface with dairy industry wastewater: an experimental investigation. *3 Biotech*, *10*(1). https://doi.org/10.1007/S13205-019-2008-X

Ahmed, M. F., Lim, C. K., Mokhtar, M. Bin, & Khirotdin, R. P. K. (2021). Predicting Arsenic (As) Exposure on Human Health for Better Management of Drinking Water Sources. *International Journal of Environmental Research and Public Health 2021, Vol. 18, Page 7997*, *18*(15), 7997. https://doi.org/10.3390/IJERPH18157997

Allaguvatova, R., Myasina, Y., Zakharenko, V., & Gaysina, L. (2019). A simple method for the cultivation of algae Chlorella vulgaris Bejerinck. *IOP Conference Series: Earth and Environmental Science*, *390*(1). https://doi.org/10.1088/1755-1315/390/1/012020

Al-Mahdi, A. Y., Ahmida, M. A., Ali, A., Alabed, A., & Abdsalam, R. (2019). Assessment of arsenic, lead, mercury and coliform count in serdang lake, Selangor Malaysia. *Pakistan Journal of Biotechnology*, *16*(1), 21–25. https://doi.org/10.34016/PJBT.2019.16.1.4

Alvarado, S., Guédez, M., Lué-Merú, M. P., Nelson, G., Alvaro, A., Jesús, A. C., & Gyula, Z. (2008). Arsenic removal from waters by bioremediation with the aquatic plants Water Hyacinth (Eichhornia crassipes) and Lesser Duckweed (Lemna minor). *Bioresource Technology*, *99*(17), 8436–8440. https://doi.org/10.1016/j.biortech.2008.02.051

Andres, J., & Bertin, P. N. (2016). The microbial genomics of arsenic. *FEMS Microbiology Reviews*, *40*(2), 299–322. https://doi.org/10.1093/FEMSRE/FUV050

Arora, N., Gulati, K., Tripathi, S., Pruthi, V., & Poluri, K. M. (2018). Algae as a budding tool for mitigation of arsenic from aquatic systems. *Mechanisms of Arsenic Toxicity and Tolerance in Plants*, 269–297. https://doi.org/10.1007/978-981-13-1292-2_12

Arsenic. (2022, December 7). World Health Organization . https://www.who.int/news-room/fact-sheets/detail/arsenic

Ashraf, M. A., Maah, MOHD. J., & Yusof, I. (2011). *Analysis of Physio-chemical Parameters and Distribution of Heavy Metals in Soil and Water of Ex-Mining Area of Bestari Jaya, Peninsular Malaysia*. Asian Journal of Chemistry. https://asianjournalofchemistry.co.in/Journal/ViewArticle.aspx?ArticleID=23_8_44

Bahar, M. M., Megharaj, M., & Naidu, R. (2013). Toxicity, transformation and accumulation of inorganic arsenic species in a microalga Scenedesmus sp. isolated from soil. *Journal of Applied Phycology*, *25*(3), 913–917. https://doi.org/10.1007/S10811-012-9923-0

Bahar, M. M., Megharaj, M., & Naidu, R. (2016). Influence of phosphate on toxicity and bioaccumulation of arsenic in a soil isolate of microalga Chlorella sp. *Environmental*

Science and Pollution Research, *23*(3), 2663–2668. https://doi.org/10.1007/S11356-015-5510-7

Balamurugan, G. (1991). Tin mining and sediment supply in peninsular malaysia with special reference to the Kelang River Basin. *The Environmentalist*, *11*(4), 281–291. https://doi.org/10.1007/BF01266561

Bártová, K., Hilscherová, K., Babica, P., Maršálek, B., & Bláha, L. (2011). Effects of microcystin and complex cyanobacterial samples on the growth and oxidative stress parameters in green alga Pseudokirchneriella subcapitata and comparison with the model oxidative stressor-herbicide paraquat. *Environmental Toxicology*, *26*(6), 641–648. https://doi.org/10.1002/tox.20601

Bau Lake remains arsenic. (n.d.). The Borneo Post. Retrieved June 5, 2023, from https://www.theborneopost.com/2014/04/27/bau-lake-remains-arsenic/

Beal, J., Farny, N. G., Haddock-Angelli, T., Selvarajah, V., Baldwin, G. S., Buckley-Taylor, R., Gershater, M., Kiga, D., Marken, J., Sanchania, V., Sison, A., Workman, C. T., Pehlivan, M., Roige, B. B., Aarnio, T., Kivisto, S., Koski, J., Lehtonen, L., Pezzutto, D., … Zhou, J. (2020). Robust estimation of bacterial cell count from optical density. *Communications Biology*, *3*(1). https://doi.org/10.1038/S42003-020-01127-5

Berg, M., & Sutula, M. (2015). *Factors affecting the growth of cyanobacteria with special emphasis on the Sacramento-San Joaquin Delta - Applied Marine Sciences, Inc.*

Chakraborti, D., Basu, G. K., Biswas, B., Chowdhury, U., Rahman, M. M., Paul, K., Chowdhury, R., Chanda, C., Lodh, D., & Ray, S. L. (2001). Characterization of arsenic bearing sediments in Gangetic delta of West Bengal-India. *Books.Google.ComD Chakraborti, GK Basu, BK Biswas, UK Chowdhury, MM Rahman, K Paul, TR ChowdhuryArsenic Exposure and Health Effects, 2001•books.Google.Com*, *4*, 27–52. https://books.google.com/books?hl=en&lr=&id=kpT2eIxOCi8C&oi=fnd&pg=PA27&ots=EpJV2hIo-J&sig=xJ_QX5WV5rqqW7qGUBcWM1of4Lg

Chen, Y. G., & Hur, S. (2021). Cellular origins of dsRNA, their recognition and consequences. *Nature Reviews Molecular Cell Biology 2021 23:4*, *23*(4), 286–301. https://doi.org/10.1038/s41580-021-00430-1

Chioccioli, M., Hankamer, B., & Ross, I. L. (2014). Flow cytometry pulse width data enables rapid and sensitive estimation of biomass dry weight in the microalgae Chlamydomonas reinhardtii and Chlorella vulgaris. *PLoS ONE*, *9*(5). https://doi.org/10.1371/JOURNAL.PONE.0097269

da Silva, J. C., & Lombardi, A. T. (2020). Chlorophylls in microalgae: Occurrence, distribution, and biosynthesis. *Pigments from Microalgae Handbook*, 1–18. https://doi.org/10.1007/978-3-030-50971-2_1/FIGURES/5

Danish, M. I., Qazi, I. A., Zeb, A., Habib, A., Awan, M. A., & Khan, Z. (2013). Arsenic removal from aqueous solution using pure and metal-doped Titania nanoparticles coated on glass beads: Adsorption and column studies. *Journal of Nanomaterials*, *2013*. https://doi.org/10.1155/2013/873694

Das, S., Lizon, F., Gevaert, F., Bialais, C., Duong, G., Ouddane, B., & Souissi, S. (2023). Assessing indicators of arsenic toxicity using variable fluorescence in a commercially valuable microalgae: Physiological and toxicological aspects. *Journal of Hazardous Materials*, *452*, 131215. https://doi.org/10.1016/J.JHAZMAT.2023.131215

Degen, J., Uebele, A., Retze, A., Schmid-Staiger, U., & Trösch, W. (2001). A novel airlift photobioreactor with baffles for improved light utilization through the flashing light effect. *Journal of Biotechnology*, *92*(2), 89–94. https://doi.org/10.1016/S0168-1656(01)00350-9

Difference between ssDNA and dsDNA. (n.d.). BYJU's. Retrieved January 31, 2024, from https://byjus.com/biology/difference-between-ssdna-and-dsdna/

Earth's Fresh Water. (2023). National Geographic. https://education.nationalgeographic.org/resource/earths-fresh-water/

Fernandez Valiente, E., & Leganes, F. (1990). Regulatory Effect of pH and Incident Irradiance on the Levels of Nitrogenase Activity in the Cyanobacterium Nostoc UAM 205. *Journal of Plant Physiology*, *135*(5), 623–627. https://doi.org/10.1016/S0176-1617(11)80647-4

Ferrari, S. G., Silva, P. G., González, D. M., Navoni, J. A., & Silva, H. J. (2013). Arsenic tolerance of cyanobacterial strains with potential use in biotechnology. *Revista Argentina de Microbiologia*, *45*(3), 174–179. https://doi.org/10.1016/S0325-7541(13)70021-X

Foster, S., Thomson, D., & Maher, W. (2008). Uptake and metabolism of arsenate by anexic cultures of the microalgae Dunaliella tertiolecta and Phaeodactylum tricornutum. *Marine Chemistry*, *108*(3–4), 172–183. https://doi.org/10.1016/J.MARCHEM.2007.11.005

Garbinski, L. D., Rosen, B. P., & Chen, J. (2019). Pathways of arsenic uptake and efflux. *Environment International*, *126*, 585–597. https://doi.org/10.1016/J.ENVINT.2019.02.058

García-Salgado, S., Quijano, M. A., & Bonilla, M. M. (2012). Arsenic speciation in edible alga samples by microwave-assisted extraction and high performance liquid chromatography coupled to atomic fluorescence spectrometry. *Analytica Chimica Acta*, *714*, 38–46. https://doi.org/10.1016/J.ACA.2011.12.001

Gemici, Ü., Tarcan, G., Helvaci, C., & Somay, A. M. (2008). High arsenic and boron concentrations in groundwaters related to mining activity in the Bigadiç borate deposits (Western Turkey). *Applied Geochemistry*, *23*(8), 2462–2476. https://doi.org/10.1016/J.APGEOCHEM.2008.02.013

Gene Expression. (n.d.). National Library of Medicine (NIH). Retrieved January 31, 2024, from https://www.ncbi.nlm.nih.gov/probe/docs/applexpression/

Gene Expression Is Analyzed by Tracking RNA. (n.d.). Scitable by Nature Education. Retrieved January 31, 2024, from https://www.nature.com/scitable/topicpage/gene-expression-is-analyzed-by-tracking-rna-6525038/

Genome. (n.d.). Retrieved January 31, 2024, from https://www.genome.gov/genetics-glossary/Genome

Genuário, D. B., Silva-Stenico, M. E., Welker, M., Beraldo Moraes, L. A., & Fiore, M. F. (2010). Characterization of a microcystin and detection of microcystin synthetase genes from a Brazilian isolate of Nostoc. *Toxicon*, *55*(4), 846–854. https://doi.org/10.1016/j.toxicon.2009.12.001

Gitau, M. M., Farkas, A., Balla, B., Ördög, V., Futó, Z., & Maróti, G. (2021). Strain-specific biostimulant effects of chlorella and chlamydomonas green microalgae on medicago truncatula. *Plants*, *10*(6). https://doi.org/10.3390/PLANTS10061060/S1

Gonçalves, A. L., Pires, J. C. M., & Simões, M. (2016). The effects of light and temperature on microalgal growth and nutrient removal: an experimental and mathematical approach. *RSC Advances*, *6*(27), 22896–22907. https://doi.org/10.1039/C5RA26117A

Gong, Y., Ao, H. Y., Liu, B. B., Wen, S., Wang, Z., Hu, D. J., Zhang, X. Z., Song, L. R., & Liu, J. T. (2011). Effects of inorganic arsenic on growth and microcystin production of a Microcystis strain isolated from an algal bloom in Dianchi Lake, China. *Chinese Science Bulletin*, *56*(22), 2337–2342. https://doi.org/10.1007/s11434-011-4576-y

Gong, Y., Chou, H. N., Tu, C. D., Liu, X., Liu, J., & Song, L. (2009). Effects of arsenate on the growth and microcystin production of Microcystis aeruginosa isolated from Taiwan as influenced by extracellular phosphate. *Journal of Applied Phycology*, *21*(2), 225–231. https://doi.org/10.1007/S10811-008-9353-1/FIGURES/3

Gong, Y., Song, L., Wu, X., Xiao, B., Fang, T., & Liu, J. (2009). Effects of arsenate on microcystin content and leakage of microcystis strain PCC7806 under various phosphate regimes. *Environmental Toxicology*, *24*(1), 87–94. https://doi.org/10.1002/tox.20392

Grande, J. A., Beltrán, R., Sáinz, A., Santos, J. C., de la Torre, M. L., & Borrego, J. (2005). Acid mine drainage and acid rock drainage processes in the environment of Herrerías Mine (Iberian Pyrite Belt, Huelva-Spain) and impact on the Andevalo Dam. *Environmental Geology*, *47*(2), 185–196. https://doi.org/10.1007/s00254-004-1142-9

Green micro algae (Chlorella vulgaris) . (n.d.). Phytocode. Retrieved October 31, 2023, from https://phytocode.net/phytoglossary/green-micro-algae-chlorella-vulgaris/

Griffiths, M. J., Garcin, C., Van Hille, R. P., & Harrison, S. T. L. (2011). *Interference by pigment in the estimation of microalgal biomass concentration by optical density*. https://doi.org/10.1016/j.mimet.2011.02.005

Gul, A., Bulut, G., & Sirkeci, A. A. (2013). Beneficiation of an arsenic bearing complex sulphide ore by flotation. *Physicochemical Problems of Mineral Processing*, *49*(1), 203–212. https://doi.org/10.5277/PPMP130118

Hadiyanto, H., Soetrisnanto, D., & Christwardhana, M. (2014). Phytoremediation of Palm Oil Mill Effluent Using Pistia Stratiotes Plant and Algae Spirulina sp for Biomass Production. *International Journal of Engineering*, *27*(12 (C)). https://doi.org/10.5829/IDOSI.IJE.2014.27.12C.02

Hani Binti Abu Hamid, S. (2015). *A STUDY ON THE POTENTIAL OF EX-MINING LAKES AS ALTERNATIVE WATER SOURCES*.

Hashim, M., Nayan, N., Saleh, Y., Mahat, H., Mat Said, Z., & Fhei Shiang, W. (2018). Water quality assessment of former tin mining lakes for recreational purposes in Ipoh city, Perak, Malaysia. *Indonesian Journal of Geography*, *50*(1), 25–33. https://doi.org/10.22146/IJG.15665

Herath, I., Vithanage, M., Bundschuh, J., Maity, J. P., & Bhattacharya, P. (2016). Natural Arsenic in Global Groundwaters: Distribution and Geochemical Triggers for Mobilization. *Current Pollution Reports 2016 2:1*, *2*(1), 68–89. https://doi.org/10.1007/S40726-016-0028-2

Higashi, S., Nakashima, S., & Takeshita, T. (1985). Bioaccumulation of Arsenic by Freshwater Algae and the Application to the Removal of Inorganic Arsenic from an Aqueous Phase. Part II. By Chlorella vulgaris Isolated from Arsenic-Polluted Environment. *Separation Science and Technology*, *20*(2–3), 153–161. https://doi.org/10.1080/01496398508058356

Huang, F., Dang, Z., Guo, C. L., Lu, G. N., Gu, R. R., Liu, H. J., & Zhang, H. (2013). Biosorption of Cd(II) by live and dead cells of Bacillus cereus RC-1 isolated from cadmium-contaminated soil. *Colloids and Surfaces B: Biointerfaces*, *107*, 11–18. https://doi.org/10.1016/J.COLSURFB.2013.01.062

Huang, W. J., Wu, C. C., & Chang, W. C. (2014). Bioaccumulation and toxicity of arsenic in cyanobacteria cultures separated from a eutrophic reservoir. *Environmental Monitoring and Assessment*, *186*(2), 805–814. https://doi.org/10.1007/S10661-013-3418-6

ITIS - Report: Nostoc commune. (2023, March 27). ITIS Taoxonomy. https://www.itis.gov/servlet/SingleRpt/SingleRpt?search_topic=TSN&search_value=1147#null

Jekel, M., & Amy, G. L. (2006). Arsenic removal during drinking water treatment. *Interface Science and Technology*, *10*(C), 193–206. https://doi.org/10.1016/S1573-4285(06)80080-3

Jena, J., Nayak, M., Sekhar Panda, H., Pradhan, N., Sarika, C., Ku. Panda, P., V. S. K Rao, B., B. N. Prasad, R., & Behari Sukla, L. (2012). Microalgae of Odisha Coast as a Potential Source for Biodiesel Production. *World Environment*, *2*(1), 12–17. https://doi.org/10.5923/J.ENV.20120201.03

Jozefczak, M., Remans, T., Vangronsveld, J., & Cuypers, A. (2012). Glutathione Is a Key Player in Metal-Induced Oxidative Stress Defenses. *International Journal of Molecular Sciences*, *13*(3), 3145. https://doi.org/10.3390/IJMS13033145

Kapaj, S., Peterson, H., Liber, K., & Bhattacharya, P. (2006). Environmental Epidemiology Unit, Department of Public Health and Policy. *Journal of Environmental Science and Health Part A*, *41*, 2399–2428. https://doi.org/10.1080/10934520600873571

Karadjova, I. B., Slaveykova, V. I., & Tsalev, D. L. (2008). The biouptake and toxicity of arsenic species on the green microalga Chlorella salina in seawater. *Aquatic Toxicology*, *87*(4), 264–271. https://doi.org/10.1016/J.AQUATOX.2008.02.006

Khalili, A., Najafpour, G. D., Amini, G., & Samkhaniyani, F. (2015). Influence of nutrients and LED light intensities on biomass production of microalgae Chlorella vulgaris. *Biotechnology and Bioprocess Engineering*, *20*(2), 284–290. https://doi.org/10.1007/S12257-013-0845-8

Khuntia, S., Majumder, S. K., & Ghosh, P. (2014). Oxidation of As(III) to As(V) using ozone microbubbles. *Chemosphere*, *97*, 120–124. https://doi.org/10.1016/J.CHEMOSPHERE.2013.10.046

Kimura, S., Nakajima, M., Yumoto, E., Miyamoto, K., Yamane, H., Ong, M., Tomita-Yokotani, K., & Asami, T. (2020). Cytokinins affect the akinete-germination stage of a terrestrial filamentous cyanobacterium, Nostoc sp. HK-01. *Plant Growth Regulation*, *92*(2), 273–282. https://doi.org/10.1007/S10725-020-00636-X/FIGURES/5

Knauer, K., & Hemond, H. (2000). Accumulation and reduction of arsenate by the freshwater green alga Chlorella sp. (Chlorophyta). *Journal of Phycology*, *36*(3), 506–509. https://doi.org/10.1046/J.1529-8817.2000.99056.X

Koki, I. B., Low, K. H., Juahir, H., Abdul Zali, M., Azid, A., & Zain, S. M. (2018). Consumption of water from ex-mining ponds in Klang Valley and Melaka, Malaysia: A health risk study. *Chemosphere*, *195*, 641–652. https://doi.org/10.1016/J.CHEMOSPHERE.2017.12.112

Koki, I. B., Zain, S. M., Hin, L. K., Azid, A., Juahir, H., & Zali, M. A. (2019). Development of water quality index of ex-mining ponds in Malaysia. *Malaysian Journal of Fundamental and Applied Sciences*, *15*(1), 54–60. https://doi.org/10.11113/MJFAS.V15N2019.1079

Lavrinovičs, A., Mežule, L., & Juhna, T. (2020). Microalgae starvation for enhanced phosphorus uptake from municipal wastewater. *Algal Research*, *52*, 102090. https://doi.org/10.1016/J.ALGAL.2020.102090

Leong, Y. K., & Chang, J.-S. (2020). *Bioremediation of heavy metals using microalgae: Recent advances and mechanisms*. https://doi.org/10.1016/j.biortech.2020.122886

Levy, J. L., Stauber, J. L., Adams, M. S., Maher, W. A., Kirby, J. K., & Jolley, D. F. (2005). Toxicity, biotransformation, and mode of action of arsenic in two freshwater microalgae (Chlorella sp. and Monoraphidium arcuatum). *Environmental Toxicology and Chemistry*, *24*(10), 2630–2639. https://doi.org/10.1897/04-580R.1

Li, Y., Lin, Y., Loughlin, P. C., & Chen, M. (2014). Optimization and effects of different culture conditions on growth of Halomicronema hongdechloris – a filamentous cyanobacterium containing chlorophyll f. *Frontiers in Plant Science*, *5*(FEB), 67. https://doi.org/10.3389/fpls.2014.00067

Liu, J., Qiu, Y., He, L., Luo, K., & Wang, Z. (2021). Effect of iron and phosphorus on the microalgae growth in co-culture. *Archives of Microbiology*, *203*(2), 733–740. https://doi.org/10.1007/S00203-020-02074-9/FIGURES/3

Lloyd, J. R., & Oremland, R. S. (2006). Microbial transformations of arsenic in the environment: From soda lakes to aquifers. *Elements*, *2*(2), 85–90. https://doi.org/10.2113/GSELEMENTS.2.2.85

Low, K. H., Koki, I. B., Juahir, H., Azid, A., Behkami, S., Ikram, R., Mohammed, H. A., & Zain, S. M. (2016). Evaluation of water quality variation in lakes, rivers, and ex-mining ponds in Malaysia (review). *Desalination and Water Treatment*, *57*(58), 28215–28239. https://doi.org/10.1080/19443994.2016.1185382

Maeda, S., Fujita, S., Ohki, A., Yoshifuku, I., Higashi, S., & Takeshita, T. (1988). Arsenic accumulation by arsenic-tolerant freshwater blue-green alga (Phormidium sp.). *Applied Organometallic Chemistry*, *2*(4), 353–357. https://doi.org/10.1002/aoc.590020412

Maeda, S., Kumeda, K., Maeda, M., Higashi, S., & Takeshita, T. (1987). Bioaccumulation of arsenic by freshwater algae (Nostoc sp.) and the application to the removal of inorganic arsenic from an aqueous phase. *Applied Organometallic Chemistry*, *1*(4), 363–370. https://doi.org/10.1002/AOC.590010411

Martín, J. F., & Liras, P. (2021). Molecular Mechanisms of Phosphate Sensing, Transport and Signalling in Streptomyces and Related Actinobacteria. *International Journal of Molecular Sciences*, *22*(3), 1–20. https://doi.org/10.3390/IJMS22031129

Masojídek, J., Kopecký, J., Giannelli, L., & Torzillo, G. (2011). Productivity correlated to photobiochemical performance of Chlorella mass cultures grown outdoors in thin-layer cascades. *Journal of Industrial Microbiology and Biotechnology*, *38*(2), 307–317. https://doi.org/10.1007/S10295-010-0774-X

Media Preparation Recipe Template. (2019, November 5). CCAP (Culture Collection of Algae and Protozoa). https://www.ccap.ac.uk/wp-content/uploads/MR_BG11_customerorders.pdf

Miazek, K., Iwanek, W., Remacle, C., Richel, A., & Goffin, D. (2015a). Effect of Metals, Metalloids and Metallic Nanoparticles on Microalgae Growth and Industrial Product Biosynthesis: A Review. *International Journal of Molecular Sciences 2015, Vol. 16, Pages 23929-23969*, *16*(10), 23929–23969. https://doi.org/10.3390/IJMS161023929

Miazek, K., Iwanek, W., Remacle, C., Richel, A., & Goffin, D. (2015b). Effect of Metals, Metalloids and Metallic Nanoparticles on Microalgae Growth and Industrial Product Biosynthesis: A Review. *International Journal of Molecular Sciences*, *16*(10), 23929. https://doi.org/10.3390/IJMS161023929

Minchin, S., & Lodge, J. (2019). Understanding biochemistry: structure and function of nucleic acids. *Essays in Biochemistry*, *63*(4), 433. https://doi.org/10.1042/EBC20180038

Minhas, A. K., Hodgson, P., Barrow, C. J., & Adholeya, A. (2020). Two-phase method of cultivating Coelastrella species for increased production of lipids and carotenoids. *Bioresource Technology Reports*, *9*, 100366. https://doi.org/10.1016/J.BITEB.2019.100366

Miretzky, P., Saralegui, A., & Fernández Cirelli, A. (2006). Simultaneous heavy metal removal mechanism by dead macrophytes. *Chemosphere*, *62*(2), 247–254. https://doi.org/10.1016/j.chemosphere.2005.05.010

Miyashita, S. I., Fujiwara, S., Tsuzuki, M., & Kaise, T. (2012). Cyanobacteria produce arsenosugars. *Environmental Chemistry*, *9*(5), 474–484. https://doi.org/10.1071/EN12061

Miyashita, S., Murota, C., Kondo, K., Fujiwara, S., Tsuzuki, M., Miyashita, S., Murota, C., Kondo, K., Fujiwara, S., & Tsuzuki, M. (2015). Arsenic metabolism in cyanobacteria. *Environmental Chemistry*, *13*(4), 577–589. https://doi.org/10.1071/EN15071

Møller, C. L., Vangsøe, M. T., & Sand-Jensen, K. (2014). Comparative growth and metabolism of gelatinous colonies of three cyanobacteria, Nostoc commune, Nostoc pruniforme and Nostoc zetterstedtii, at different temperatures. *Freshwater Biology*, *59*(10), 2183–2193. https://doi.org/10.1111/fwb.12421

Munoz, L. P. (2014). *THE MECHANISMS OF ARSENIC DETOXIFICATION BY THE GREEN MICROALGAE CHLORELLA VULGARIS* [Middlesex University]. https://www.researchgate.net/publication/314113049_THE_MECHANISMS_OF_ARSENIC_DETOXIFICATION_BY_THE_GREEN_MICROALGAE_CHLORELLA_VULGARIS

Mur, L. R., Skulberg, O. M., & Utkilen, H. (1999). *Toxic Cyanobacteria in Water: A guide to their public health consequences, monitoring and management*.

National Research Council (U.S.). Subcommittee on Arsenic in Drinking Water. (1999). *Arsenic in drinking water*. National Academy Press.

Nostoc . (2022, August). Alchetron. https://alchetron.com/Nostoc#nostoc-49fa003c-c069-42b9-93d3-c1bee299bf7-resize-750.png

Ong, G. H., Yap, C. K., Maziah, M., Suhaimi, H., & Tan, S. G. (2013). An investigation of arsenic contamination in Peninsular Malaysia based on Centella asiatica and soil samples. *Environmental Monitoring and Assessment*, *185*(4), 3243–3254. https://doi.org/10.1007/S10661-012-2787-6

Orji, K. U., Sapari, N. B., Yusof, K. W., Robabeh, A., & Olisa, E. (2009). Water Quality Assessment of Ex-mining Lakes in Perak, Malaysia as Alternative Source of Water Supply. *Applied Mechanics and Materials*, *567*, 177–182. https://doi.org/10.4028/WWW.SCIENTIFIC.NET/AMM.567.177

Oxidative phosphorylation . (n.d.). Khan Academy. Retrieved January 30, 2024, from https://www.khanacademy.org/science/ap-biology/cellular-energetics/cellular-respiration-ap/a/oxidative-phosphorylation-etc

Parvin, M., Zannat, M. N., & Habib, M. A. B. (2007). Two Important Techniques for Isolation of Microalgae. *Asian Fisheries Science*, *20*, 117–124. https://doi.org/10.33997/j.afs.2007.20.1.010

Patel, A., Tiwari, S., & Prasad, S. M. (2021). Arsenate and arsenite-induced inhibition and recovery in two diazotrophic cyanobacteria Nostoc muscorum and Anabaena sp.: study on time-dependent toxicity regulation. *Environmental Science and Pollution Research*, *28*(37), 51088–51104. https://doi.org/10.1007/S11356-021-13800-1

Podder, M. S., & Majumder, C. B. (2015). Phycoremediation of arsenic from wastewaters by Chlorella pyrenoidosa. *Groundwater for Sustainable Development*, *1*(1–2), 78–91. https://doi.org/10.1016/J.GSD.2015.12.003

Poong, S. W., Lim, P. E., Lai, J. W. S., & Phang, S. M. (2017). Optimization of high quality total RNA isolation from the microalga, Chlorella sp. (Trebouxiophyceae, Chlorophyta) for next-generation sequencing. *Phycological Research*, *65*(2), 146–150. https://doi.org/10.1111/PRE.12165

Poulhazan, A., Arnold, A. A., Warschawski, D. E., & Marcotte, I. (n.d.). *Chapter X Solid-state NMR study of microalgal membranes*.

Ramanan, S., Tang, J., & Velayudhan, A. (2000). Isolation and preparative purification of microcystin variants. *Journal of Chromatography A*, *883*(1–2), 103–112. https://doi.org/10.1016/S0021-9673(00)00378-2

Ramírez-Romero, A., Martin, M., Boyer, A., Bolzoni, R., Matricon, L., Sassi, J. F., Steyer, J. P., & Delrue, F. (2023). Microalgae adaptation as a strategy to recycle the aqueous phase from hydrothermal liquefaction. *Bioresource Technology*, *371*, 128631. https://doi.org/10.1016/J.BIORTECH.2023.128631

Randrianarison, G., & Ashraf, M. A. (2017). Microalgae: a potential plant for energy production. *Http://Dx.Doi.Org/10.1080/24749508.2017.1332853*, *1*(2), 104–120. https://doi.org/10.1080/24749508.2017.1332853

Ratha, S. K., Rao, P. H., Govindaswamy, K., Jaswin, R. S., Lakshmidevi, R., Bhaskar, S., & Chinnasamy, S. (2016). A rapid and reliable method for estimating microalgal biomass using a moisture analyser. *Journal of Applied Phycology*, *28*(3), 1725–1734. https://doi.org/10.1007/S10811-015-0731-1

Rivera, O. (2023, November 18). *RNA Integrity Assessment via Agarose Gel Electrophoresis*. Benchling. https://benchling.com/protocols/f4ed4SZs/rna-integrity-assessment-via-agarose-gel-electrophoresis

Rodriguez Castro, M. C., Urrea, G., & Guasch, H. (2015). Influence of the interaction between phosphate and arsenate on periphyton's growth and its nutrient uptake capacity. *Science of the Total Environment*, *503–504*, 122–132. https://doi.org/10.1016/J.SCITOTENV.2014.06.094

Rosen, B. P. (2002a). Biochemistry of arsenic detoxification. *FEBS Letters*, *529*(1), 86–92. https://doi.org/10.1016/S0014-5793(02)03186-1

Rosen, B. P. (2002b). Biochemistry of arsenic detoxification. *FEBS Letters*, *529*(1), 86–92. https://doi.org/10.1016/S0014-5793(02)03186-1

Ross, H. B. (2014). Flow Cytometry Pulse Width Data Enables Rapid and Sensitive Estimation of Biomass Dry Weight in the Microalgae Chlamydomonas reinhardtii and Chlorella vulgaris. *PLoS ONE*, *9*(5). https://doi.org/10.1371/journal.pone.0097269

Safi, C., Zebib, B., Merah, O., Pontalier, P. Y., & Vaca-Garcia, C. (2014). Morphology, composition, production, processing and applications of Chlorella vulgaris: A review. *Renewable and Sustainable Energy Reviews*, *35*, 265–278. https://doi.org/10.1016/J.RSER.2014.04.007

Safi, C., Zebib, B., Merah, O., Pontalier, P.-Y., Vaca-Garcia, C., Vaca, C., & Morphology, G. (2014). *Morphology, composition, production, processing and applications of Chlorella*

vulgaris: A review composition, production, processing and applications of Chlorella vulgaris: A review. Renewable and Sustainable Energy Reviews. *35*. https://doi.org/10.1016/j.rser.2014.04.007ï

Sakai, N., Alsaad, Z., Thuong, N. T., Shiota, K., Yoneda, M., & Ali Mohd, M. (2017). Source profiling of arsenic and heavy metals in the Selangor River basin and their maternal and cord blood levels in Selangor State, Malaysia. *Chemosphere*, *184*, 857–865. https://doi.org/10.1016/J.CHEMOSPHERE.2017.06.070

Samudi Yasir, M., bt Ahmad Kabir, N., Yahaya, R., Ab Majid Pusat Pengajian Fizik Gunaan, A., & Sains dan Teknologi, F. (2008). KANDUNGAN LOGAM BERAT DAN RADIONUKLID TABII DALAM IKAN, AIR, TUMBUHAN DAN SEDIMEN DI BEKAS TASIK LOMBONG. *The Malaysian Journal of Analytical Sciences*, *12*(1).

Sánchez-Riego, A. M., López-Maury, L., & Florencio, F. J. (2014). Genomic responses to arsenic in the cyanobacterium Synechocystis sp. PCC 6803. *PLoS ONE*, *9*(5). https://doi.org/10.1371/JOURNAL.PONE.0096826

Sanders, J. G. (1979). EFFECTS OF ARSENIC SPECIATION AND PHOSPHATE CONCENTRATION ON ARSENIC INHIBITION OF SKELETONEMA COSTATUM (BACILLARIOPHYCEAE). *Journal of Phycology*, *15*(4), 424–428. https://doi.org/10.1111/J.1529-8817.1979.TB00714.X

Sanders, J. G., & Windom, H. L. (1980). The uptake and reduction of arsenic species by marine algae. *Estuarine and Coastal Marine Science*, *10*(5), 555–567. https://doi.org/10.1016/S0302-3524(80)80075-2

Schmidt, J. J., Gagnon, G. A., & Jamieson, R. C. (2016). Microalgae growth and phosphorus uptake in wastewater under simulated cold region conditions. *Ecological Engineering*, *95*, 588–593. https://doi.org/10.1016/J.ECOLENG.2016.06.114

Schor, A. R., Buie, C. R., Anam, K., Rahman, Y., Hidhayati, N., Febrieni, V. N., Sedjati, S., & Yudiati, E. (2020). Optimization of light intensity on growth rate and total lipid content of Chlorella vulgaris. *Earth and Environmental Science*. https://doi.org/10.1088/1755-1315/584/1/012040

Segundo-Val, I. S., & Sanz-Lozano, C. S. (2016). Introduction to the Gene Expression Analysis. *Methods in Molecular Biology (Clifton, N.J.)*, *1434*, 29–43. https://doi.org/10.1007/978-1-4939-3652-6_3

Shanab, S., Essa, A., & Shalaby, E. (2012). Bioremoval capacity of three heavy metals by some microalgae species (Egyptian isolates). *Plant Signaling and Behavior*, *7*(3), 392–399. https://doi.org/10.4161/psb.19173

Shi, Q., Ju, M., Zhu, X., Gan, H., Gu, R., Wu, Z., Meng, Z., Dou, G., & Yao, S. (2019). Pharmacokinetic Properties of Arsenic Species after Intravenous and Intragastrical Administration of Arsenic Trioxide Solution in Cynomolgus Macaques Using HPLC-ICP-MS. *Molecules*. https://doi.org/10.3390/molecules24020241

Singh, A. P., Goel, R. K., & Kaur, T. (2011). Mechanisms Pertaining to Arsenic Toxicity. *Toxicology International*, *18*(2), 87. https://doi.org/10.4103/0971-6580.84258

Singh, J., & Saxena, R. C. (2015). An Introduction to Microalgae: Diversity and Significance. *Handbook of Marine Microalgae: Biotechnology Advances*, 11–24. https://doi.org/10.1016/B978-0-12-800776-1.00002-9

Singh, N. K., Gupta, G., Upadhyay, A. K., & Rai, U. N. (2018). Potentials of aquatic plants and algae for arsenic accumulation. In *Mechanisms of Arsenic Toxicity and Tolerance in Plants* (pp. 257–267). Springer Singapore. https://doi.org/10.1007/978-981-13-1292-2_11

Song, L., Sano, T., Li, R., Watanabe, M. M., Liu, Y., & Kaya, K. (1998). Microcystin production of *Microcystis viridis* (cyanobacteria) under different culture conditions. *Phycological Research*, *46*(s2), 19–23. https://doi.org/10.1046/j.1440-1835.1998.00120.x

Spencer, D. F., Liow, P. S., & Lembi, C. A. (2011). Growth response to temperature and light in Nostoc spongiaeforme (Cyanobacteria). *Journal of Freshwater Ecology*, *26*(3), 357–363. https://doi.org/10.1080/02705060.2011.559745

Suhendrayatna, Ohki, A., Kuroiwa, T., & Maeda, S. (1997). *Arsenic compounds in the freshwater green microalgae Chlorella vulgaris after exposure to arsenite*. APPLIED ORGANOMETALLIC CHEMISTRY. https://sci-hub.hkvisa.net/https://onlinelibrary.wiley.com/doi/10.1002/(SICI)1099-0739(199902)13:2%3C127::AID-AOC810%3E3.0.CO;2-K

Takeuchi, M., Kawahata, H., Prasad, L. G., Kita, N., Morishita, Y., Ono, Y., & Komai, T. (2007). Arsenic resistance and removal by marine and non-marine bacteria. *Journal of Biotechnology*, *3*(127), 434–442.

Thanh, T., Omar, H., Abdullah, M. P., Chi, V. T. Q., Noroozi, M., Ky, H., & Napis, S. (2009). Rapid and effective method of RNA isolation from green microalga Ankistrodesmus convolutus. *Molecular Biotechnology*, *43*(2), 148–153. https://doi.org/10.1007/S12033-009-9182-8

Thoburn, J. (1978). Malaysia's tin supply problems. *Resources Policy*, *4*(1), 31–34. https://doi.org/10.1016/0301-4207(78)90063-6

USGS Water Science School. (n.d.). Retrieved October 26, 2023, from https://water.usgs.gov/edu/gallery/watercyclekids/earth-water-distribution.html

Vale, M. A., Ferreira, A., Pires, J. C. M., & Gonçalves, A. L. (2020). CO2 capture using microalgae. *Advances in Carbon Capture*, 381–405. https://doi.org/10.1016/B978-0-12-819657-1.00017-7

Wang, D., & Farhana, A. (2023). Biochemistry, RNA Structure. *StatPearls*. https://www.ncbi.nlm.nih.gov/books/NBK558999/

Wang, N. S. (n.d.). *Measurements of Cell Biomass Concentration*. Retrieved October 10, 2023, from https://user.eng.umd.edu/~nsw/ench485/lab9c.htm

Wang, N. X., Li, Y., Deng, X. H., Miao, A. J., Ji, R., & Yang, L. Y. (2013). Toxicity and bioaccumulation kinetics of arsenate in two freshwater green algae under different

phosphate regimes. *Water Research*, *47*(7), 2497–2506. https://doi.org/10.1016/J.WATRES.2013.02.034

Wang, Y., Wang, S., Xu, P., Liu, C., Liu, M., Wang, Y., Wang, C., Zhang, C., & Ge, Y. (2015). Review of arsenic speciation, toxicity and metabolism in microalgae. *Reviews in Environmental Science and Biotechnology*, *14*(3), 427–451. https://doi.org/10.1007/S11157-015-9371-9/TABLES/3

Wang, Z., Luo, Z., & Yan, C. (2013). Accumulation, transformation, and release of inorganic arsenic by the freshwater cyanobacterium Microcystis aeruginosa. *Environmental Science and Pollution Research*, *20*(10), 7286–7295. https://doi.org/10.1007/S11356-013-1741-7

Water Science School. (2018). *Freshwater (Lakes and Rivers) and the Water Cycle*. U.S. Geological Survey. https://www.usgs.gov/special-topics/water-science-school/science/freshwater-lakes-and-rivers-and-water-cycle

Xiao, Z., Li, X., & Huo, S. (2022). *Arsenic Accumulation and Biotransformation Affected by Nutrients (N and P) in Common Blooming-Forming Microcystis wesenbergii (Komárek) Komárek ex Komárek (Cyanobacteria)*. https://doi.org/10.3390/w14020245

Xing, W., Wu, H., Hao, B., Huang, W., & Liu, G. (2013). Bioaccumulation of heavy metals by submerged macrophytes: Looking for hyperaccumulators in eutrophic lakes. *Environmental Science and Technology*, *47*(9), 4695–4703. https://doi.org/10.1021/es303923w

Xue, X. M., Yan, Y., Xiong, C., Raber, G., Francesconi, K., Pan, T., Ye, J., & Zhu, Y. G. (2017). Arsenic biotransformation by a cyanobacterium Nostoc sp. PCC 7120. *Environmental Pollution*, *228*, 111–117. https://doi.org/10.1016/j.envpol.2017.05.005

Xue, X.-M., Ye, J., Raber, G., Francesconi, K. A., Li, G., Gao, H., Yan, Y., Rensing, C., & Zhu, Y.-G. (2017). *Arsenic Methyltransferase is Involved in Arsenosugar Biosynthesis by Providing DMA*. https://doi.org/10.1021/acs.est.6b04952

Yaakob, M. A., Mohamed, R. M. S. R., Al-Gheethi, A., Ravishankar, G. A., & Ambati, R. R. (2021). Influence of Nitrogen and Phosphorus on Microalgal Growth, Biomass, Lipid, and Fatty Acid Production: An Overview. *Cells 2021, Vol. 10, Page 393*, *10*(2), 393. https://doi.org/10.3390/CELLS10020393

Yan, G., Chen, X., Du, S., Deng, Z., Wang, L., & Chen, S. (2019a). Genetic mechanisms of arsenic detoxification and metabolism in bacteria. *Current Genetics*, *65*(2), 329–338. https://doi.org/10.1007/S00294-018-0894-9

Yan, G., Chen, X., Du, S., Deng, Z., Wang, L., & Chen, S. (2019b). Genetic mechanisms of arsenic detoxification and metabolism in bacteria. *Current Genetics*, *65*(2), 329–338. https://doi.org/10.1007/s00294-018-0894-9

Yau, S. K., Yusoff, F. M., Khong, N. M. H., Foo, S. C., & Lai, J. I. (2016). Improved Pre-treatment Protocol for Scanning Electron Microscopy Coupled wi...: EBSCOhost. *Pertanika Journal of Tropical Agricultural Science*, *39*(3). https://web.p.ebscohost.com/ehost/detail/detail?vid=0&sid=e2c3a201-96ca-4705-b12b-

112d1b8393aa%40redis&bdata=JkF1dGhUeXBlPXNoaWImc2l0ZT1laG9zdC1saXZlJnNjb3BlPXNpdGU%3d#AN=119631056&db=asn

Yin, X. X., Zhang, Y. Y., Yang, J., & Zhu, Y. G. (2011). Rapid biotransformation of arsenic by a model protozoan Tetrahymena thermophila. *Environmental Pollution*, *159*(4), 837–840. https://doi.org/10.1016/j.envpol.2010.12.033

Yoshida, T., Makita, Y., Nagata, S., Tsutsumi, T., Yoshida, F., Sekijima, M., Tamura, S., & Ueno, Y. (1998). Acute oral toxicity of microcystin-LR, a cyanobacterial hepatotoxin, in mice. *Natural Toxins*, *5*(3), 91–95. https://doi.org/10.1002/1522-7189(1997)5:3<91::aid-nt1>3.0.co;2-h

Younger, P. L., & Wolkersdorfer, C. (2004). Mining Impacts on the Fresh Water Environment: Technical and Managerial Guidelines for Catchment Scale Management ERMITE-Consortium. *Mine Water and the Environment*, *23*, S2–S80. https://doi.org/10.1007/s10230-004-0028-0

Yu, H., Jia, S., & Dai, Y. (2009). Growth characteristics of the cyanobacterium Nostoc flagelliforme in photoautotrophic, mixotrophic and heterotrophic cultivation. *Journal of Applied Phycology*, *21*(1), 127–133. https://doi.org/10.1007/s10811-008-9341-5

Zhang, S., Rensing, C., & Zhu, Y. G. (2014). Cyanobacteria-mediated arsenic redox dynamics is regulated by phosphate in aquatic environments. *Environmental Science and Technology*, *48*(2), 994–1000. https://doi.org/10.1021/ES403836G

Zhu, F., Yang, M., Luo, Z. xi, Yu, R. lian, Hu, G. ren, & Yan, Y. (2020). Bioaccumulation and biotransformation of arsenic in Leptolyngbya boryana. *Environmental Science and Pollution Research*, *27*(24), 29993–30000. https://doi.org/10.1007/S11356-020-09294-Y

Zuhairi, W., Yaacob, W., Mohd, S., Hazwani, P. &, Mutalib, A., Geologi, P., Sekitaran, S., Alam, S., Sains, F., & Teknologi, D. (2009). *Acid mine drainage and heavy metals contamination at abandoned and active mine sites in Pahang*. https://doi.org/10.1088/1755-1315/646/1/012047